สมบัติทางแสงของละอองลอยเหนือบริเวณอำเภอพิมาย จังหวัดนครราชสีมา ภาคตะวันออกเฉียงเหนือของประเทศไทย

ว่าที่ ร.ต. ธวัชชัย สุดใจ

วิทยานิพนธ์นี้เป็นส่วนหนึ่งของการศึกษาตามหลักสูตรปริญญาวิทยาศาสตรมหาบัณฑิต
สาขาวิชาโลกศาสตร์ ภาควิชาธรณีวิทยา
คณะวิทยาศาสตร์ จุฬาลงกรณ์มหาวิทยาลัย
ปีการศึกษา 2552

AEROSOL OPTICAL PROPERTIES OVER AMPHOE PHIMAI, CHANGWAT NAKHON RATCHASIMA, NORTH EASTERN THAILAND

Acting SubLt. Thawatchai Sudjai

A Thesis Submitted in Partial Fulfillment of the Requirements
for the Degree of Master of Science Program in Earth Sciences

Department of Geology

Faculty of Science

Chulalongkorn University

Academic Year 2009

Thesis Title	AEROSOL OPTICAL PROPERTIES OVER AMPHOE PHIMAI, CHANGWAT NAKHON RATCHASIMA, NORTH EASTERN THAILAND
By	Acting SubLt. Thawatchai Sudjai
Field of Study	Earth Sciences
Thesis Advisor	Sathon Vijarnwannaluk, Ph.D.

Accepted by the Faculty of science, Chulalongkorn University in Partial Fulfillment of the Requirements for the Master's Degree

..... Dean of the Faculty of Science

(Professor Supot Hannongbua, Dr.rer.nat)

THESIS COMMITTEE

..... Chairman

(Assistant Professor Somchai Nakapadungrat, Ph.D.)

..... Thesis Advisor

(Sathon Vijarnwannaluk, Ph.D.)

..... Examiner

(Assistant Professor Sombat Yumuang, Ph.D.)

..... External Examiner

(Vanisa Surapipith, Ph.D.)

ธวัชชัย สุดใจ : สมบัติทางแสงของละอองลอยเหนือบริเวณอำเภอพิมาย จังหวัดนครราชสีมา ภาคตะวันออกเฉียงเหนือของประเทศไทย. (AEROSOL OPTICAL PROPERTIES OVER AMPHOE PHIMAI, CHANGWAT NAKHON RATCHASIMA, NORTH EASTERN THAILAND) อ. ที่ปรึกษาวิทยานิพนธ์หลัก : ดร.สธน วิจารณ์วรรณลักษณ์,123 หน้า.

การตรวจวัดปริมาณรังสีตรง (Direct radiation) และรังสีอ้อม (Diffuse radiation) โดยใช้เครื่องไอสกายเรดิโอมิเตอร์ (i-Skyradiometer) และวิเคราะห์ด้วยโปรแกรม Skyrad.pack V4.2 สามารถที่จะนำมาหาค่าคุณสมบัติทางฟิสิกส์เชิงแสงของละอองลอย อันประกอบไปด้วยค่าของความหนาเชิงแสงของละอองลอย (Aerosol Optical Depth, AOD), ค่าอัลบีโดสำหรับการกระจัดกระจายเดี่ยวของละอองลอย (Single Scattering Albedo, SSA) และค่าการแจกแจงขนาดของละอองลอย (Volume size distribution, Vol)

ในงานวิจัยนี้นั้นได้ทำการตรวจวัดปริมาณรังสี ณ สถานีวิจัยชั้นบรรยากาศ อำเภอพิมาย ระหว่างปี พ.ศ. 2549 ถึงปี พ.ศ. 2550 โดยใช้ความยาวคลื่นที่ 500 นาโนมิเตอร์ พบว่าค่า AOD และ SSA นั้นมีค่าสูงในช่วงเดือนมีนาคมและกันยายน และมีค่าที่ต่ำในเดือนมิถุนายนถึงกรกฎาคมและธันวาคมถึงมกราคม โดยในปี พ.ศ. 2549 มีค่าเฉลี่ยรายเดือนของ AOD สูงสุดอยู่ที่ 0.75 ในเดือนมีนาคมและมีค่าต่ำสุดอยู่ที่ 0.28 ในเดือนมิถุนายน ค่าเฉลี่ยรายเดือนของ SSA อยู่ที่ 0.94 ในเดือนตุลาคมและต่ำสุดอยู่ที่ 0.87 ในเดือนพฤษภาคมและมิถุนายน ในปี พ.ศ. 2550 มีค่าเฉลี่ยรายเดือนของ AOD สูงสุดอยู่ที่ 0.89 ในเดือนมีนาคมและมีค่าต่ำสุดอยู่ที่ 0.32 ในเดือนมิถุนายน ค่าเฉลี่ยรายเดือนของ SSA อยู่ที่ 0.90 ในเดือนมีนาคมและตุลาคม และต่ำสุดอยู่ที่ 0.83 ในเดือนธันวาคม สำหรับค่า Vol นั้นละอองลอยขนาดเล็ก (Fine mode) ส่วนใหญ่มีขนาดเฉลี่ยของรัศมีเท่ากับ 0.17 ไมโครมิเตอร์ ละอองลอยขนาดใหญ่ (Coarse mode) นั้นโดยส่วนมากจะมีขนาดใหญ่กว่า 16.54 ไมโครมิเตอร์ เท่ากันทั้งในปี พ.ศ. 2549 และ พ.ศ. 2550 จากการคำนวณทางเดินได้แบบย้อนหลัง (Backward trajectory) ของอนุภาคละอองลอยจะพบว่าในฤดูหนาวนั้นละอองลอยส่วนใหญ่จะมีเส้นทางการเดินทางของอนุภาคมาจากบริเวณทิศตะวันออกเฉียงเหนือของประเทศไทย ในฤดูร้อนนั้นอนุภาคละอองลอยจะมีทิศทางการพัดพามาจากทางบริเวณทิศตะวันออกของประเทศไทย ส่วนในฤดูฝนนั้นอนุภาคละอองลอยส่วนใหญ่จะเส้นทางการเดินทางของอนุภาคมาจากทิศตะวันตกเฉียงใต้ของประเทศไทย

ภาควิชา....ธรณีวิทยา....ลายมือชื่อนิสิต.....

สาขาวิชา...โลกศาสตร์...ลายมือชื่อ อ.ที่ปรึกษาวิทยานิพนธ์หลัก.....

ปีการศึกษา.....2552.....

4972319023 : MAJOR EARTH SCIENCES

KEYWORDS : AEROSOL / AEROSOL OPTICAL DEPTH / SINGLE SCATTERING ALBEDO / VOLUME SIZE DISTRIBUTION / BACKWARD TRAJECTORY

THAWATCHAI SUDJAI : AEROSOL OPTICAL PROPERTIES OVER AMPHOE PHIMAI, CHANGWAT NAKHON RATCHASIMA, NORTH EASTERN THAILAND. THESIS ADVISOR : SATHON VIJARNWANNALUK, Ph.D., 123 pp.

Measurement of diffuse and direct solar irradiance can be used to determine the aerosol optical properties such as an aerosols optical depth (AOD), single scattering albedo (SSA), and volume size distribution (Vol), in the atmosphere. In this study, i-skyradiometer at Observatory for Atmospheric Research at Phimai, Thailand are used to observed these properties.

The period of data is between 2006-2007, Skyrad.pack V4.2 program with double precision method was used for data analysis. In 2006, on select wavelength : 500 nm, it clears that AOD and SSA value are very high in two periods, March and September. They are lower in June to July and December to January. The highest monthly average of AOD is 0.75 in March and the lowest is 0.28 in June. The highest monthly average of SSA is 0.94 in October and the lowest is 0.87 in May and June. In 2007, as in 2006, AOD and SSA value is very high in two periods, March and September. They are lower in June to July and December to January. The highest monthly average of AOD is 0.89 in March and the lowest is 0.32 in June. The highest monthly average of SSA is 0.90 in March and October. The lowest monthly of average SSA is 0.83 in December. It is found that the average volume of size of aerosol particle in coarse mode is larger than 16.54 micrometer and the size of aerosol particle in fine mode is 0.17 micrometer both of two years. The backward trajectories in winter season show the source of aerosol particle came from the north-east of Thailand, in continental. In summer season most of the aerosol particle came from the east. And in rainy season, the aerosol particle came from the south-west.

Department : .....GEOLOGY.....Student's signature.....

Field of study : ...EARTH SCIENCES...Advisor's signature.....

Academic year : .....2009.....

ACKNOWLEDGEMENTS

I would like to acknowledge my thesis advisors, Dr.Sathon Vijarnwannaluk, and Miss Boossarasiri Thana, Mr. Akkaneewut Chabangborn for their valuable suggestion and recommendation.

In addition, I would like to make sincere thanks to Prof.Dr.Tamio TAKAMURA (Center for Environmental Remote Sensing, CEReS) and Dr. **Kikuchi NOBUYUKI** (Japan Aerospace Exploration Agency, JAXA) and his staffs as well as Dr.Pradeep Khatri for establishing and maintaining the SKYNET sites in Thailand of this study. And also, thank you to related government agencies namely Thai Meteorological Department, Bureau of Royal Rainmaking and Agricultural Aviation.

Lastly, I would like to thanks my parents and families, and also my colleagues for their encouraging and stimulating to the fruitfulness of my research works.

CONTENTS

Page

Page

LIST OF TABLES

LIST OF FIGURES

Figure Page

Figure Page

Figure Page

CHAPTER I
INTRODUCTION

1.1 Overview

Earth is a simple sphere but it is not simple in terms of life and environment. The earth consists of lithosphere, hydrosphere, atmosphere and biosphere. All of the parts effected each other. When each part changes, other part will be changed altogether.

Atmosphere is one of the important parts of the earth. It effects everything. It has a role like a movement of life. It makes wind, storm, thunderstorm, cloud, rain, snow. Any change in the atmosphere always has an effect on every aspect on earth.

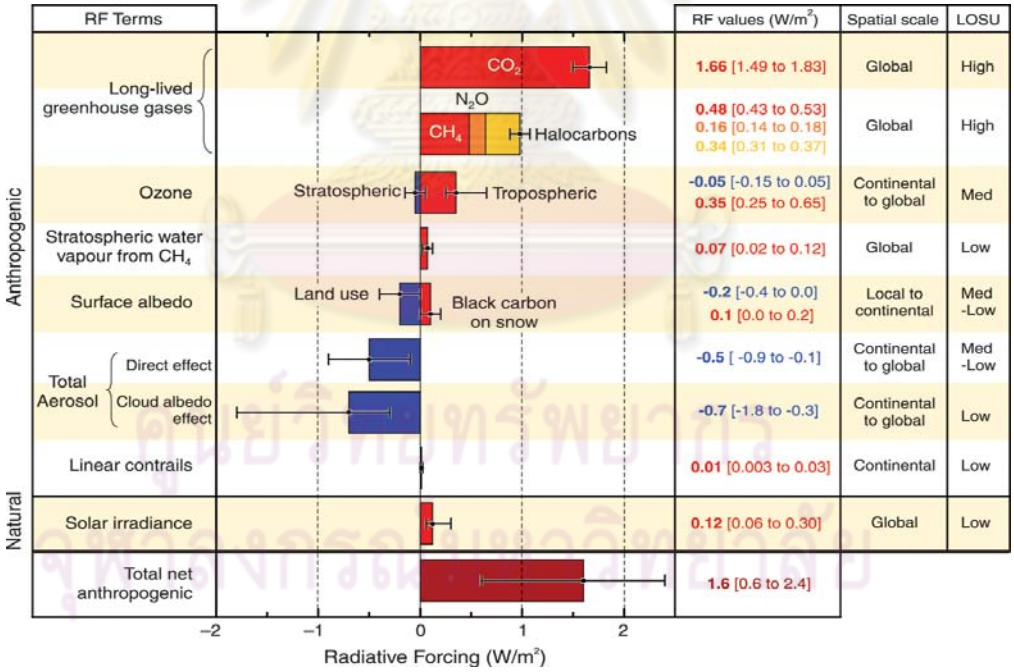

Figure 1.1 IPCC fourth assessment reports, climate change 2007 (IPCC, 2007).

Aerosol particle, in the atmosphere, is a mysterious element of the climate system. IPCC, Inter Governmental Panel on Climate Change, summarize atmospheric component effect on climate, which express as level of scientific understanding (LOSU) in figure 1.1. Most of the greenhouse gases, such as Methane (CH_4), Water vapour (H_2O), Carbon dioxide (CO_2), Ozone (O_3), have mostly positive radiative forcing effect. In addition, LOSU is quite high to medium for these gases. According to Ramanathan, 2000, the greenhouse gases will increase the energy of earth's surface balance by 3 W/m^2. In contrary, LOSU of aerosols effect is quite low relative to the greenhouse gas, therefore we are not exactly sure that it will provide position or negative radiative forcing effect.

Aerosols influence the Earth-atmosphere system in two different ways. The first is the direct effect, by which aerosols scatter and absorb solar and thermal infrared radiation, therefore altering the radiative balance of the Earth-atmosphere system. The second is the indirect effect, the aerosols modify the microphysical processes and the radiative properties and lifetime of clouds (Heywood and Boucher, 2000).

The semi-direct effect is separate from the indirect aerosol effect, by which increases in aerosol concentration lead to increases in cloud albedo and lifetime by microphysical interactions. The semi-direct aerosol effect may have a significant warming impact on climate by 'burning off' low clouds that scatter solar radiation back to space but have little impact on outgoing long wave radiation (Johnson, 2003).

In this study, 5 chapters were presented. Chapter I is the introduction, chapter II is the theory and literature review, chapter III is about instruments and methodology, chapter IV is the results and discussion and finally chapter V is the conclusions and suggestions.

1.2 Statement of Problem

Even though the aerosol particles have on effect to our life, climate both in local and global scale, but there are very few studies in Thailand. Thailand is a great agriculture country. The situation of weather is very significant. This research helps us to know some properties of aerosols in this area. In addition, because the effect of aerosols also takes on global area, the aerosols data can fill in the gap of the global data. It is a key to predict our future climate. Especially, these data can be checked and compared with those obtained by other methods such as the data obtained by satellite.

1.3 Objective

The objective of this study is to understand annual variation of aerosol optical properties which are the aerosol optical depth (AOD), Single scattering albedo (SSA) and aerosol volume size distributions. The data will be collected by i-Skyradiometer (model POM-02) which is manufactured by PREDE Company Japan. SKYRAD.pack algorithm will be used to analyze the observation data. The detail of instrument and data analysis present in chapter III. After that, aerosol optical properties will be consider together with HYSPLIT (Hybrid Single Particle Lagrangian Integrated Trajectory Model) model that provide by NOAA (National Oceanic and Atmospheric Administration) in order to analyze the source of aerosol.

1.4 Scope of Investigation

i-Skyradiometer has been installed at the observatory for atmospheric research at Phimai, Nakhon Ratchasima since January 2005. The observatory is in the northeast of Bangkok. It was established by the cooperation between Thai-Japanese scientists in order to understand aerosol effect in the monsoon region. In this study, the focus is on the data from 2006 to 2007.

1.5 Expected Result

It is expected that i-Skyradiometer will provide the comprehensive information of physical properties of aerosols such as Aerosol Optical Depth (AOD), Single Scattering Albedo (SSA), and volume size distributions over study area.

CHAPTER II

THEORY AND LITERATURE REVIEWS

2.1 Radiation budget

The Earth has an average incoming solar radiation around 342 Wm^{-2} (IPCC, 2007). Some part of it is being reflected by clouds, aerosol, atmospheric gases, and the surface of the Earth. The other part of incoming radiation is being absorbed by the atmosphere and the surface. To maintain the thermodynamics equilibrium of the earth-atmosphere system, energy has to be transported back to space. Our earth and its atmosphere do it by emitting the outgoing long wave (thermal) radiation to space, as show in figure 2.1.

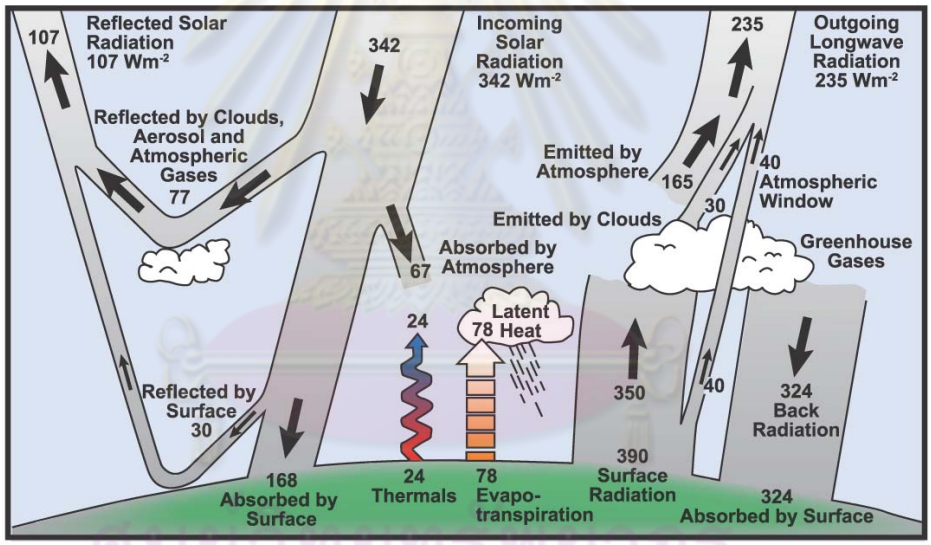

Figure 2.1 Estimate of the Earth's annual and global mean energy balance (Kiehl and Trenberth, 1997).

Aerosol is one important part of the radiation budget. It plays both role of absorbing and reflecting incoming solar radiation. It can change the balance and side of radiative forcing. Positive or negative radiative forcing may get the Earth to warm up or cool down, respectively. In addition, aerosol particles not only effect the radiation budget, but it also effects some properties of cloud, precipitation (Flossmann, 1998) and our health.

2.2 Earth Climate

Earth's climate varies with time and location, because the Earth's orbit is ellipse and the Earth's axis is tilt by 23 ½ degree. This tilt in orbital axis causes the change in seasons, as show in figure 2.2.

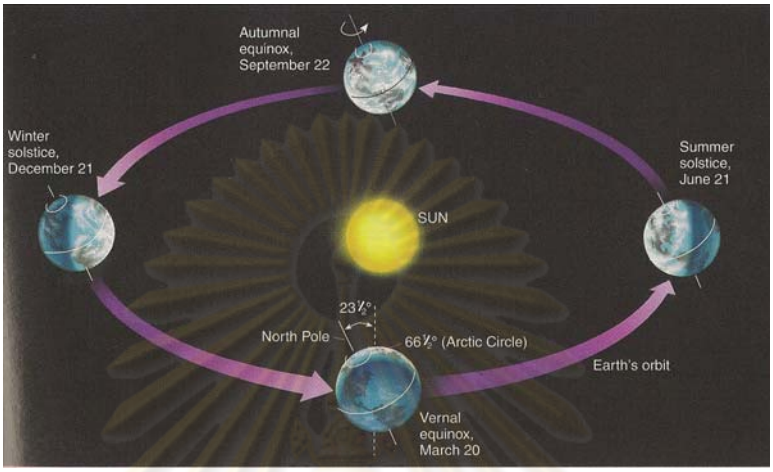

Figure 2.2 The Earth revolves about the sun (Ahrens, 2008).

During the day, the temperature changes with time because of incoming solar radiation and outgoing the Earth infrared radiation. In day time, the Earth receives energy from sunlight, temperature increases from 6 am to 4 pm, as in figure 2.3. During the night, the Earth radiated energy out, therefore the temperature decreases to the lowest point again at 6 am. Relative humidity changes in opposite to temperature. It is higher on 6 am and lower on 4 pm, as in figure 2.4.

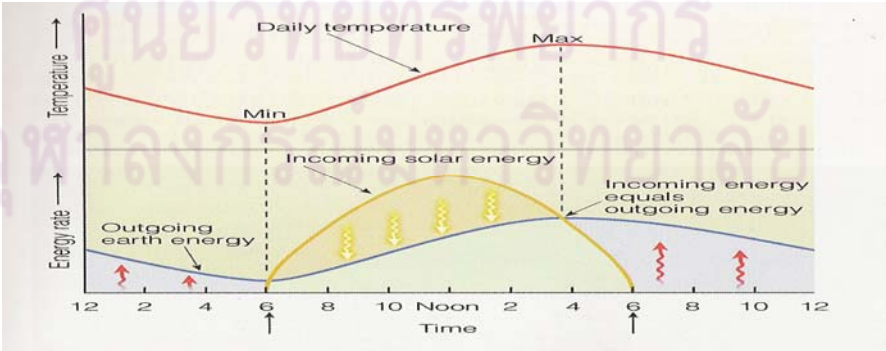

Figure 2.3 The daily variation in air temperature (Ahrens, 2008).

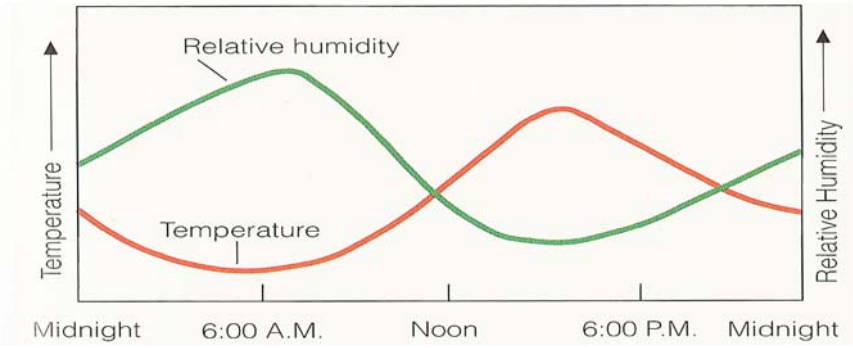

Figure 2.4 The daily variation in relative humidity (Ahrens, 2008).

According to Global warming situation, a famous topic of scientist on this century is the increasing global mean temperature. A yellow line in figure 2.5, the temperature is rising during the period of 25 years (1981 to 2005) with anomalies relative to the 1961 to 1990 (IPCC, 2007). For the period of 50, 100 and 150 years, the global mean temperature rise also but at lower rate. Over the past 100 years (1906 to 2005) surface temperature increase about 0.74 °C.

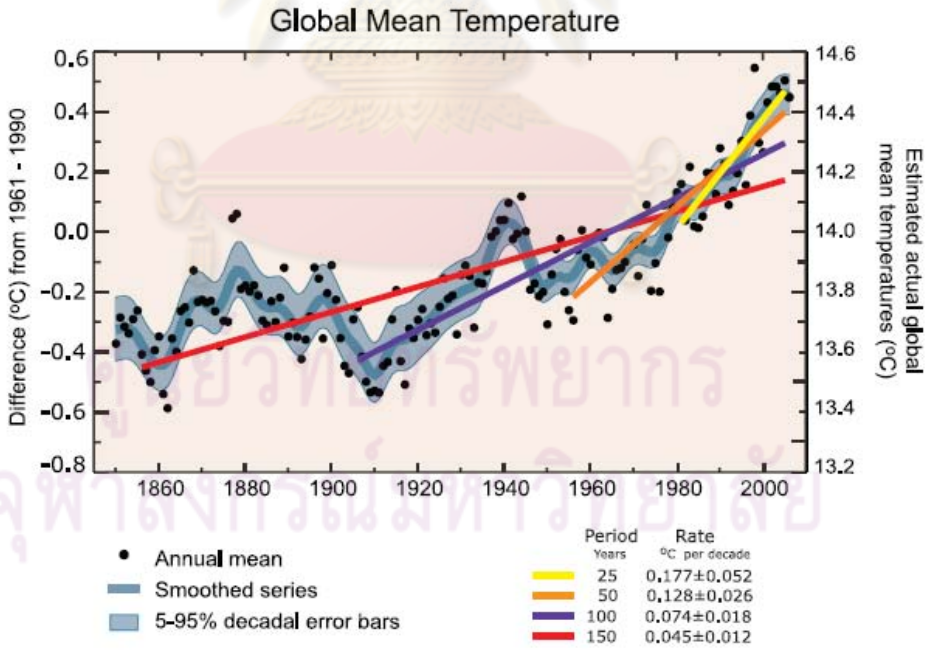

Figure 2.5 The global mean temperature (IPCC, 2007)

2.3 Radiation

Radiation, electromagnetic wave, comes from the Sun through a space to our earth. Radiation involves in many process of the Earth, i.e. : water cycle, winds, biology cycle.

2.3.1 Propagation

Radiation can propagate through space with the speed of c_0 = 299,792,458 m·s^{-1} (Roland, 2005). From wave model of radiation, the wave-length λ (m·cycle^{-1}) is associated to the frequency, ν (Hz = cycle·s^{-1}) by:

$$\lambda \cdot \nu = c_0 \tag{2.5}$$

2.3.2 Emission

Everything has emitted some radiation, when its temperature is higher than absolute zero. By Planck's law, the amount of blackbody monochromatic (single wavelength or color) radiation flux, called irradiance, E_λ^* can be express by :

$$E_\lambda^* = \frac{c_1}{\lambda^5 \cdot \left[\exp(c_2 / \lambda \cdot T) - 1\right]} \tag{2.6}$$

Where T is an absolute temperature and two constants are ;

$$c_1 = 3.74 \times 10^8 W \cdot m^{-2} \cdot \mu m^4 \tag{2.7}$$

$$c_2 = 1.44 \times 10^4 \mu m \cdot K \tag{2.8}$$

For the peak of wavelength radiation from object that warmer than absolute zero is can represent by Wien's law;

$$\lambda_{\max} = \frac{a}{T} \tag{2.9}$$

where a = 2897 μm·K.

The total amount of emission irradiance can be found by Stefan-Boltzmann law (2.10), where σ_{SB} = 5.67x10^{-8} W·m^{-2}·K^{-4} is the Stefan-Boltzmann constant.

$$E_2^* = \sigma_{SB} \cdot T^4 \tag{2.10}$$

2.3.3 Distributions

Inverse square law (2.11) can represent a decrease of radiation that emitted from a spherical source of distance from the center of the sphere.

$$\frac{E_2^*}{E_1^*} = \left(\frac{R_1}{R_2}\right)^2 \tag{2.11}$$

where R_1 and R_2 are the distance from a center of each sphere.

2.3.4 Absorption, Reflection and Transmission

Radiation from the Sun can be absorbed, reflected and transmitted. When it reaches any object, a fraction of incoming (incident) radiation might also be absorbed in to the substance. Absorptivity is defined as;

$$absorptivity = \frac{E_\lambda absorbed}{E_\lambda incident} = a_\lambda \tag{2.12}$$

Some fraction of incoming radiation can be reflected back, the reflectivity is ;

$$reflectivity = \frac{E_\lambda reflected}{E_\lambda incident} = r_\lambda \tag{2.13}$$

And a fraction transmitted through some object, or transmissivity, is;

$$transmissivity = \frac{E_\lambda transmitted}{E_\lambda incident} = t_\lambda \tag{2.14}$$

The sum all of them must total 1, as 100% of the radiation at any wavelength must be accounted (2.15) and table 2.1 is example of emissivities value.

$$1 = a_\lambda + r_\lambda + t_\lambda \quad \text{or} \quad E_{\lambda\, incoming} == E_{\lambda\, absorbed} + E_{\lambda\, reflected} + E_{\lambda\, transmitted} \tag{2.15}$$

Table 2.1 Typical infrared emissivities (Roland B, 2005).

Surface	*e*	Surface	*e*
Soil, peat	0.97-0.98	Snow, fresh	0.99
Asphalt	0.95	Concrete	0.71-0-9
gravel	0.92	Cloud, low	1.0
Urban	0.85-0.95	Cloud, cirrus	0.3
Leaf 1 μm	0.05-0.53	Cloud, alto	0.9
Sand wet	0.98	Ice	0.96
paper	0.89-0.95	Silver	0.02
Aluminum	0.01-0.05	Grass	0.9-0.95
Human skin	0.95	Plaster, white	0.91

The percentage of total reflected to total incoming solar radiation is called the albedo, A, by 2.16 and example of albedo value is in table 2.2.

$$A = \frac{E_{reflected}}{E_{incoming}} \cdot 100 \tag{2.16}$$

Table 2.2 Typical albedo (Roland, 2005).

Surface	*A*	Surface	*A*
Snow, fresh	75-95	Road, asphalt	5-15
Snow, old	35-70	Concrete	15-37
Water, deep	5-20	Buildings	9
Soil, dark wet	6-8	Urban, mean	15
Clay, wet	23	Field, fallow	5-12
Cloud, thick	70-95	Rice paddy	12
Cloud, thin	20-65	corn	18

2.3.5 Beer's Law

Beer's law provides the relationship between incident radiative flux and outgoing transmitted radiative flux (2.17). The let Δs be the path length of particle within the air, n be the number density of absorbing particles in the air, and b be the absorption cross section of each particle as in figure 2.6. Then the transmitted radiative flux is related to the incident radiative flux by;

$$E_{transmitted} = E_{incident} \cdot e^{-n \cdot b \cdot \Delta s} \tag{2.17}$$

It can also be written using an absorption coefficient, k (2.18);

$$E_{transmitted} = E_{incident} \cdot e^{-k \cdot \rho \cdot \Delta s} \tag{2.18}$$

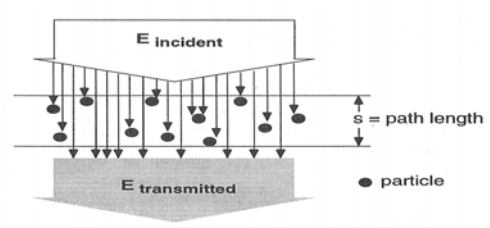

Figure 2.6 Reduction of radiation across a path due to absorption by particles (Roland, 2005).

2.4 Atmosphere

2.4.1 Atmospheric Structure and some behavior

Layers of the atmosphere include the Thermosphere, Mesosphere, Stratosphere and Troposphere. Their level is, higher than 84.9 km, 47 to 84.9 km, 11 to 47 km and 0 to 11 km, respectively (Roland, 2000). The layer is separated by temperature structure, as in figure 2.7. The boundaries between 2 layers are call Mesopause, Stratopause and Tropopause. Almost of all clouds and weather occur in the troposphere.

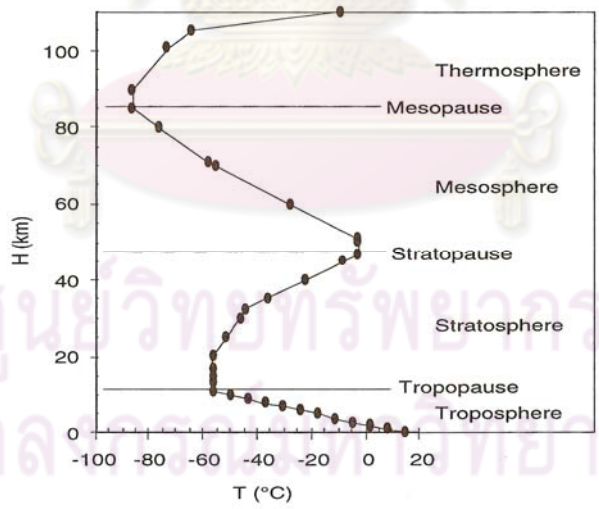

Figure 2.7 Standard temperature profiles vs. geopotential height (Roland, 2000).

Atmosphere has a lot of cloud. Cloud is something that we can see regularly in the sky. Clouds have four major groups, i.e. high clouds, middle clouds, low clouds and clouds with vertical development. High clouds are cirrus, cirrostratus and cirrocumulus. Middle is altostratus and altocumulus. Low clouds are stratus,

stratocumulus and nimbostratus. And, clouds with vertical development are cumulus and cumulonimbus. Figure 2.8 show each clouds type and level of its origin.

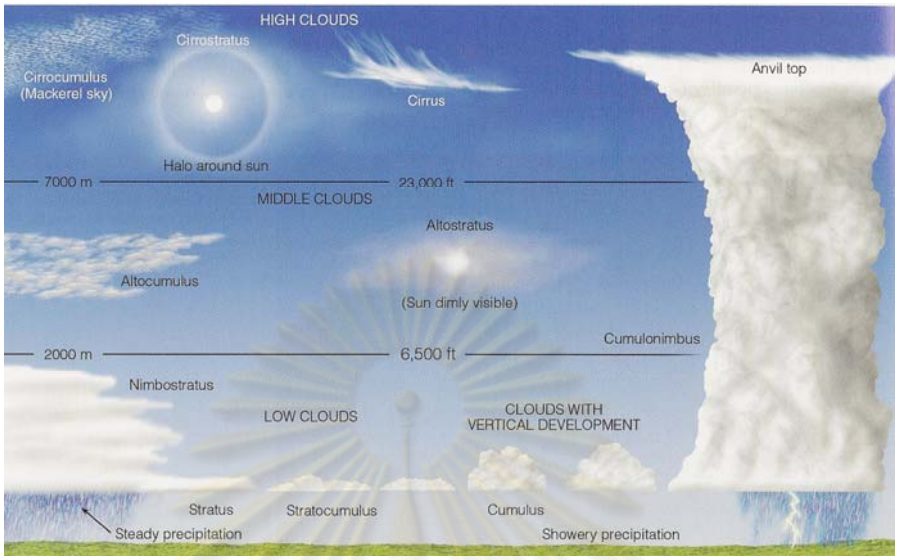

Figure 2.8 A generalized illustration of basic cloud types based on height above the surface and vertical development (Ahrens, 2007).

In figure 2.9 shows the process of water circulation. When sea water of the ocean receives energy from the Sun, sea water evaporates to water vapor then it is condensation in to liquid, cloud, and precipitation to the earth surface. Rain or snow from precipitation melt and run down to low level. And finally, it becomes sea water again. All of the cycle process is called hydrologic cycle (Ahrens, 2007).

Figure 2.9 The hydrologic cycle (Ahrens, 2007).

2.4.2 Thermodynamic State

The thermodynamic state of the air is represented by three factors, its pressure, density, and temperature (Roland, 2005).

Pressure P is the force F per unit area A that perpendicular to the surface as in (2.1):

$$P = F / A \tag{2.1}$$

Density ρ is defined as mass m per unit volume V (2.2):

$$\rho = m / V \tag{2.2}$$

Temperature T is associated with greater average molecular speeds (ν_{rms}), according to (2.3):

$$T = a \cdot m_w \cdot \nu_{rms}^{\ 2} \tag{2.3}$$

where a = 4.0 x 10^{-5} K.$m^{-2}s^{-2}$ is a constant.

Equation of state is the relationship between pressure, density, and temperature of the air. On different fluids, there is different equation of state. It depends on their molecular properties. For dry air a simple equation of state of the gases in the atmosphere known as the ideal gas law is;

$$P = \rho \cdot \Re_d \cdot T \tag{2.4}$$

where $\Re_d$ = 0.287053 kPa•K^{-1}•m^3•kg^{-1}

= 281.053 J• K^{-1}•kg^{-1}

is called the gas constant for dry air.

2.4.3 Relation between atmosphere and aerosol

There are many relations between aerosol particle and atmosphere. First of all, atmosphere contains many aerosol particles. For example, the global annual mineral aerosol particles releases to atmosphere are around 1000-2000 Tg•yr^{-1}

(Duce, 1995). For this reason, aerosol can change properties of the atmosphere. Aerosol make uncertainty in climate forecasts (Charlson and Heintzenberg, 1995). Forcing measure in watts per square meter (Wm^{-2})is refer to changes in heat balance due to anthropogenic or externally imposed changes in the chemical composition of the atmosphere. Atmospheric aerosol particles both of in atmosphere and clouds cause of much larger uncertainties in forcing. In addition, aerosol particle change some process of the atmosphere. Cloud properties are one that effected by it. Aerosol particles directly determine the number of drops formed. This, in turn, effects the growth of the cloud, precipitation formation, and the radiative cloud properties (Flossmann, 1998). All of that, almost all aerosol particles is coming from surface to atmosphere and return to the surface. It is natural life cycle of aerosol particles in the atmosphere.

2.5 Aerosols

"Aerosols is a suspension of solid or liquid particles in gas, usually air; or a colloid" (Reist, 1993). Aerosols can be discharge to our environment both by natural process and anthropogenic process. It effects our health; pollution our climate.

From this definition, aerosols can be dust, fumes, smoke, mists, fog, haze, and smog, etc. Aerosols can be divided in to three major groups. First is the monodisperse aerosol, which contains particle of only one size. Second is the polydisperse aerosol, which contains particles more than one size. And last, the homogeneous aerosols, which have similar chemical properties within its group (Reist, 1993).

2.5.1 Specific of Aerosols

Because aerosols are not entirely liquid, they can have many shapes. In general, shape of aerosols can be divided into three classes. First, an isometric particle, which all three dimension are roughly to same. Second, platelets particles, which it have two long sides and a small thickness. Third, a fibers particle, which has great length in one direction compared to much smaller lengths in the other direction (Reist, 1993).

Normally, aerosol size (diameters) is set between 0.01 μm to 100 μm (Reist, 1993). The reason of this is because the smallest particle should be at the transition point from molecule into particle. And aerosol particles larger than 100 μm do not normally remain suspended in the air long enough to be of much interest in aerosol science. Table 2.3 shows example of aerosols particles in diameters.

Table 2.3 Typical particle diameters in μm (Reist, 1993).

Tobacco smoke	0.25	Lycopodium	20
Ammonium chloride	0.1	Atmospheric fog	2–o0
Sulfuric acid mist	0.3–5	Pollens	15–70
Zinc oxide fume	0.05	"Aerosol" spray products	1–100
Flour dust	15–20	Talc	10
Pigments	1–5	Photochemical aerosols	0.01–1

2.5.2 Kind of Aerosols

Aerosols can be divided by many factors, For example; source of aerosol, properties of aerosol both chemically and physically, size of aerosol particle. Aerosols have four large types. They are sulfate, carbonaceous, dust and sea salt aerosols. Chemical species of aerosol are sulfates, nitrates, silicates, sea salt, soot and organic matter. If divided by size, aerosols compose of fine mode for small size and coarse mode for large size. When divided by source, aerosol can be dividing in to natural and anthropogenic aerosols, primary aerosol, secondary aerosols, marine time aerosols, continental aerosol and desert aerosol (Reist, 1993).

2.5.3 Effect of Aerosols

Aerosols have a three effect to our climate. First is direct effect, which includes scattering and absorption. Second is indirect effect and the last is semi-direct effect.

Aerosols influence the Earth-atmospheric system in two different ways. The first is the direct effect, by which aerosols scatter and absorb solar and thermal infrared radiation, thus altering the radiative balance of the Earth-atmospheric system.

The second is the indirect effect, the aerosols modify the microphysical and the radiative properties and lifetime of clouds (Heywood and Boucher, 2000).

The semi-direct effect is different from the indirect aerosol effect. The increases in aerosol concentration lead to increases in cloud albedo and lifetime of microphysical interactions. The semi-direct aerosol effect may have a significant warming impact on climate by 'burning off' low clouds that scatter solar radiation back to space but have little impact on outgoing long wave radiation. (Johnson, 2003).

2.5.4 Aerosols in Thailand

There are very few studies about aerosols in Thailand. In 2005, Kim et al. used ground-based solar radiation measurements to observe aerosol radiative forcing over East Asia. They found that aerosol in Sri Samrong area, in figure 2.10, from 1997 to 2000 is more of an absorbing biomass burning aerosols. The total volume of fine mode is larger than course mode. Fine mode of aerosols is about 0.2 μm, course mode is about 5 μm and single scattering value is about 0.88 (Kim et al., 2005).

Figure 2.10 The observatory for atmospheric research at Sri Samrong, Thailand.

2.5.5 Aerosol Optical Properties

Aerosol optical properties are important to understand the effects of its to our climate. It contains Aerosol Optical Depth (AOD), Single Scattering Albedo (SSA) and Volume size distributions (Vol).

AOD is the vertical integral of the aerosol concentration weighted with the effective cross-sectional area of the particles intercepting (by scattering and absorption) the solar radiation at the wavelength of interest (Ramanathan et al., 2001).

Single Scattering Albedo (SSA) is the factor composing scattering effects of aerosols to absorbing effects. The higher the SSA, mean the more scattering. The aerosol volume size distribution is the mean size of the aerosols from the spectral optical depth measurements of an air column of unit cross section (Krishna et al., 1998).

2.6 Method of Determining Scattering Parameter

From i-Skyradiometer, the direct solar flux density (2.19) can be measured. Lets, F_0 be the flux at the top of the atmosphere, τ is the total optical thickness, and m_0 is the optical air mass which can be approximated as $m_0 = 1/\text{Cos}\ \theta_0$ as long as $\theta_0 \leq 45^\circ$ (Nakajima et al., 1996). The monochromatic direct solar flux density F (in $Wm^{-2}\mu m^{-1}$) is given by (2.19);

$$F = F_0 \exp(-m_0\tau) \tag{2.19}$$

In the above process, aerosols optical depth value can be calculated. If ω is the single-scattering albedo of the whole air mass, $P(\theta)$ is the total phase function at scattering angle θ, $\Delta\Omega$ is the solid view angle of the sky radiometer, and $q(\theta)$ indicates the multiple scattering (MS) contribution, the monochromatic diffuse sky flux density E (in $Wm^{-2}\mu m^{-1}$) can be expressed by (2.20);

$$E(\theta_0, \phi) \equiv E(\theta) = Fm_0\Delta\Omega[\omega\tau P(\theta) + q(\theta)] \tag{2.20}$$

For more accurate relation, the diffuse flux normalizes by the direct flux by;

$$R(\theta) \equiv \frac{E(\theta)}{Fm_o\Delta\Omega} = \omega\tau P(\theta) + q(\theta) \equiv \beta(\theta) + q(\theta) \tag{2.21}$$

The differential scattering coefficient, $\beta(\theta) \equiv \omega\tau P(\theta)$, is obtained by an iterative regression incorporating a MS algorithm from $R(\theta)$. Followed by $\beta(\theta)$ and possibly τ data, the volume size distributions of the atmospheric aerosol can derived.

By definition the aerosol optical thickness is (2.22);

$$\tau_A(\lambda) \equiv \int_{r_m}^{r_M} \pi r^2 Q_{ext}(x, \tilde{m}) n(r) dr \tag{2.22}$$

where Q_{ext} is the efficiency factor for extinction as given by the Mie theory for spherical particles, $x = (2\pi/\lambda)r$ is the size parameter, n(r) is the columnar radius distributions of aerosol, r_m and r_M are minimum and maximum aerosol radii, respectively, and $\tilde{m}$ = m-ki is the aerosol complex refractive index. For aerosol single scattering albedo, SSA or ω_A, is $\omega_A = \tau_{AS} / \tau_A$ where τ_{AS} is the optical thickness for scattering by replace the efficiency factor to Q_{ext} (Nakajima et al., 1996).

The aerosol difference scattering coefficient representative of the whole atmospheric column is defined as;

$$\beta_A(\theta) = \int_{r_m}^{r_M} [i_1(\theta, x, \tilde{m}) + (i_2(\theta, x, \tilde{m})] n(r) dr \tag{2.23}$$

where i_1 and i_2 are Mie intensity function. The aerosol phase function is defined as ;

$$p_A(\theta) \equiv \beta_A(\theta) / \omega_A \tau_A \tag{2.24}$$

The columnar aerosol radius distributions, *n(r)*, are the number of particles within an air column of unit cross section, for a unit radius interval (in inverse square centimeters time inverse micrometers). If the columnar volume spectrum *v(r)* is used; it is defined as the volume of aerosol for an air column of unit cross section, within a unit of logarithmic radius interval: $v(r) \equiv dV / d \ln r$ (in cubic centimeters per square centimeters). The relation between v(r) and n(r) is $v(r) = (4\pi/3) r^4 n(r).$

As a result, the two quantities τ_A and β_A can expressed as;

$$\tau_A(\lambda) = (2\pi/\lambda) \int_{r_m}^{r_M} K_{ext}(x, \tilde{m}) v(r) d \ln r \tag{2.25}$$

$$\beta_A(\theta) = (2\pi/\lambda) \int_{r_m}^{r_M} K(\theta, x, \tilde{m}) v(r) d \ln r \tag{2.26}$$

where K_{ext} and K are kernel function defined as ;

$$K_{ext}(x) = (\frac{3}{4})\frac{Q_{ext}(x)}{x} \tag{2.27}$$

$$K(\theta, x, \tilde{m}) = (\frac{3}{2})\frac{i_1 + i_2}{x^3} \tag{2.28}$$

The behavior of K_{ext} and K approximately determines the radius interval of reliable information content for the aerosol optical and physical features. For all process, it can be shown as flow chart in figure 2.11.

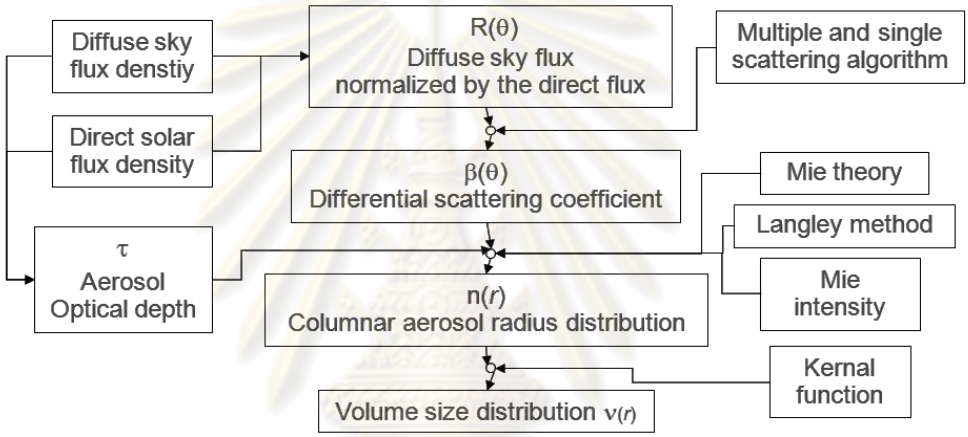

Figure 2.11 Flow chart of methodology.

2.7 Literature Reviews

There are many paper of aerosols study around the world, but only very few about Thailand. The important point of aerosols effects is that it is not only effect globally but it also effects the rain and cloud formation. That is one of the reasons why it is very important to study aerosol in Thailand.

The sky brightness measurement from ground for remote sensing of particulate polydispersions (Nakajima, 1996) is a heart of all aerosol studies. Teruyuki Nakajima, Glauco Tonna, Ruizhong Rao, Paolo Boi, Yoram Kaufman, and Brent Holben studied. Aerosol size distributions and optical thickness from data of direct and diffuse solar radiation using the software code SKYRAD.pack. They use Skyradiometer instead

of i-Skyradiometer to measure the direct and diffuse solar radiation in the wavelength range 0.369-1.3048 μm. The same instruments and method, Kazuma Aoki and Yasushi Fujitoshi use to measure aerosol optical properties over Sapporo, Japan. And found that the aerosol optical thickness increased over a short period of time following Asian dust events and a forest fire in Siberia (Aoki and Fujiyoshi, 2003).

Over East Asia, Skyradiometer Network (SKYNET) found that aerosols in East Asia have smaller single scattering albedos than that of the same type in another area, and also found that Asian dusts become blackened during their movement because they mixed with soot particles produced over the industrial/urban area of China (Kim et al., 2005).

Aerosol optical characteristics in regional and seasonal variations over India are studied by S. Ramachandran and Ribu Cherian from 2001 to 2005. They found that Northeast India has the lowest annual mean AOD of 0.28 following by South India AOD of 0.35. AODs are higher than 0.35 in the other regions. High altitudes with low populated locations are found to have lower AODs than urban and industrialized locations. It also shows a winter low and summer high in AODs on many locations. Locations/regions dominated by pollution are found to have high FMF and high AODs, while regions in which natural (biogenic) aerosols are dominant had high FMF and range of AODs (Ramachandran and Cherian, 2008).

One of the great projects is ABC-Asia, Atmospheric Brown Cloud-Asia. The project focused on measuring the anthropogenic influence of aerosols to determine the extent of sunlight dimming and radiative forcing over the Asian region. An anthropogenic aerosol over the Indian Ocean varies with the cyclic nature of the Indian Monsoon. From November through April, the dry monsoon brings polluted air from the Indian subcontinent and Southeast Asia. As a result, nearly an order of magnitude increase of scattering and absorbing aerosols from the transition between the clean and polluted seasons was founded in 2004. The measurements indicate a large increase in the aerosol radiative forcing of the region with the arrival of the dry monsoon (Corrigan et al., 2006).

For worldwide locations measurement, AERONET is a great network of ground-based radiometers. The results show aerosols are differ in both of magnitude and spectral dependence of the absorption. The observation shows that variability of the absorption for the same aerosol type appearing due to different meteorological and source characteristics (Dubovik et al., 2000).

CHAPTER III
INSTRUMENT AND METHODOLOGY

3.1 i-Skyradiomter

i-Skyradiometer made by Prede co., ltd, is used for measure solar irradiance both direct and indirect radiation. i-Skyradiometer with Skyrad.pack V.4.2 program can compute aerosols optical thickness, refractive index, single scattering albedo, volume spectrum, sky radiance and phase function value. In this study, we use i-Skyradiometer stationed at the Observatory for Atmospheric research at Phimai as showed in figure 3.1.

Figure 3.1 i-Skyradiometer in observatory for atmospheric research at Phimai.

3.1.1 i-Skyradiometer Module

i-Skyradiometer module, compose of solar radiation sensor, sun sensor, solar tracker, rain sensor, GPS receiver, computer and cable (Prede co., LTD). The diagram of i-Skyradiometer module is show in figure 3.2.

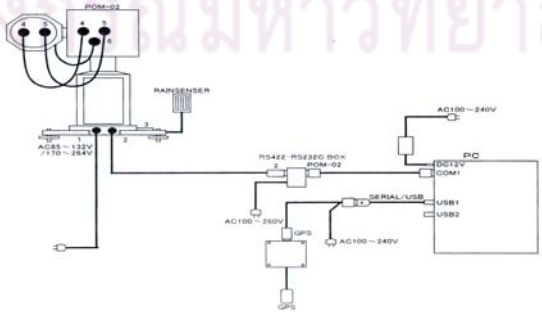

Figure 3.2 The module of i-Skyradiometer (Prede co., LTD).

3.1.2 Method of i-Skyradiometer

i-Skyradiometer is an instrument designed to measure the solar radiation, both sky radiance distributions (diffuse radiation) and direct solar irradiance (direct radiation). It measures radiation in 11 wave lengths, (315nm, 340nm, 380nm, 400nm, 500nm, 675nm, 870nm, 940nm, 1020nm, 1600nm, 2200nm) (Prede co ltd., Sky radiometer POM-02 user manual). Each wavelength corresponds to different contributors. For example, 312 nm is for optical thickness of ozone, 340 – 870 is for aerosol optical properties, 940 nm is for water vapor, and 1020 – 2200 is for cloud observation, as shown in table 3.1. In this study, we used wave length at 500 nm because the radiation maximum on this wavelength. It has not an affect of any atmospheric absorption. Otherwise, it is advantage to study of aerosol radiative forcing in the future.

Table 3.1 The observation target of each wave lengths (Prede co., LTD).

Wave lengths	Target	Wave lengths	Target
315nm	Optical thickness of Ozone	870nm	Aerosol
340nm	Aerosol	940nm	Water vapor
380nm	Aerosol	1020nm	Cloud
400nm	Aerosol	1600nm	Cloud
500nm	Aerosol	2200nm	Cloud
675nm	Aerosol		

The solar irradiance, sun light, pass in sun-shading hood to objective lens, interference filter and detector respectively. The sun-shading hood can follow the Sun by Sun sensor and Sun tracker both control by computer through the cables (signal and power). In case of raining, rain sensor is working and forces the observation to stop, as shown in figure 3.3.

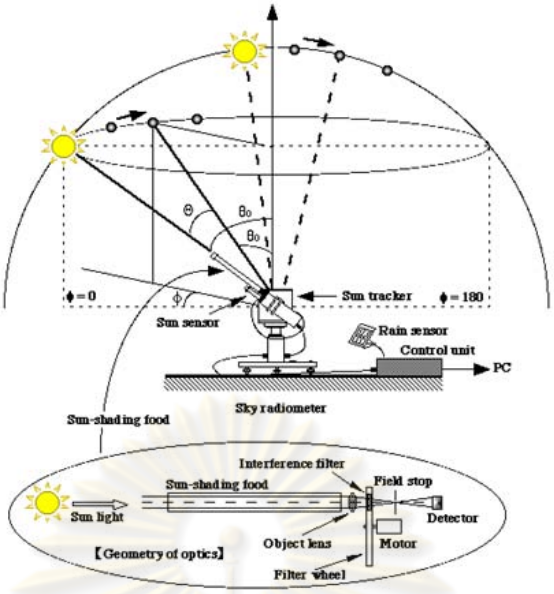

Figure 3.3 The observation of i-Skyradiometer (Prede co., LTD).

3.1.3 Observation Process

i-Skyradiometer observe the sky every 10 minute. Aerosol observations are measure in two directions, horizontal and vertical direction, as shown in figure 3.5 and figure 3.5. Scattering angle are maximum in 24 points at each Solar altitude, 0, 2, 3, 4, 5, 7, 10, 20, 25, 30, 40, 50, 60, 70, 80, 90, 100, 110, 110, 120, 130, 140, 150 and 160 degree.

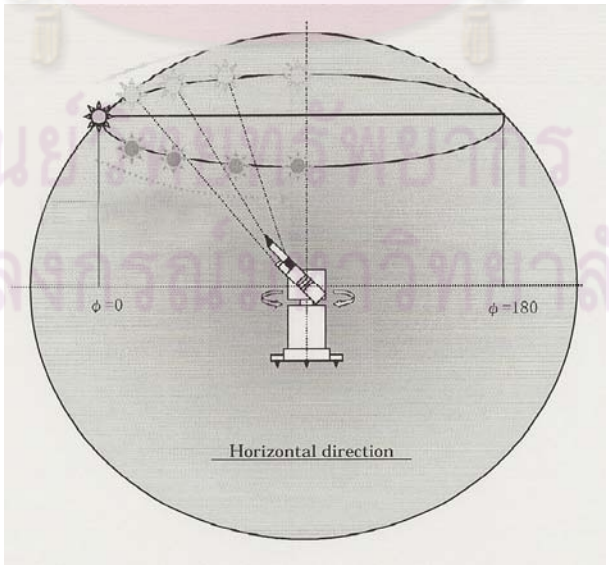

Figure 3.4 Observation of horizontal direction (Prede co., LTD).

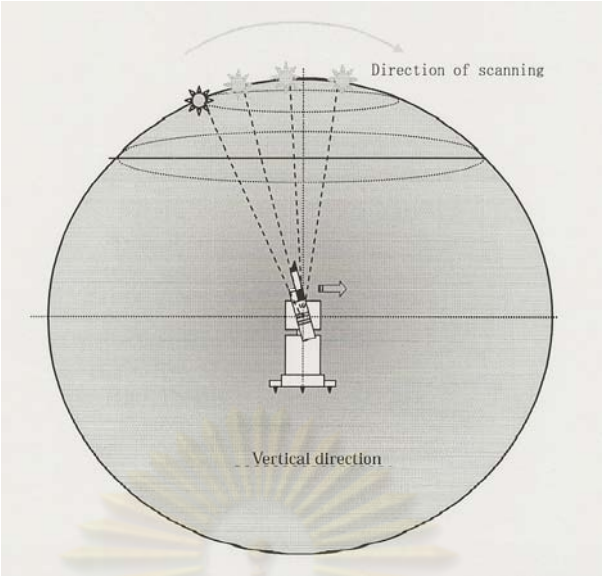

Figure 3.5 Observation of vertical direction (Prede co., LTD).

3.1.4 Data from i-Skyradiometer

i-Skyradiometer stores data that are necessary to calculate aerosols optical properties, aerosol optical depth, single scattering albeo and volume size distributions in files *.DAT type. These data will be analyzed by Skyrad.pack code program later.

A raw data pattern of dat files compose of 15 details:

1: Model of instrument.

2: S/N for body.

3: S/N for sensor.

4: Longitude and latitude.

5: Date (GMT) and time (GMT) of the start time.

6: Date (LT) and time (LT) of the start time.

7: Number of wavelengths.

8: Wavelengths.

9: Date (GMT) and time (GMT).

10: Date (LT) and time (LT).

11: H/V (H or V) gives the direction of scan; horizontal (almucantar) or vertical (principal plane).

12: Comment1 and 2.

13: Time (GMT) and time (LT).

14: Azimuth and elevation.

15: Intensities for the respective wavelengths.

The position in each detail is in figure 3.6.

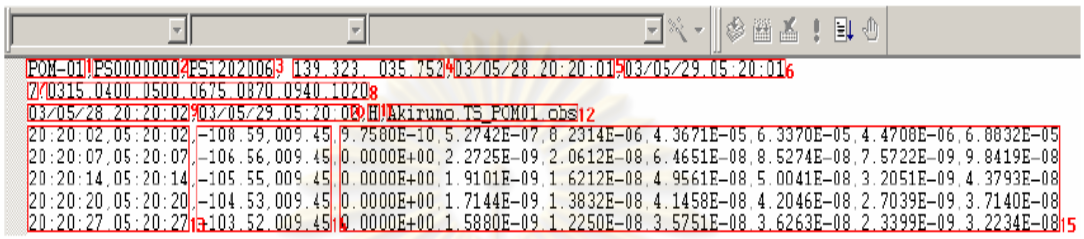

Figure 3.6 A pattern of raw data.

3.2 Program Skyrad.pack Version 4.2

Skyrad.pack V 4.2 program code use DAT file from i-Skyradiometer to find aerosols optical properties. First, it necessary to transforms raw DAT file to measured sky radiance file or DT4 file. In order to do that, it uses to use meteo.dat, ins.para and obs.para in the transform process. Meteo.dat contains the atmospheric pressure data. Ins.para contains wave lengths, solid view angles and calibration constants. And obs.para contains longitude, latitude, altitude and scattering angles of observation.

By the path of IMS, Improved multiple and single scattering, which is the radiative transfer scheme of main program, the DT4 file and tag file can generate par, vol, aur and phs files. Par file contain optical thickness, refractive index and ssa. Vol file present the volume spectrum. In side the aur and phs file are measured and retrieved sky radiance and phase function result respectively.

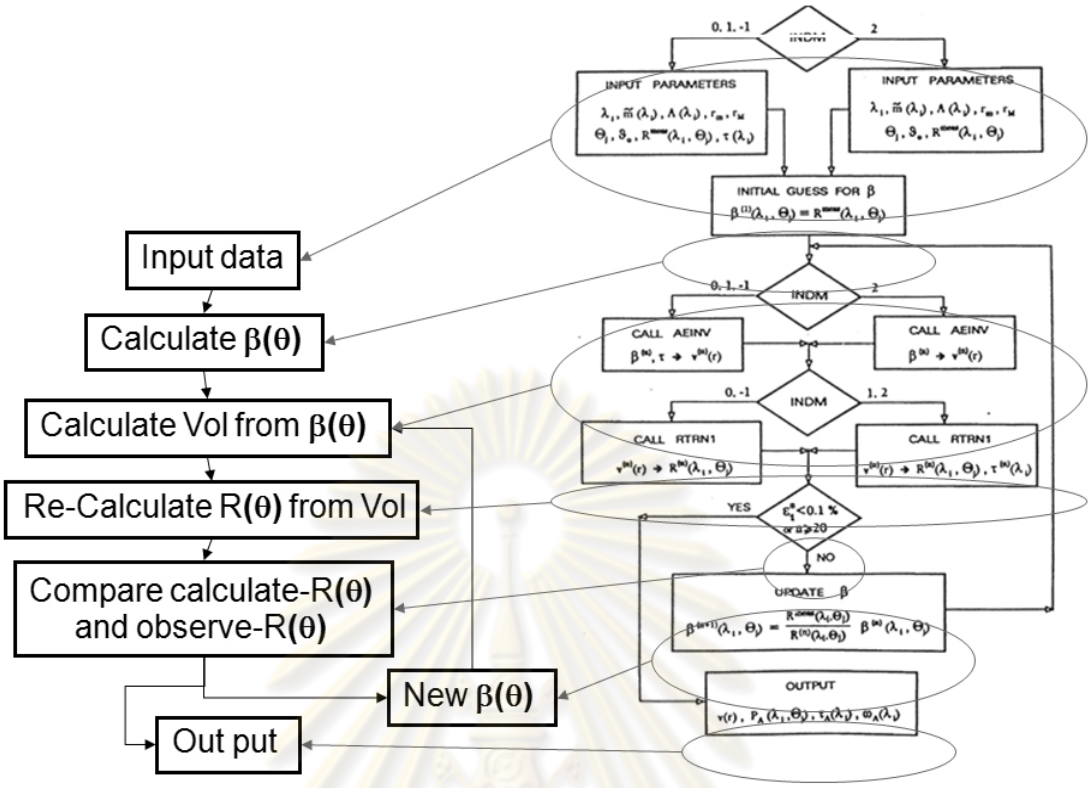

Figure 3.7 Flow chart of main program.

Part of the main program will calculate $\beta(\theta)$ from input data, which consist of DT4 file and some parameter files used before in the process to transforms the raw DAT file. From $\beta(\theta)$ value, Vol is calculated by the program, in subroutine AEINV. Then, it recalculate $R(\theta)$ from Vol value. After that, it will compare between $R(\theta)$ that come from calculate and observation. If the different can be accepted within error range, the outputs generate. Another case, recalculate new $\beta(\theta)$ occurs for re-run process, see figure 3.7.

Figure 3.8 shows the accuracy improvement of results from analysis process. All single precision of any parameter and variable was changed to double precision in the analysis program. The red line shows the result from example data, the dash blue line shows the result from single precision, the dot blue line shows the result from SGI supercomputer and the dash green line shows the result from double precision. In double precision, the result is very close to result from example and SGI super computer.

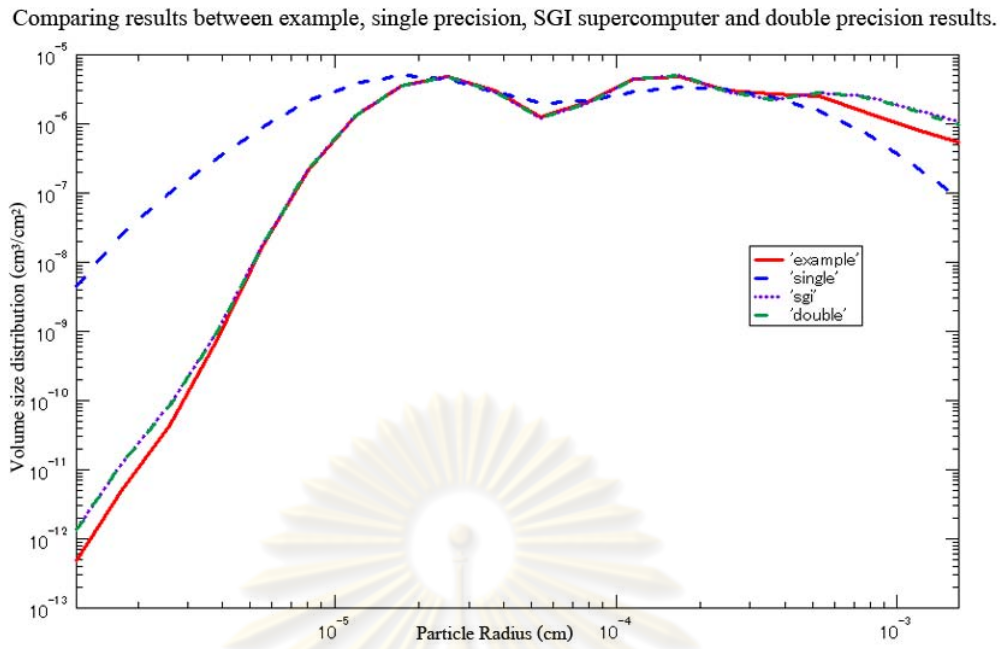

Figure 3.8 Comparing results between example, single precision, SGI supercomputer and double precision results. (Kikuchi, 2007)

3.3 Collecting Data

In this study, the data is collected by i-Skyradiometer, which was installed at observatory for atmospheric research at Phimai district, Nakhon Ratchasima province, North Eastern Thailand, as shown in figure 3.9.

Figure 3.9 Observatory for atmospheric research at Phimai.

The observatory for atmospheric research at Phimai is one of SKYNET observation sites in area of east Asia that shown in figure 3.10. SKYNET, Skyradiometer Network, focusing on long-term monitoring of aerosols and an assessment of aerosol impact on the climate system over East Asia (Kim and Sohn, 2005).

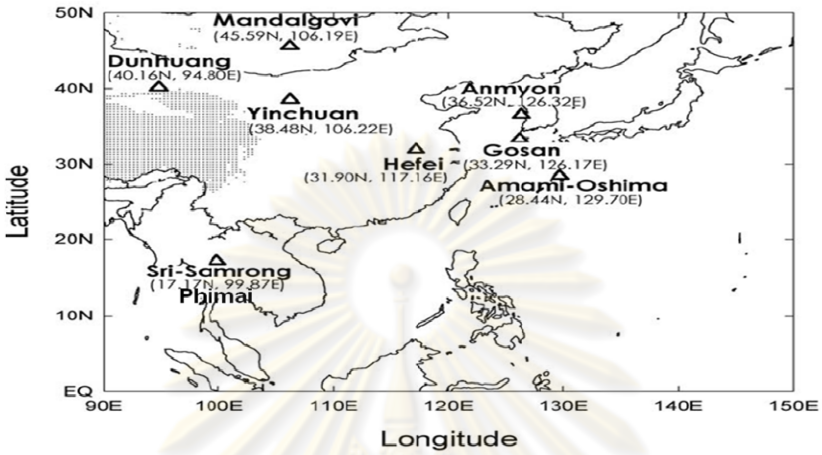

Figure 3.10 Observatory for atmospheric research in SKYNET including Phimai.

The study use data from 2006 to 2007 for 48 months. Most of the data are with complete data result, except for July and August 2008. The numbers of result files are not equal to the raw files because the program selects the input data to be process. Only correct data in range of observation criteria will be input. Table 3.2 show the number of raw files and result files on each month.

Table 3.2 The number of raw and result files obtained from The observatory for atmospheric research at Phimai in January 2006 to December 2007.

Year	2006		2007	
Month	RAW files	Result files	RAW files	Result files
January	31	30	31	31
February	28	27	28	28
March	28	18	31	30
April	29	10	30	29
May	31	21	30	18
June	30	15	30	21
July	17	5	31	19
August	18	1	30	12
September	25	13	30	15
October	18	16	24	11
November	30	30	28	23
December	31	30	31	29

3.4 Analysis Data

The results from the process come out in the raw files. Using excel, the data can be shown on graph and average for each day and month. These graph and average value made it easier to get trend, compare and explain the meaning of results. The results separate to 3 types. First is the graph of aerosols optical properties in month and year. Second is the graph of single scattering albedo in month and year. And finally is the graph of volume size distributions in month. In addition, we use trajectory and satellite photo to analyze the results for some period of time.

3.5 Compare and Investigate Data

The study is to compare and investigates data with other study. This study shows the different of the same of aerosols optical properties in other area, time and type of aerosols. Because of aerosols is a global scale effect, therefore the comparison is necessary.

CHAPTER IV
RESULTS AND DISCUSSION

There are few studies of aerosol properties in Thailand, so the activities of aerosol particles, dust or any powder, are not clear. For example, we didn't know about value of aerosol for each time of you. Size and scattering properties of aerosols are not recognized. In this study, we success in recognize all of the aerosol optical properties through the year 2006-2007.

4.1 Results

4.1.1 Aerosol optical properties in 2006

In 2006, the results are lost in many periods by analysis process and loss of raw data. Some results in April, June and August are cut off by screen correction in part of analysis. In August, the results are lost because it misses some raw data. All of the aerosol optical depth and single scattering albedo in 2006 is show in figure 4.1 and average value in figure 4.2.

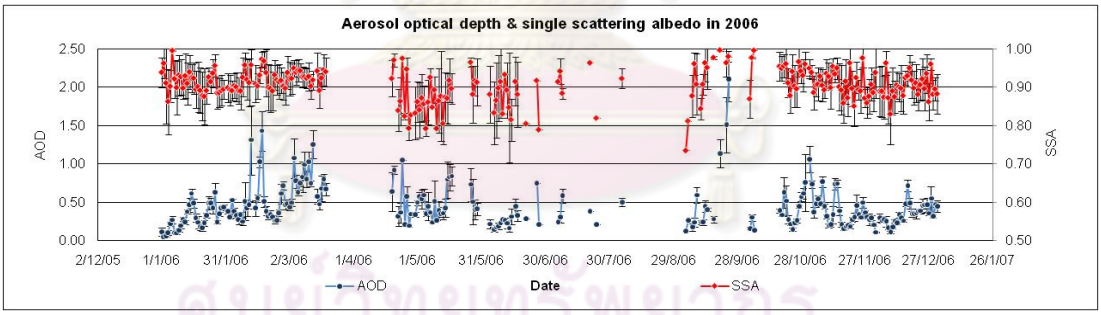

Figure 4.1 Aerosol optical depth and single scattering albedo in 2006.

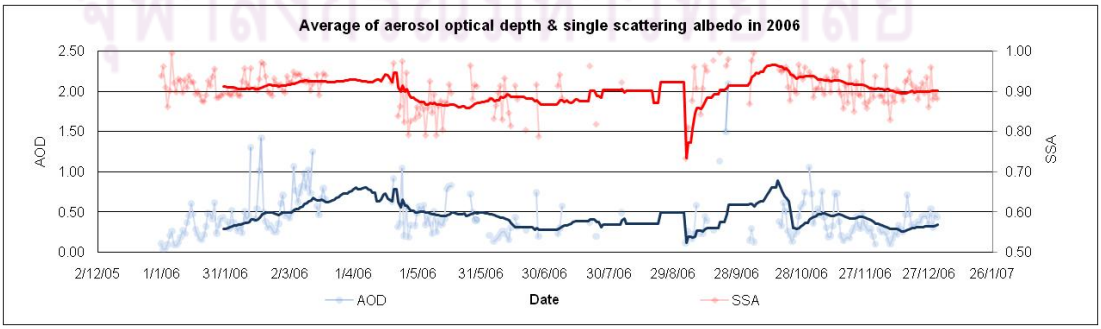

Figure 4.2 Average of aerosol optical depth and single scattering albedo in 2006.

It is clears that AOD and SSA value are very high in two periods, February to March and August to November. They are lower from May to July. The highest monthly average AOD is 0.75 in March and lowest is 0.28 in June. The highest average of SSA is 0.94 in October and lowest is 0.87 in May and June, as show in table 4.1. The point of highest AOD in this year is 2.10 on 24 September and the point of lowest is 0.05 on 2 January. In case of SSA, the point of highest is 1.00 on 20 September and lowest point is 0.73 on 4 September.

Table 4.1 Average in month of AOD and SSA in 2006.

Year	AOD		SSA	
Month	$\overline{X}$	SD	$\overline{X}$	SD
January	0.29	0.16	0.91	0.03
February	0.50	0.30	0.92	0.02
March	0.75	0.23	0.93	0.02
April	0.50	0.30	0.88	0.07
May	0.50	0.18	0.87	0.04
June	0.28	0.15	0.87	0.05
July	0.34	0.15	0.90	0.06
August	0.50	-	0.92	-
September	0.60	0.61	0.91	0.08
October	0.37	0.19	0.94	0.04
November	0.41	0.22	0.91	0.03
December	0.34	0.14	0.90	0.03

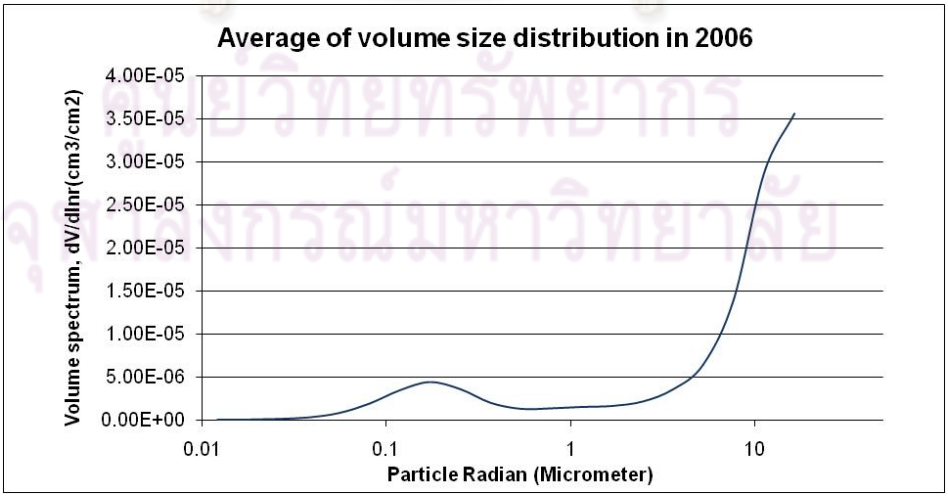

Figure 4.3 Average of volume size distributions in 2006.

In average of volume size distributions, as show in figure 4.3, for 2006, it was found that the size of aerosol particle in coarse mode is larger than 16.54 micrometer and the size of aerosol particle in fine mode is around 0.17 micrometer.

In winter season, as shown in figure 4.4, the aerosol particle is very high both in fine and coarse mode. This season has aerosol particle in fine mode more than other seasons. The aerosol particle in the summer time is very high in coarse mode like the winter time. But it has a less fine mode particle, as shown in figure 4.5.

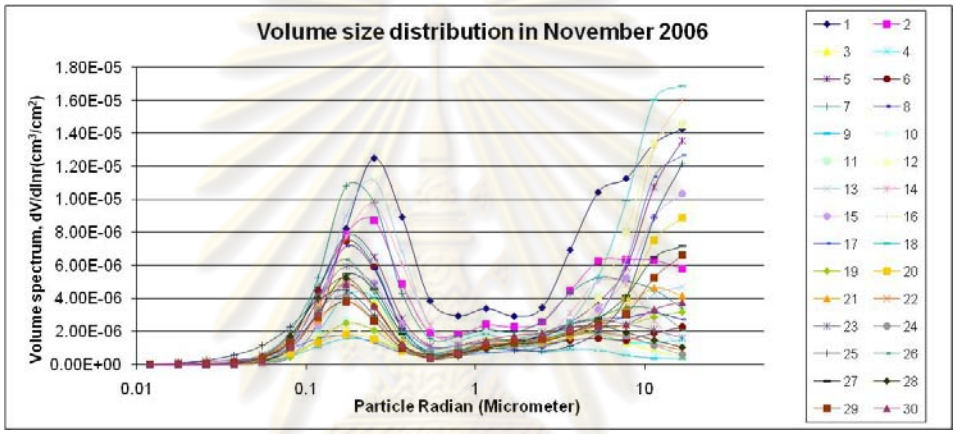

Figure 4.4 Volume size distributions in November 2006.

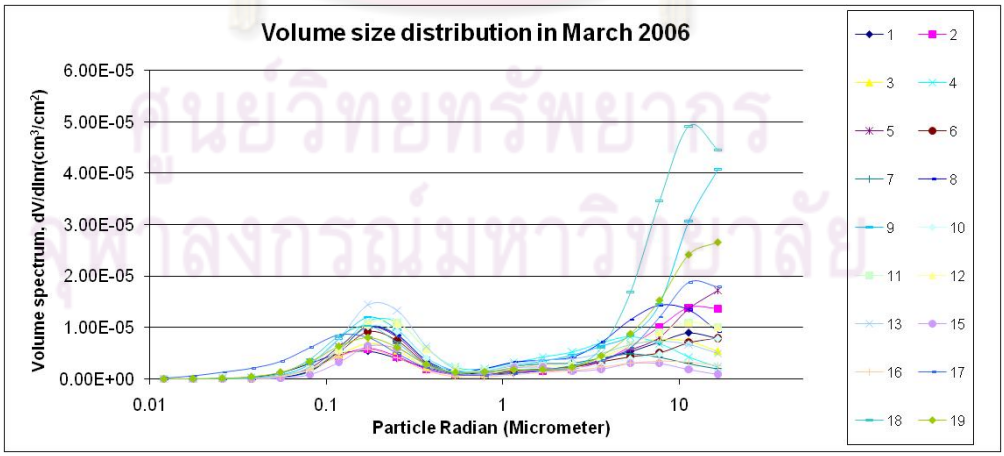

Figure 4.5 Volume size distributions in March 2006.

In rainy season, amount of aerosol particle in fine mode is opposite to the winter time. It has lesser fine mode particles but higher coarse mode particle than other season. As shown in figure 4.6.

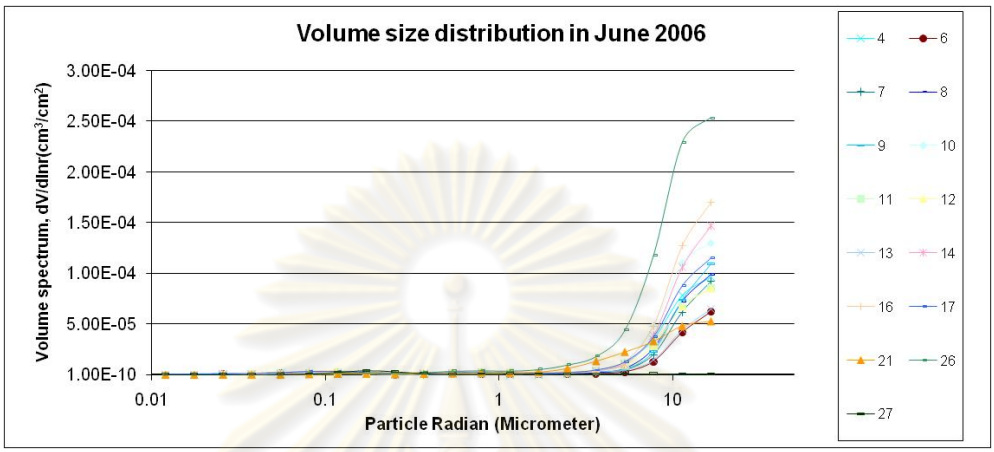

Figure 4.6 Volume size distributions in June 2006.

4.1.2 Aerosol optical properties in 2007

In 2007, the same as 2006, the results are lost in many periods by screening of program and it lost of raw data too. Some results in July, August, September and some part of October are cut off by correction part of analysis process. In some part of October, the results are lost because of the missing of raw data. All of aerosol optical depth and single scattering albedo in 2007 are shown in figure 4.7 and average value in figure 4.8.

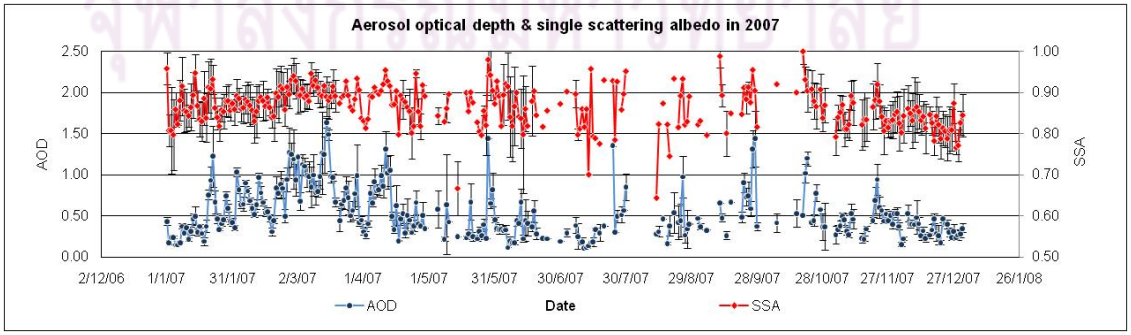

Figure 4.7 Aerosol optical depth and single scattering albedo in 2007.

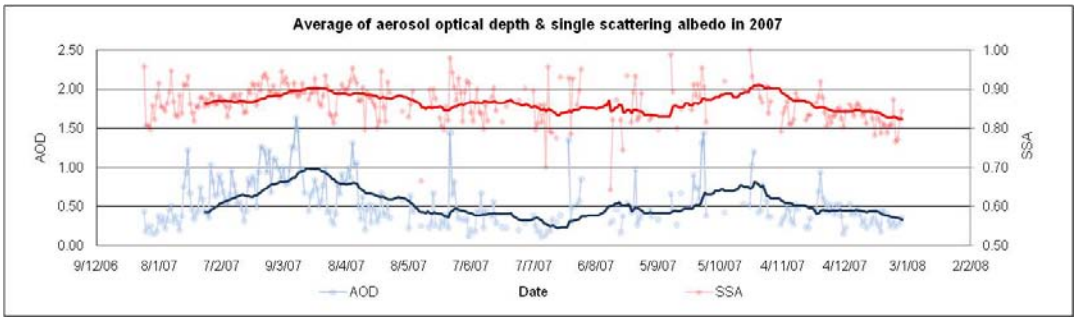

Figure 4.8 Average of aerosol optical depth and single scattering albedo in 2007.

Same as 2006, it is clears that AOD and SSA value are very high in two periods, February to March and August to November. They are lower in May to July. The highest monthly average of AOD is 0.89 in March and lowest is 0.32 in June. The highest of average SSA is 0.90 in March and October. The lowest of average SSA is 0.83 in December, as shown in table 4.2. The point of highest AOD in this year is 1.63 on 15 March and the point of lowest is 0.11 on 11 July. In case of SSA, the point of highest is 1.00 on 19 October and lowest point is 0.64 on 11 August.

Table 4.2 Average in month of AOD and SSA in 2007.

Year	AOD		SSA	
Month	$\bar{X}$	SD	$\bar{X}$	SD
January	0.42	0.24	0.87	0.04
February	0.74	0.25	0.88	0.03
March	0.89	0.30	0.90	0.02
April	0.59	0.28	0.88	0.04
May	0.46	0.31	0.86	0.07
June	0.32	0.14	0.86	0.04
July	0.38	0.30	0.85	0.07
August	0.42	0.20	0.84	0.08
September	0.65	0.34	0.87	0.06
October	0.60	0.28	0.90	0.04
November	0.45	0.16	0.84	0.03
December	0.34	0.10	0.83	0.03

For volume size distributions in 2007, it was found that the size of aerosol particle is in coarse mode is larger than 16.54 micrometer and the size of aerosol particle in fine mode is around 0.17 micrometer.

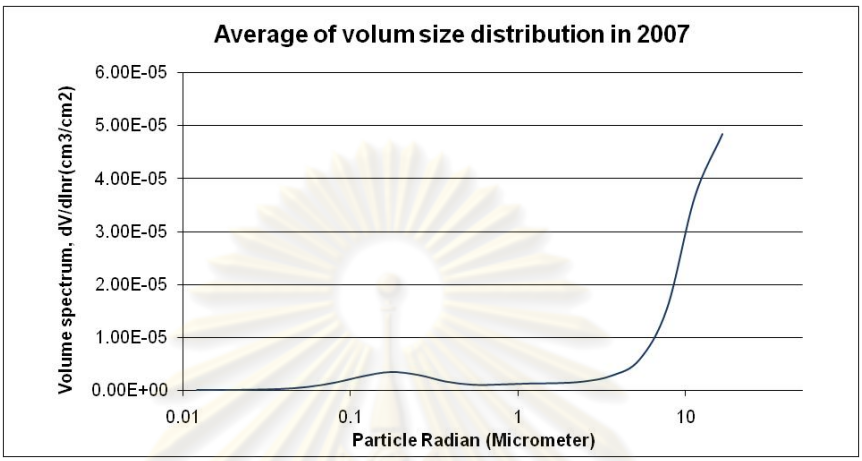

Figure 4.9 Average of volume size distributions in 2007.

In winter season, as shown in figure 4.10, the aerosol particle is very high in both of fine and coarse mode just like 2007. This season has aerosol particle in fine mode more than other seasons. When pass through summer season the aerosol particle decrease in fine mode particle, as shown in figure 4.11. Like the winter season, the aerosol particle in the summer time is very high in coarse mode.

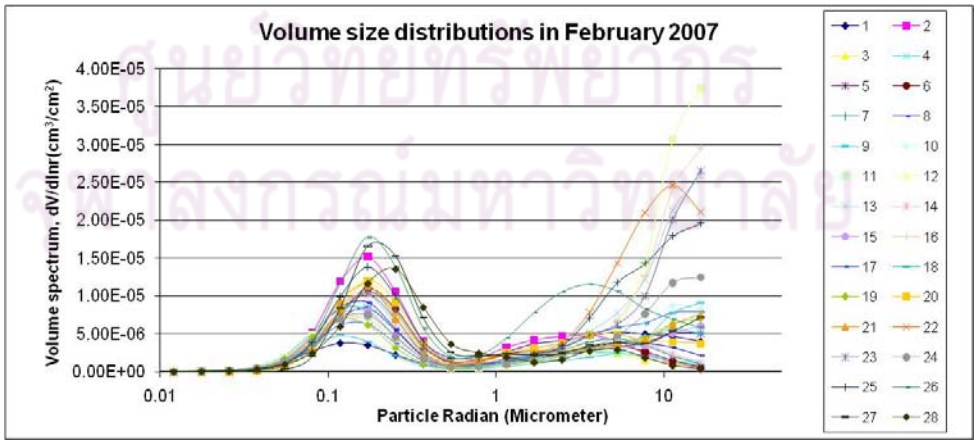

Figure 4.10 Volume size distributions in February 2007.

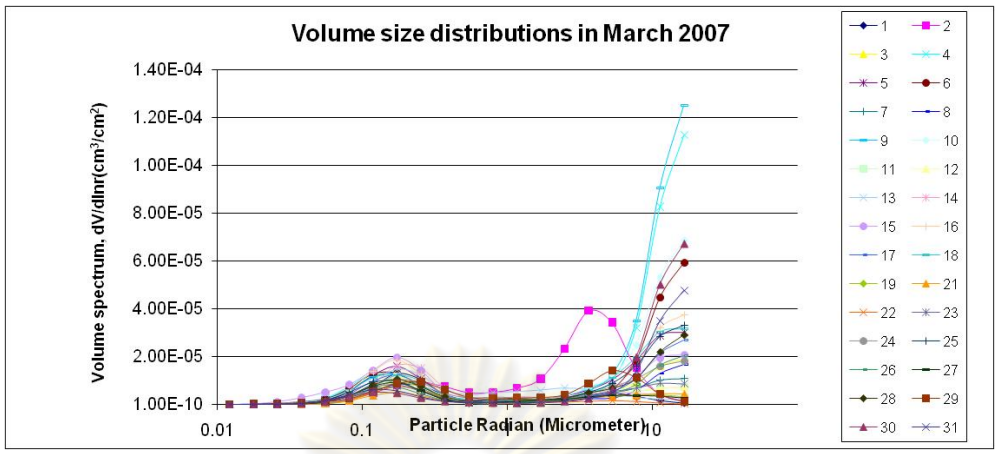

Figure 4.11 Volume size distributions in March 2007.

In rainy season, almost all of the result is very low of aerosol particle in fine mode. It has lesser fine mode particles but the higher coarse mode particles than other season, as shown in figure 4.12.

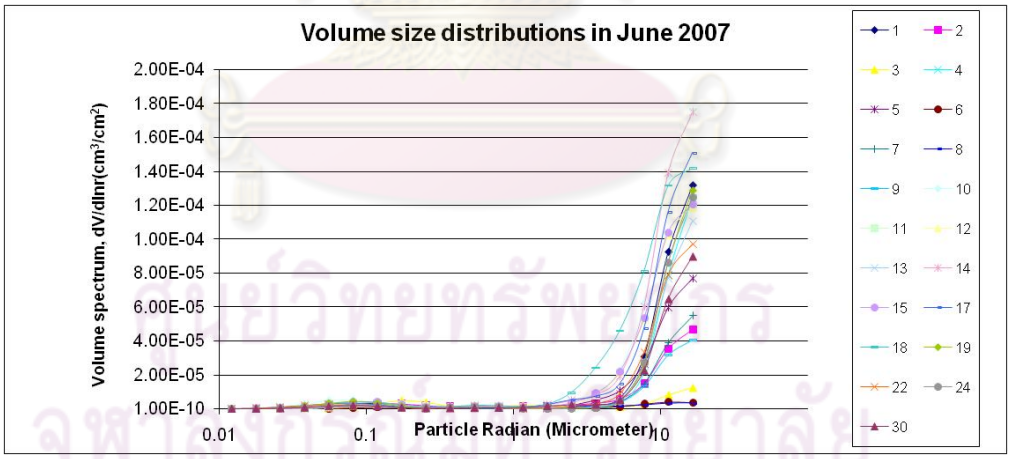

Figure 4.12 Volume size distributions in June 2007.

4.2 Discussion

The discussion will be on data in all of day, month, seasonal and year results. In case of results on some day when it high of aerosol particles, it is very interest to find the kind and source of aerosol particles that contaminate these area of Thailand. So we have to discuss the results in month, seasonal and year period to find the pattern of aerosol optical properties all over the year.

For the monthly average results in 2006 and 2007, the monthly average of aerosol optical depth in 2007 is higher than in 2006. It is clear that the pattern of aerosol particles density over the study area is high in two periods, around March and September, and lower is also in two periods, June and December, as shown in figure 4.13.

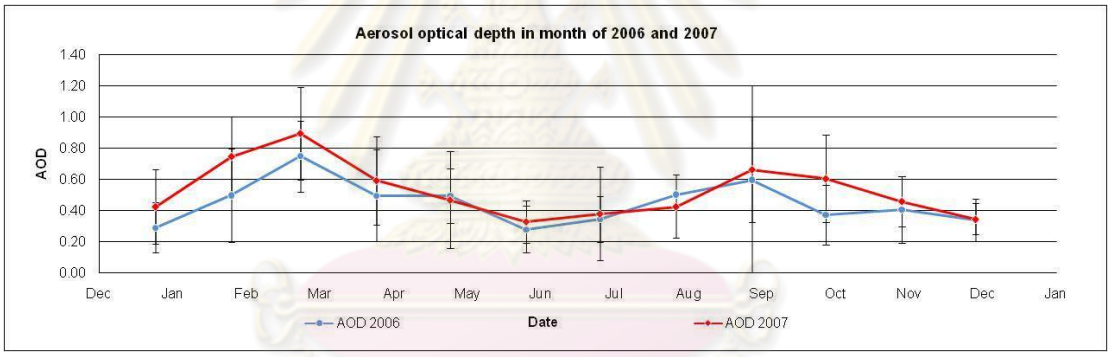

Figure 4.13 Aerosol optical depths in month of 2006 and 2007.

Single scattering albedo between 2006 and 2007 are shown in figure 4.14. In March and October, it is very high and represents non-absorbing aerosols. In April, May, June and December the aerosol particles are the absorbing aerosols. The difference between 2006 and 2007 is in July and August. In July and August 2006, single scattering albedo is increased from June to July and August but it appears to be decrease in 2007. The collective results present that the singles scattering albedo value in 2006 is higher than 2007.

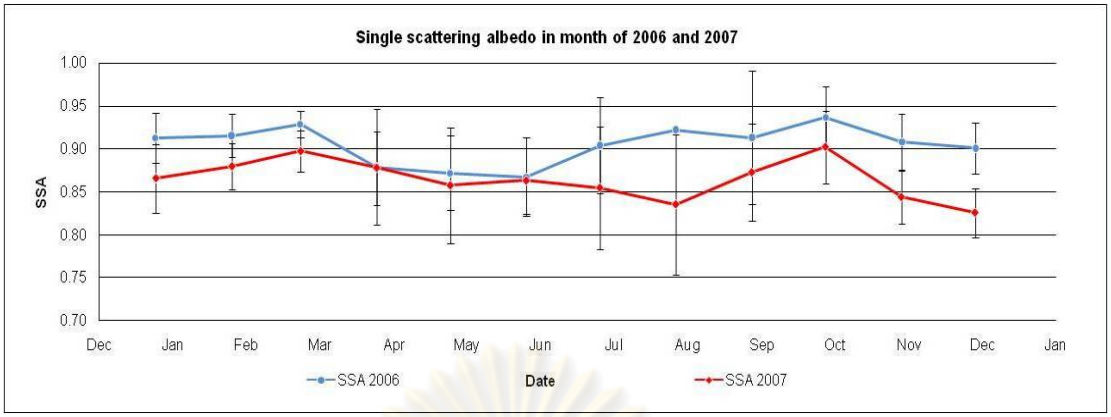

Figure 4.14 Single scattering albedo in month of 2006 and 2007.

We compare between aerosols optical depth and single scattering albedo of the two years, 2006 - 2007. They have some direct relations when aerosol optical depth is high, single scattering albedo is also high, as shown in 4.15. The aerosol particles that contaminate in study area come from same specific type, because the results of the aerosol particles in the study area have the same a pattern both in quantity and quality. Each property varies with time.

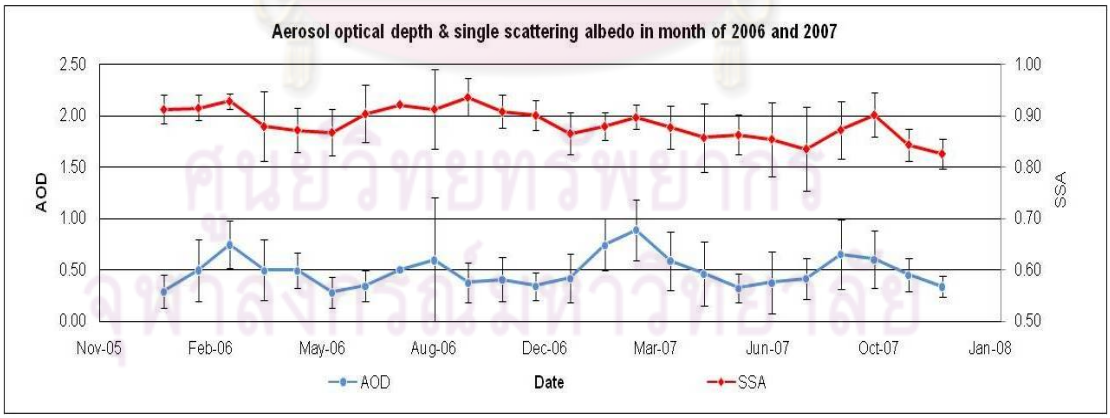

Figure 4.15 Aerosol optical depth & single scattering albedo in month of 2006 and 2007.

The frequency distribution of aerosols optical depth in 2006 and 2007 are shown in figure 4.16. The majority of aerosols optical depth is from 0.2-0.3, 22.22% in 2006 and 0.3-0.4, 21.30% in 2007. Aerosol particle, in 2007 are higher than in 2006.

In case of seasonal, figure 4.17, the high frequency of aerosols optical depth in summer is 0.3-0.4, rainy season is 0.2-0.3 and winter is 0.3-0.4. In summer and winter, area of study have higher aerosol particle than in rainy season.

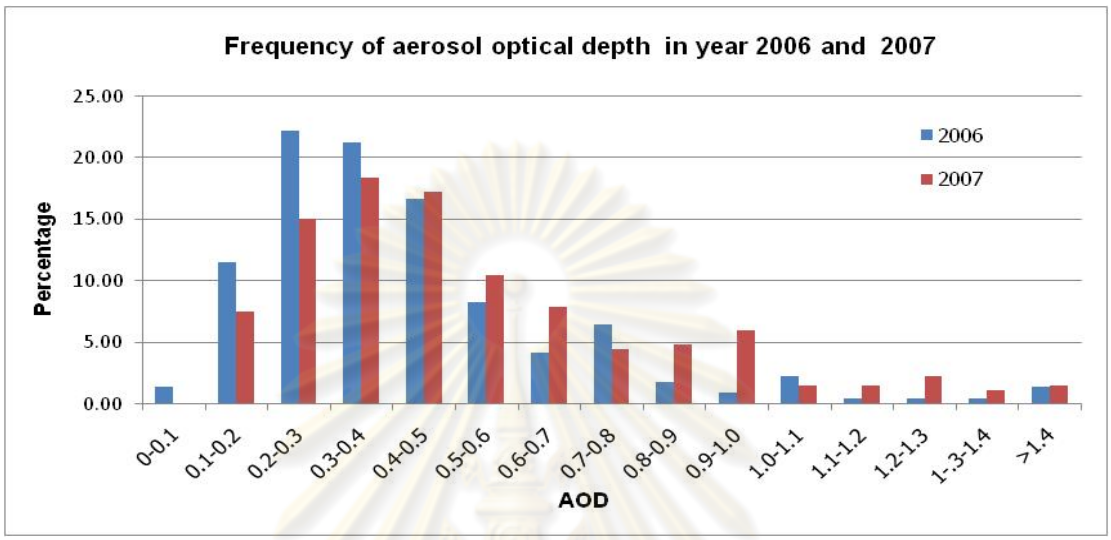

Figure 4.16 Frequency of aerosol optical depth in 2006 and 2007.

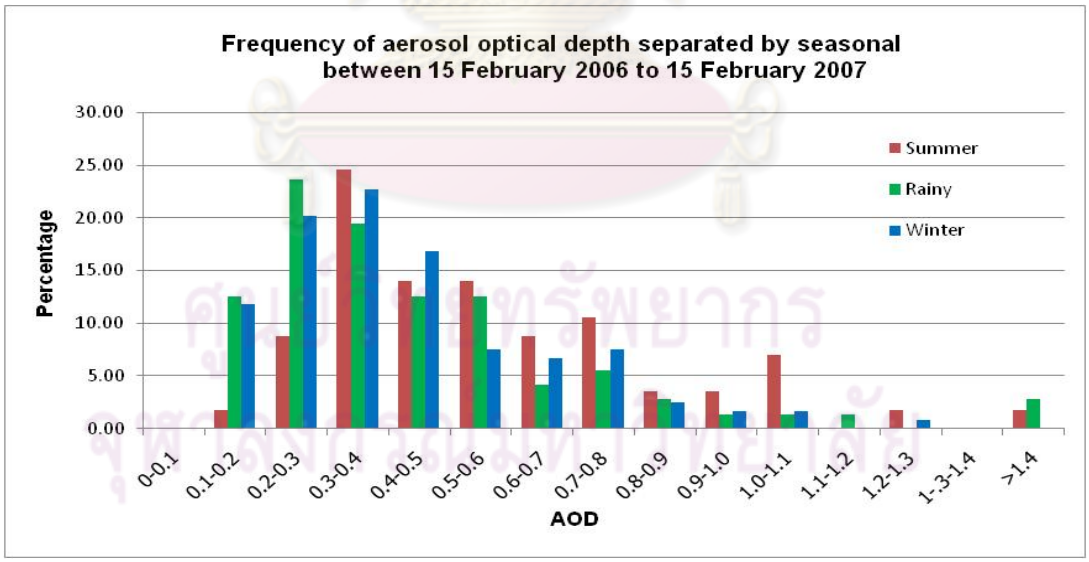

Figure 4.17 Frequency of aerosol optical depth separated by seasonal.

The single scattering albedo in year 2006, figure 6(a), is mostly in 0.90-0.95, 42.13%, and 0.85-0.90, 40.60%, in year 2007. The aerosol particle in year 2007 is absorbing radiation more than year 2006. When comparing in seasonal, figure 6(b), most of single scattering albedo value is 0.85-0.90, 51.26%, in winter, 0.85-0.90, 29.17%, in rainy season, and 0.90-0.95, 49.12% in summer. In rainy season, there are varieties of aerosol type. In winter the absorbing aerosols particle is dominated.

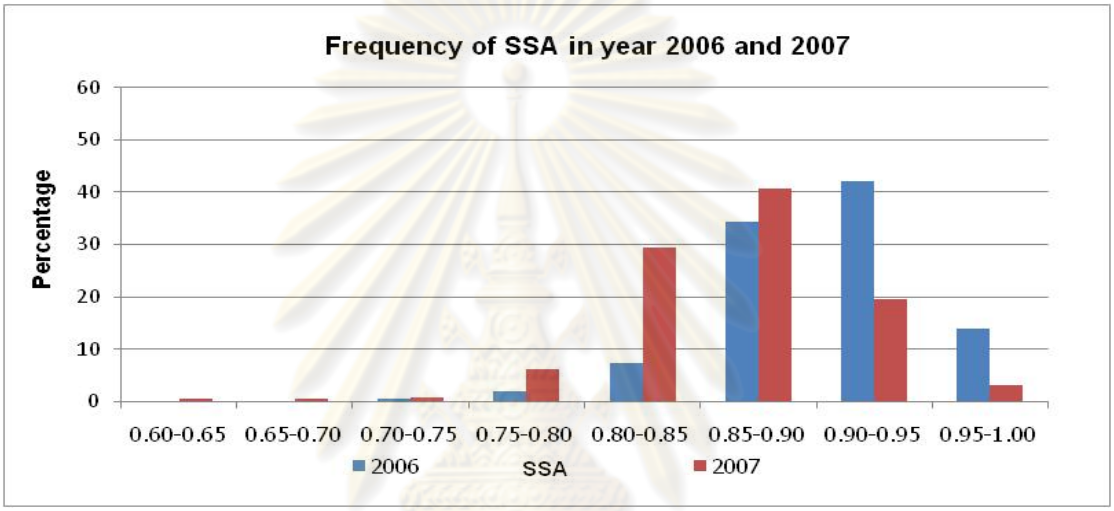

Figure 4.18 Frequency of SSA in 2006 and 2007.

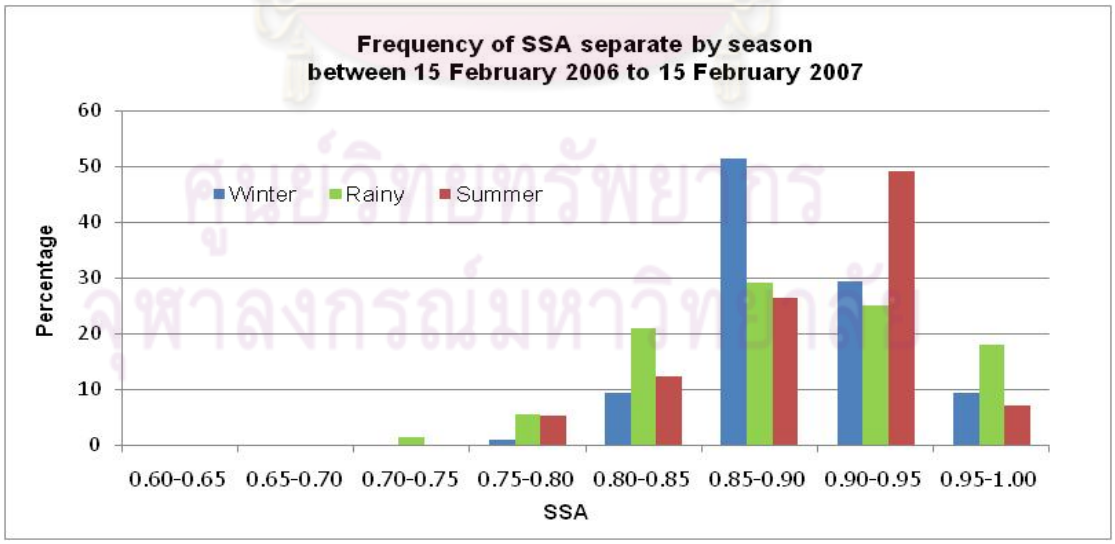

Figure 4.19 Frequency of SSA separate by season between 15 February 2006 to 15 February 2007.

The average of volume size distribution between 2 years is the same. The pattern of size of particle along 2 year is not change, see figure 4.20. The fine mode particles of two years are around 0.1729 micrometer and coarse mode is in 16.54 or greater. By seasons the volume size distribution is different. In summer the volume size is more in coarse mode than in fine mode. In rainy season the particle size is more in coarse mode and none in fine mode. In winter the fine mode particle raised and the coarse modes decline as shown in figure 4.21.

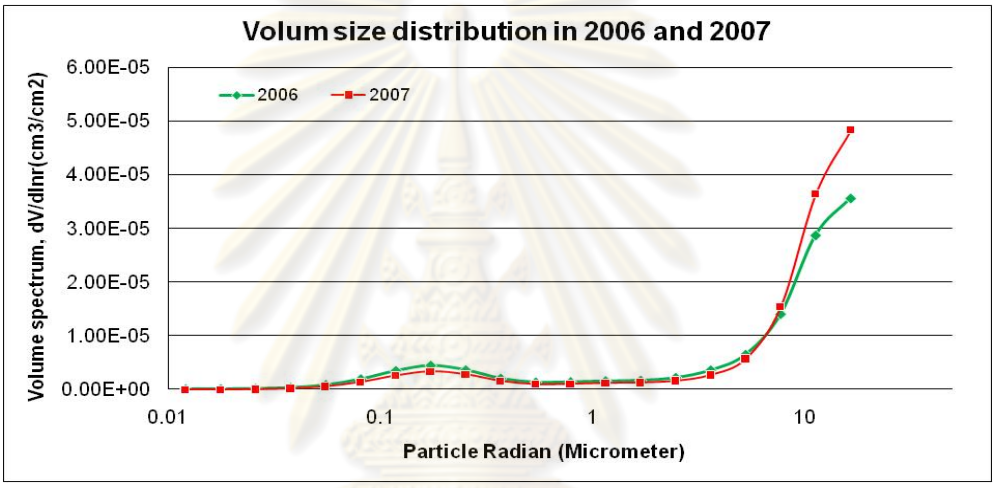

Figure 4.20 Volume size distributions in 2006 and 2007.

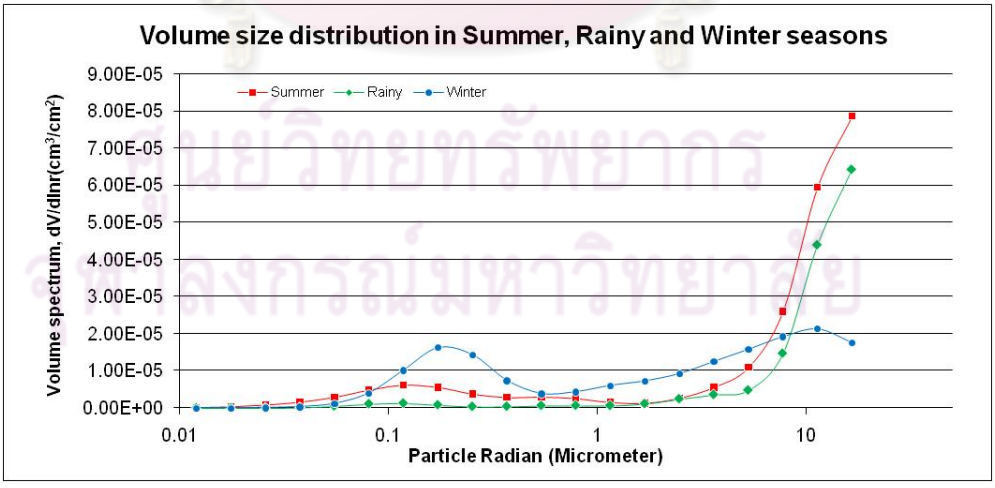

Figure 4.21 Volume size distributions in summer, rainy and winter seasons.

The high aerosol optical depth means that the study area is contaminated by a lot of aerosol particles. From single scattering albedo and back ward trajectories, we can find the kind of aerosol (absorbing or non-absorbing) and source of particles.

In winter the maximum aerosol optical depth is in 12 February 2006, figure 4.22, we found that aerosol particles came from north east of Thailand, figure 4.23, in China. The aerosol particle has both fine and coarse modes particles, see figure 4.24. From single scattering albedo, the aerosol particles are non-absorbing aerosol.

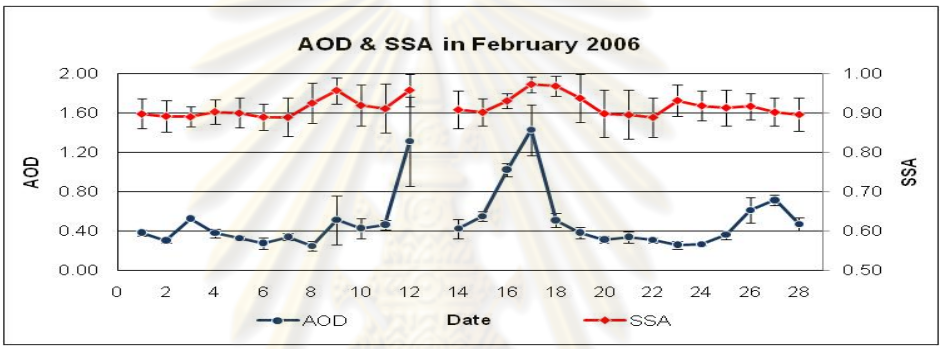

Figure 4.22 AOD & SSA in February 2006.

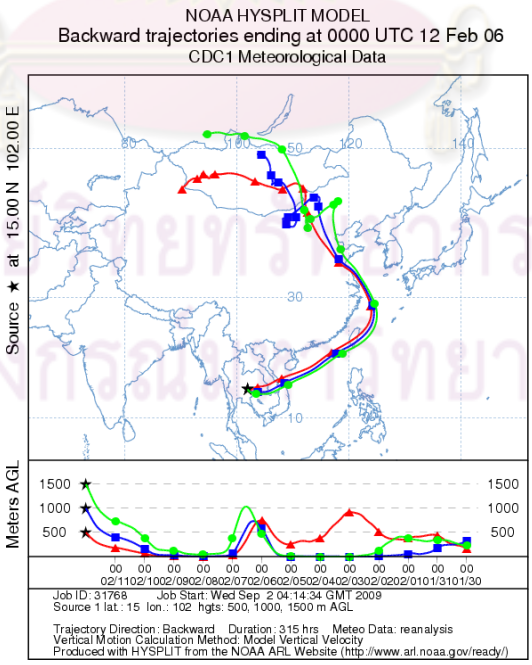

Figure 4.23 Backward trajectories on 12 February 2006.

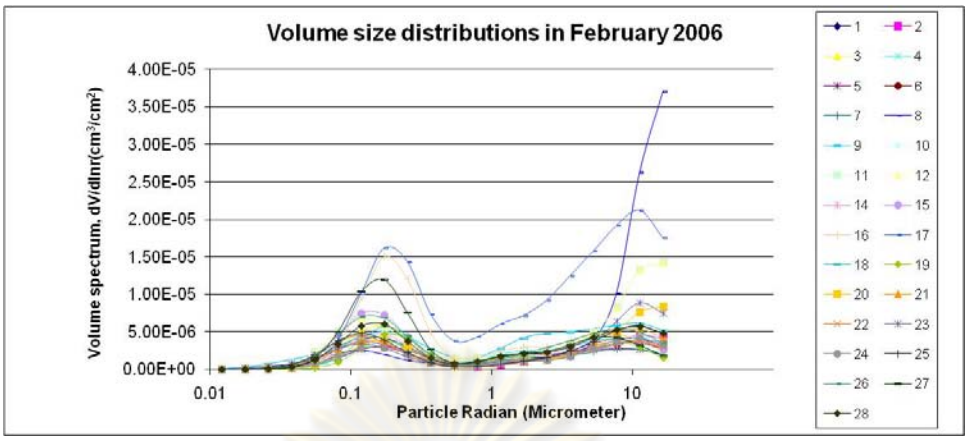

Figure 4.24 Volume size distributions in February 2007.

In summer, on 24 April 2006, the particle of higher aerosol optical depth came from east of Thailand, see figure 4.25 and figure 4.26. The sizes of particles are coarse mode, figure 4.27, and non-absorbing aerosols.

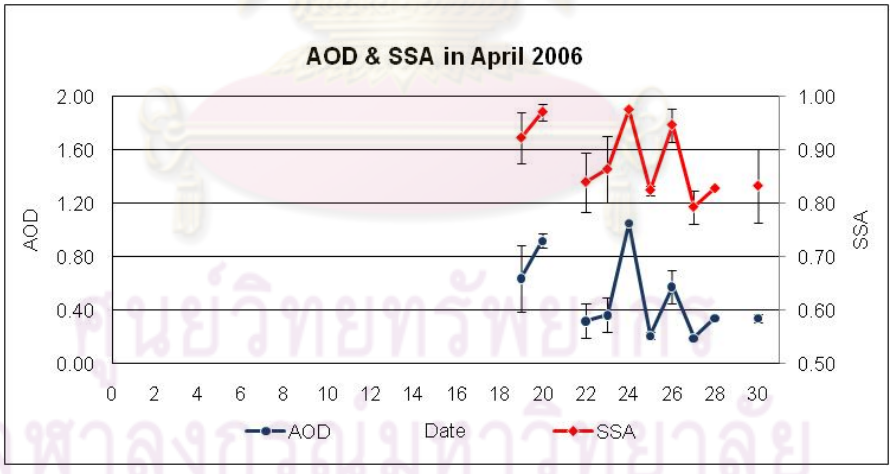

Figure 4.25 AOD & SSA in April 2006.

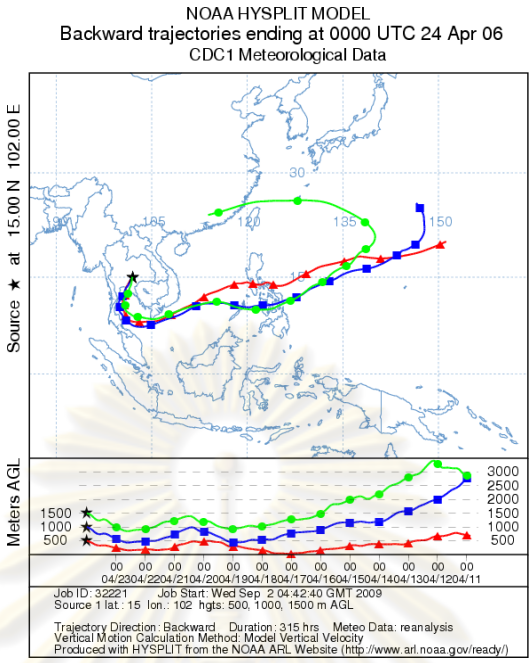

Figure 4.26 Backward trajectories on 24 April 2006.

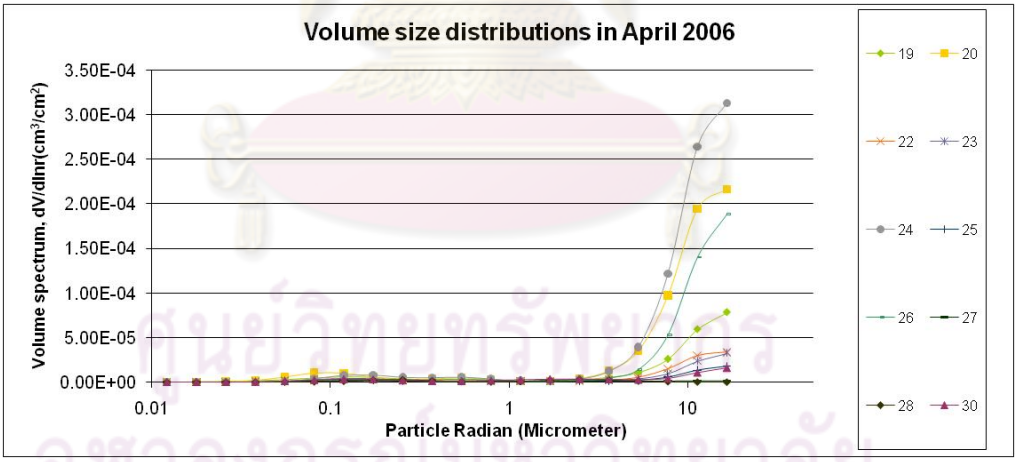

Figure 4.27 Volume size distributions in April 2006.

In rainy season, on 26 June 2006 in figure 4.28, the particle of higher aerosols optical depth came from south west of Thailand, figure 4.29. The size of particles is in coarse mode, figure 4.30, and the kind of particles is non-absorbing aerosol.

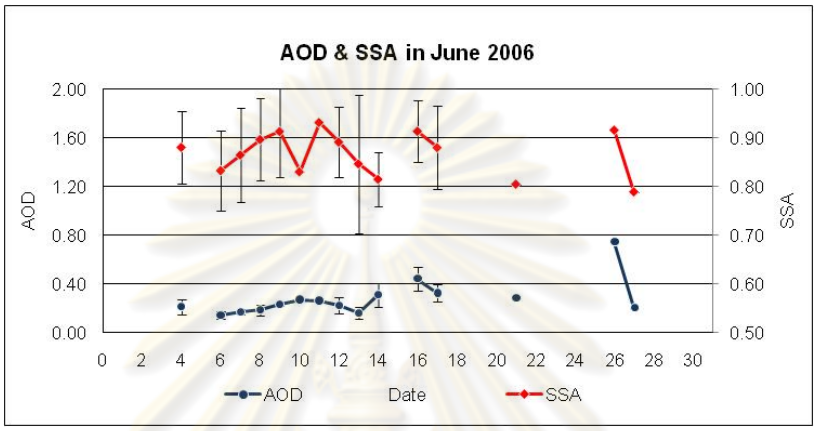

Figure 4.28 AOD & SSA in June 2006.

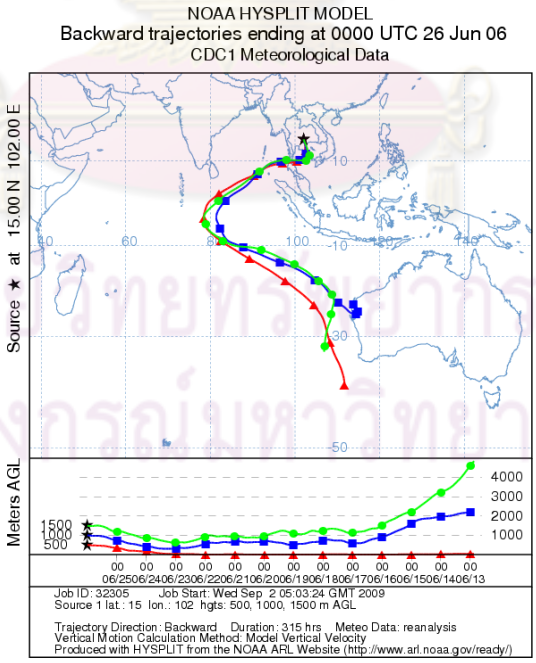

Figure 4.29 Backward trajectories on 26 June 2006.

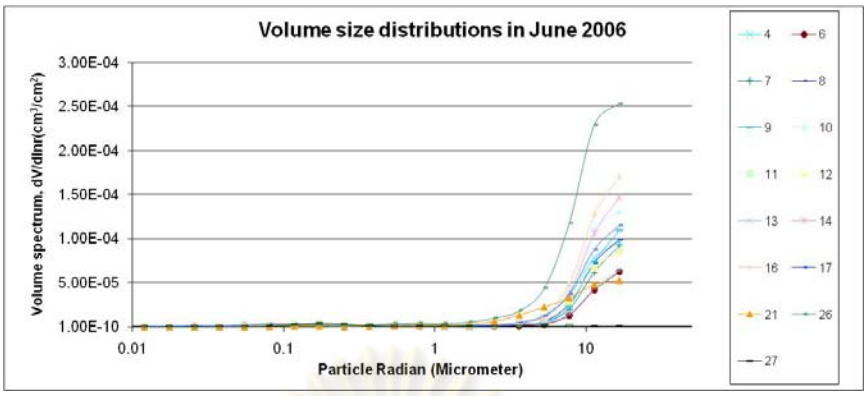

Figure 4.30 Volume size distributions in June 2006

In November 2006, on 1, 7, 18 and 22 we can see the different between source and size of aerosol particles. On November 1, aerosol optical depth is very high, figure 4.31. The particles came from around north and far of west side of Thailand, figure 4.32. It has both of coarse mode and fine mode particles, figure 4.36. It is different from 7 November that it has high value of aerosol particle too but the aerosol in coarse mode particle decreases a lot. From back ward trajectories on 7 November, figure 4.33, most of particle came from far area of west side of Thailand.

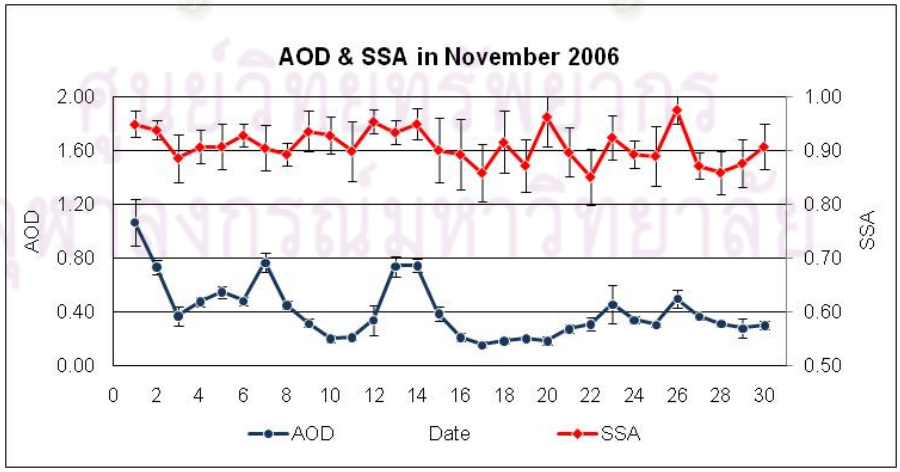

Figure 4.31 AOD & SSA in November 2006.

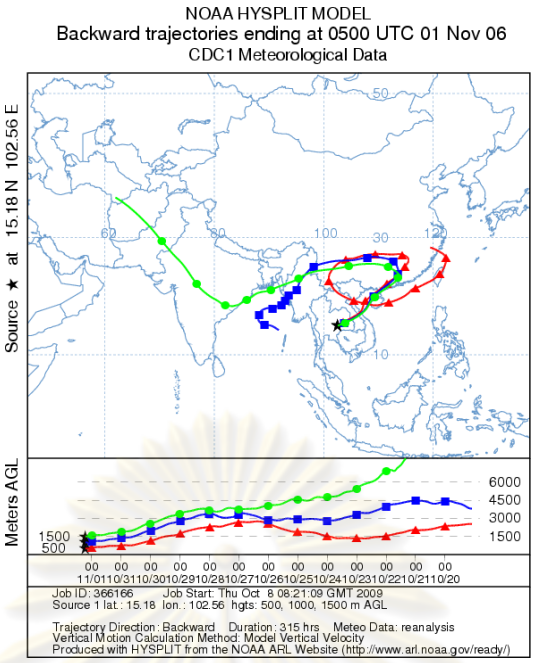

Figure 4.32 Backward trajectories on 1 November 2006.

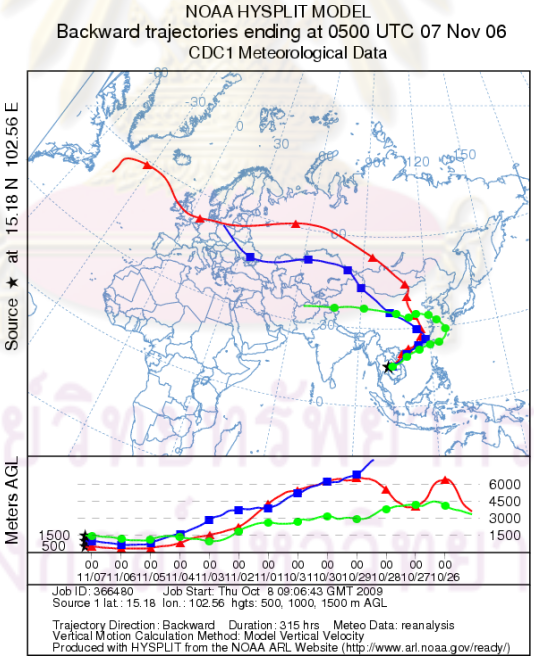

Figure 4.33 Backward trajectories on 7 November 2006.

On 18 and 22 November the trajectories of aerosol particles change from west to east, figure 4.34 and 4.35. On 18 November, size of particles is mainly coarse mode particles, figure 4.36. The back ward trajectories show that the source of aerosol particle is in the ocean. On 22 November, size of particle is mainly fine mode particles. The back ward trajectories show that the source of aerosol particle came from north east of Thailand, in continental.

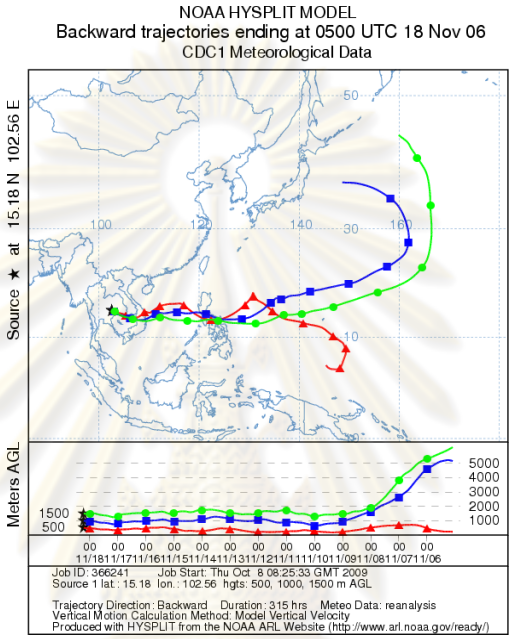

Figure 4.34 Backward trajectories on 18 November 2006.

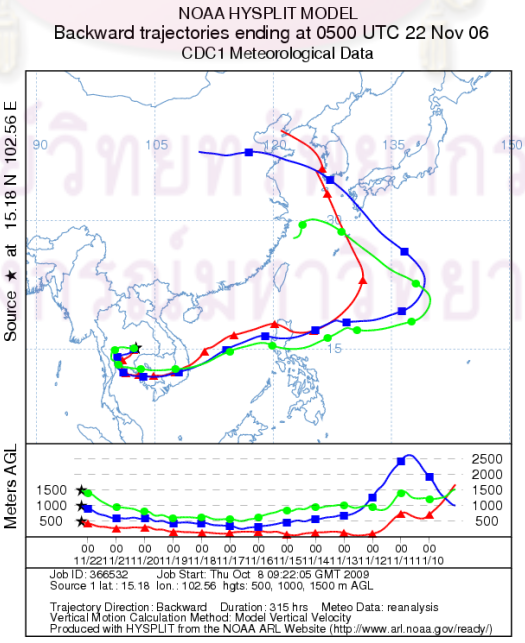

Figure 4.35 Backward trajectories on 22 November 2006.

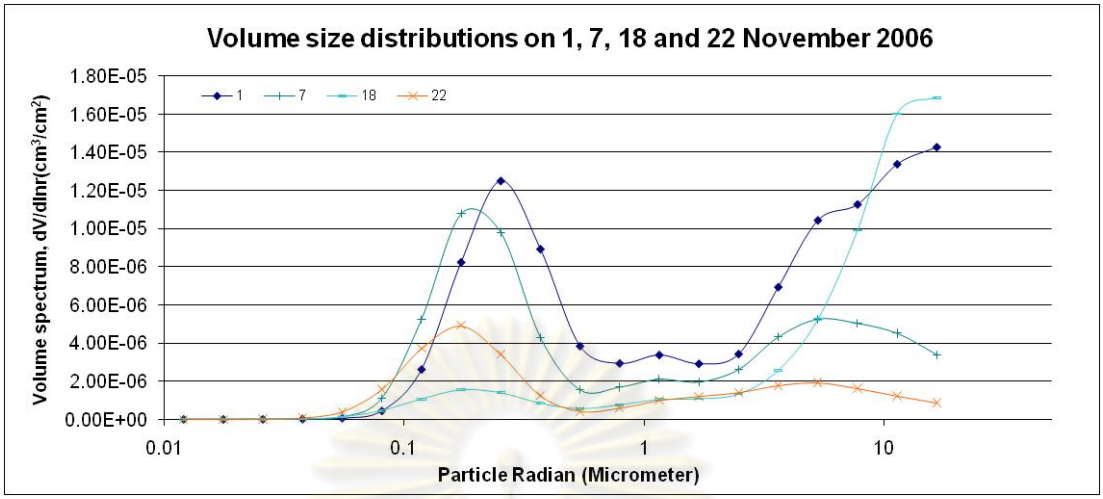

Figure 4.36 Volume size distributions on 1, 7, 18 and 22 November 2006.

In February 2007, figure 4.37, the aerosol particles of high of aerosol optical depth on day 12 came from north east of Thailand, figure 4.38. The size of particle has both of fine mode and coarse mode particles, figure 4.39. The kind of particle is absorbing aerosol.

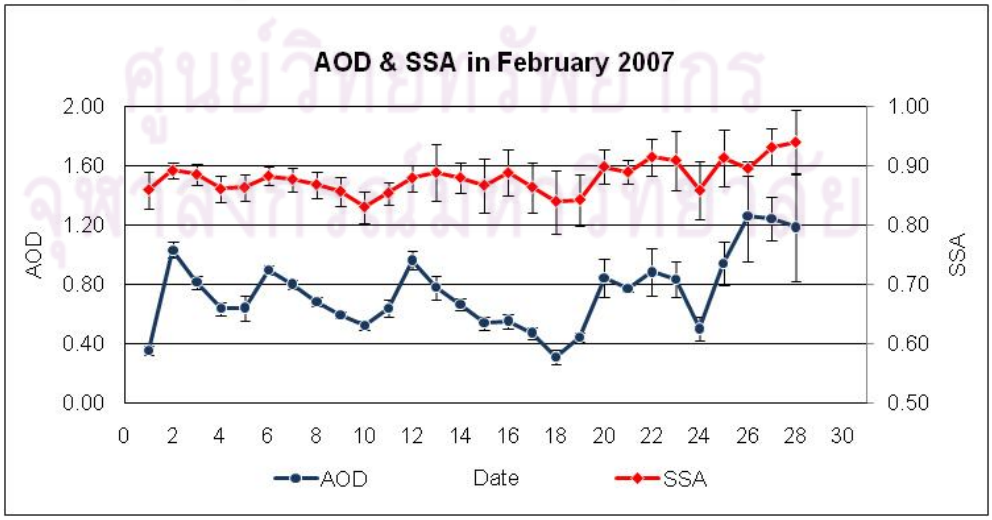

Figure 4.37 AOD & SSA in February 2007.

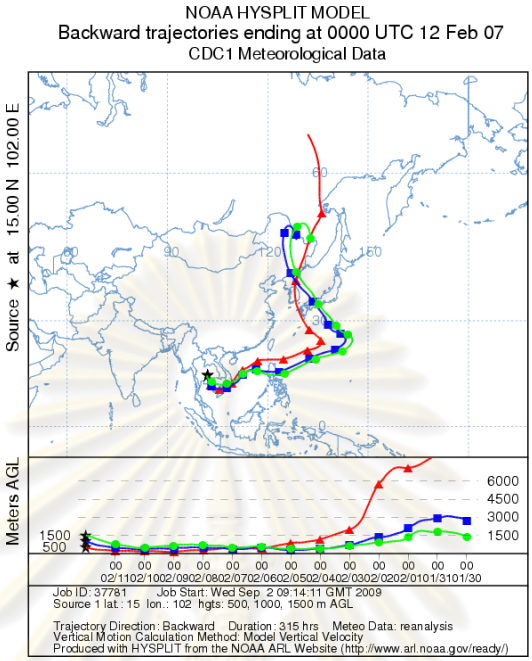

Figure 4.38 Backward trajectories on 12 February 2007.

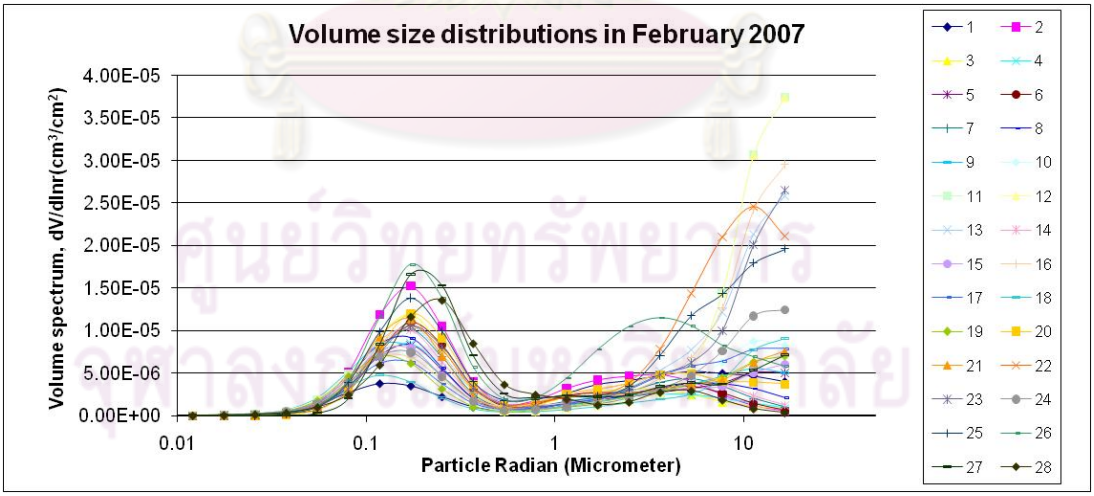

Figure 4.39 Volume size distributions in February 2007.

On 28 May 2007, figure 4.40, the aerosol particles that causing the high aerosol optical depth came from south west of Thailand, figure 4.41, in the ocean. The size of particle is completely in coarse mode, figure 4.42. The kind of aerosol particle is non-absorbing particle.

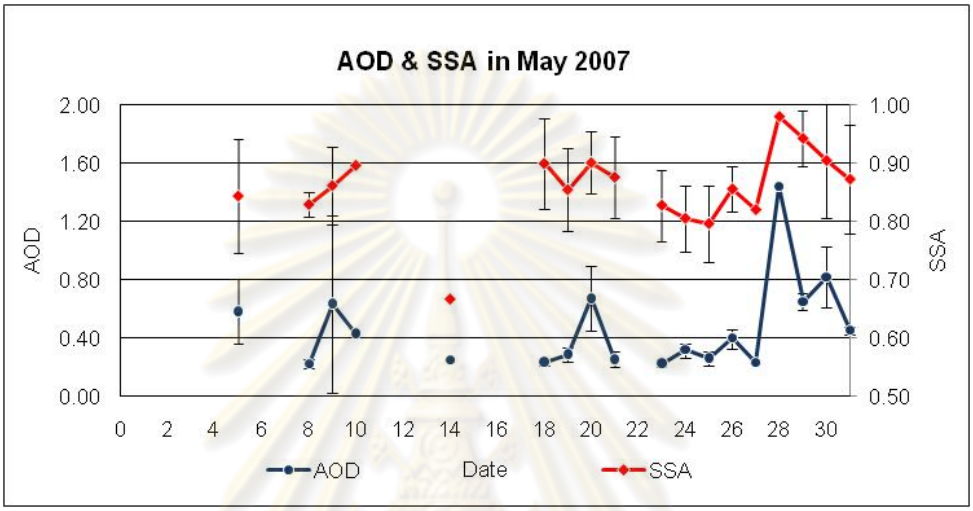

Figure 4.40 AOD & SSA in May 2007.

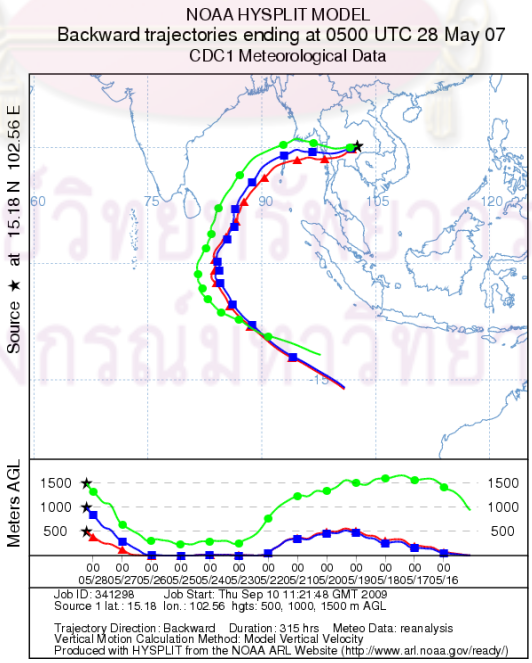

Figure 4.41 Backward trajectories on 28 May 2007.

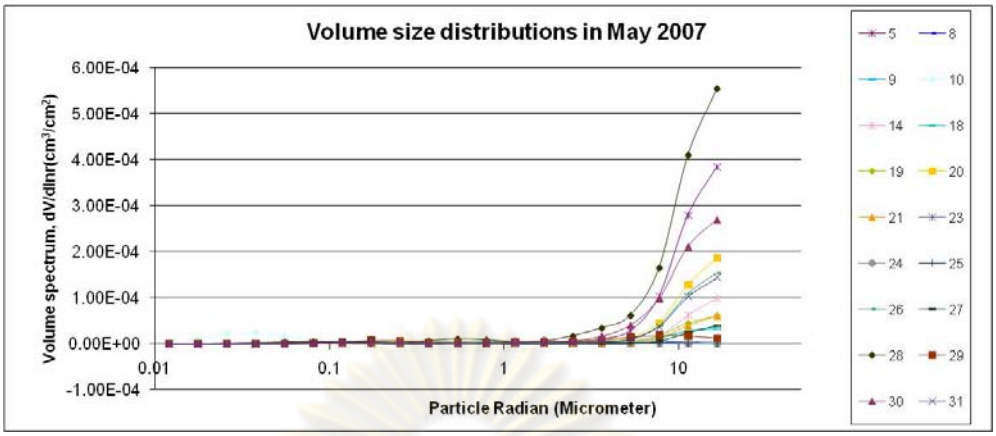

Figure 4.42 Volume size distributions in May 2007.

The area study on 22 November 2007, figure 4.43, is contaminated by aerosol particles from north east near Thailand, figure 4.44. The kind of aerosol particles is non-absorbing aerosol and size of it is mainly in coarse mode particles, figure 4.45.

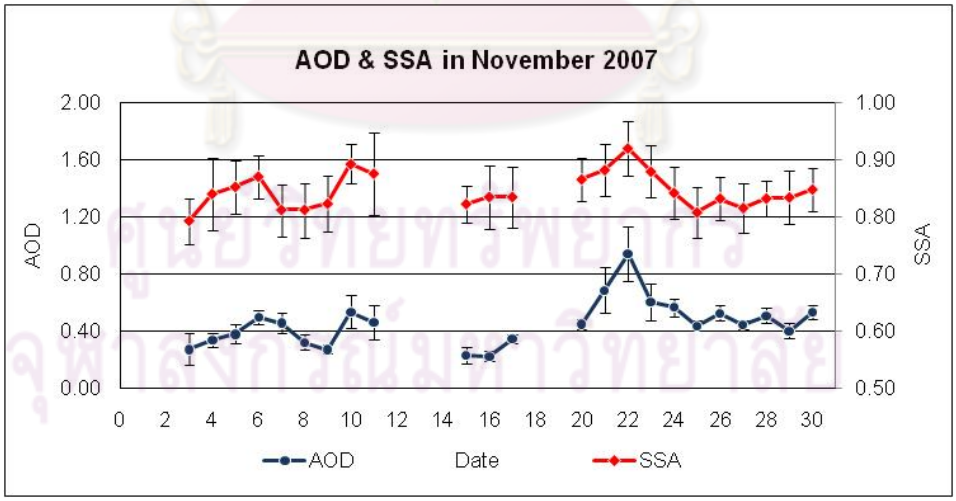

Figure 4.43 AOD & SSA in November 2007.

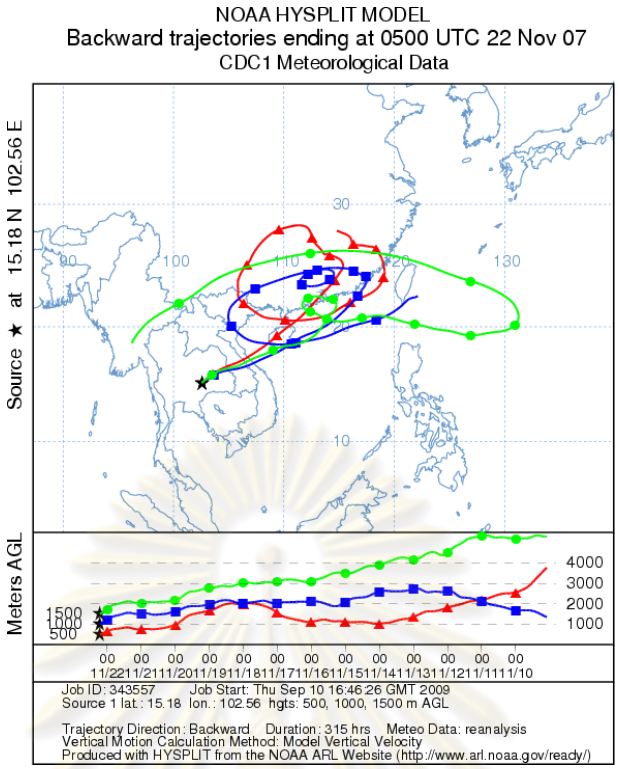

Figure 4.44 Backward trajectories on 22 November 2007.

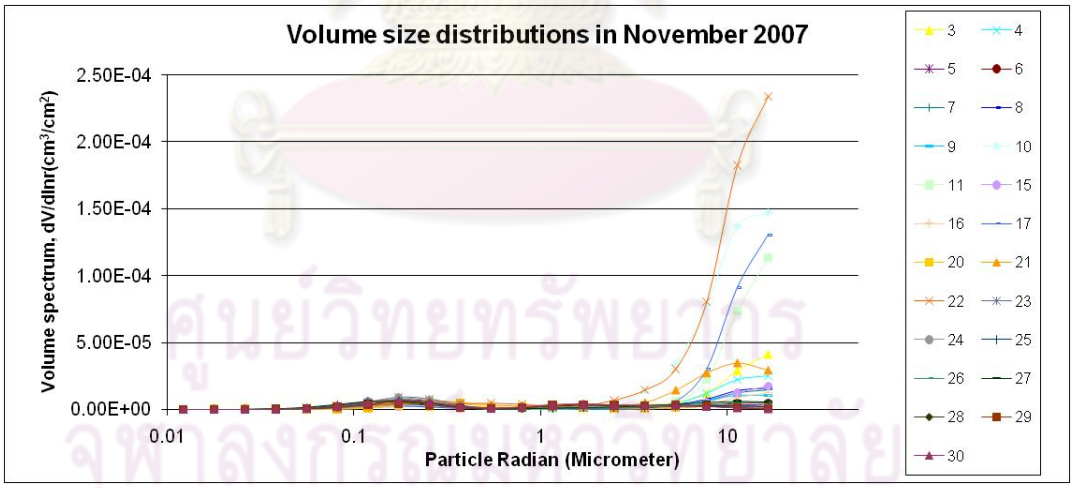

Figure 4.45 Volume size distributions in November 2007.

Wind data observed at 9 meters above ground of Observatory for Atmospheric Research at Phimai, wind direction and wind speed, were used to make wind chart. The wind chart only observes wind at surface level and point on one day data, while the backward trajectory traces the particle in various levels above mean sea level, showing in the figure 4.46 three levels; 500, 1000, and 1500 m, at receptor, i.e. Phimai. It is found that the results between them are correlated well on 26 June 2006, both the wind direction from backward trajectory and wind chart are south and south west, figure 4.46. However, on some day the wind direction were less correlated. For example; wind direction on 12 February 2007, figure 4.47, shows direction of wind is around the observatory, but the backward trajectory shown on south east direction. The different come from level of wind observation at observatory and the detail of raw data. Furthermore, wind chart can show more direction of wind than backward trajectory but it cannot show about track the wind way for long period. Backward trajectory is useful for find tracking of aerosol.

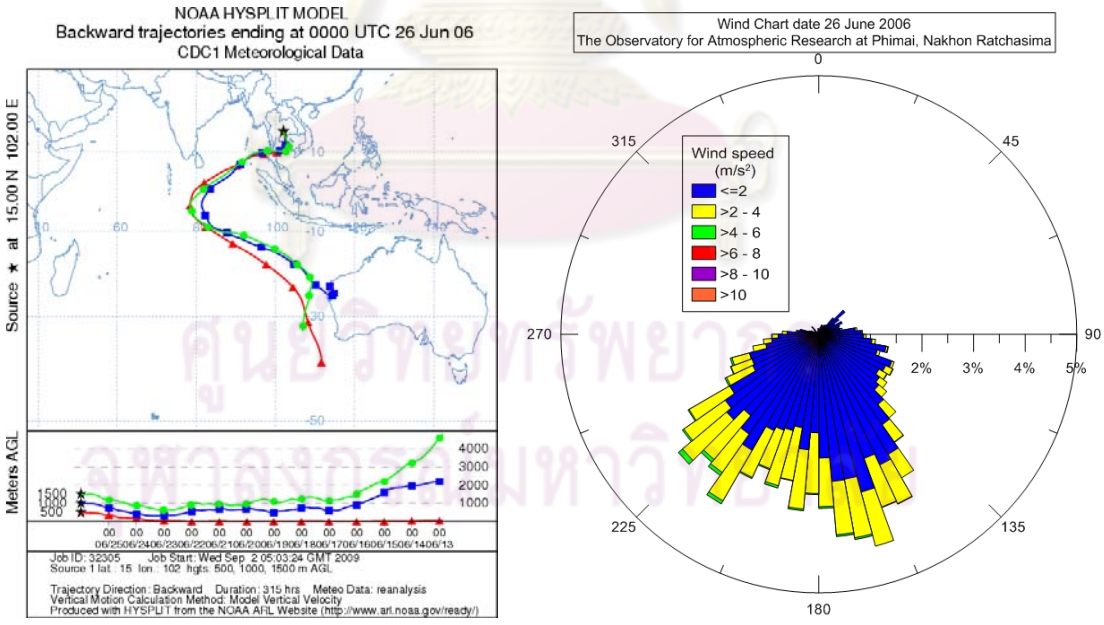

Figure 4.46 Backward trajectory and wind chart on 26 June 2006.

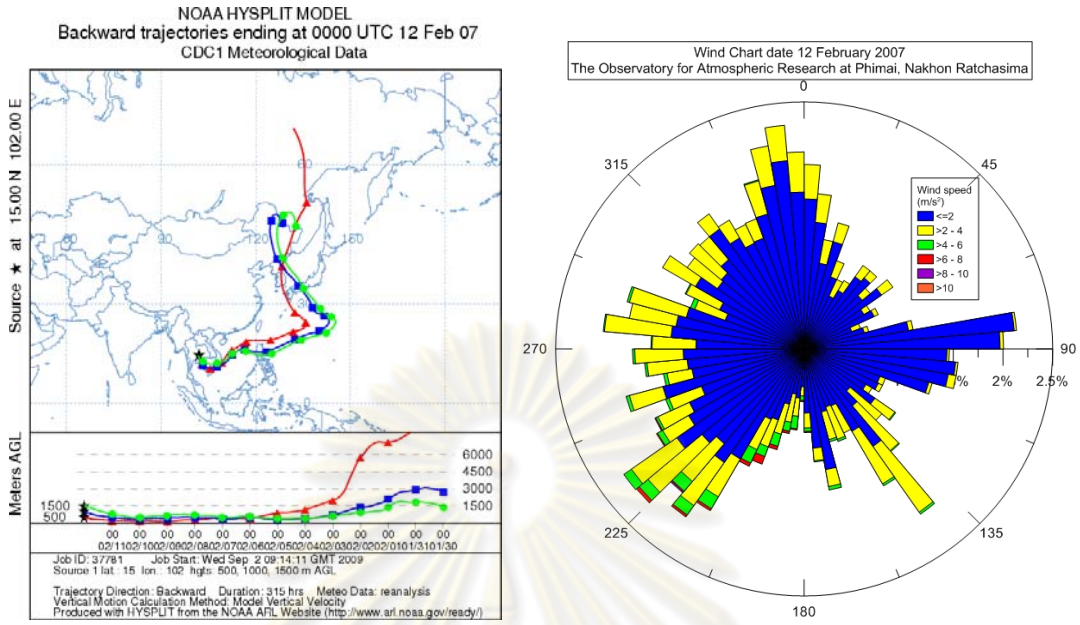

Figure 4.47 Backward trajectory and wind chart on 12 February 2007.

Wind data from observatory can show wind direction in each season. In winter, figure 4.48, wind direction is north east. In summer, figure 4.49, wind direction is east. And in rainy season, wind direction is south west, figure 4.50. Almost of wind direction from wind data of observatory is all the same of backward trajectory in each season.

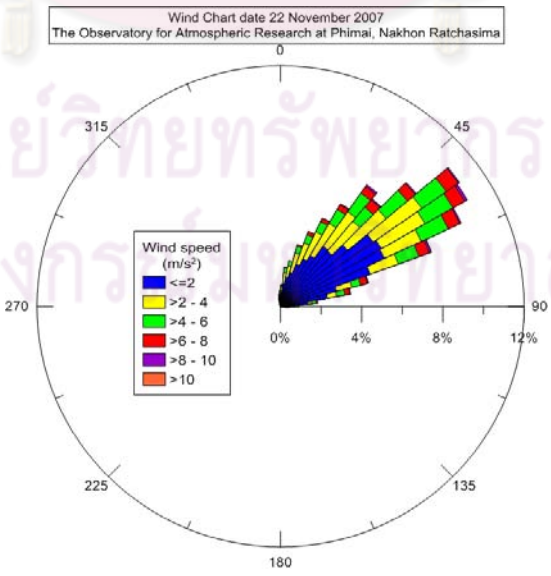

Figure 4.48 Wind chart on a typical day in winter.

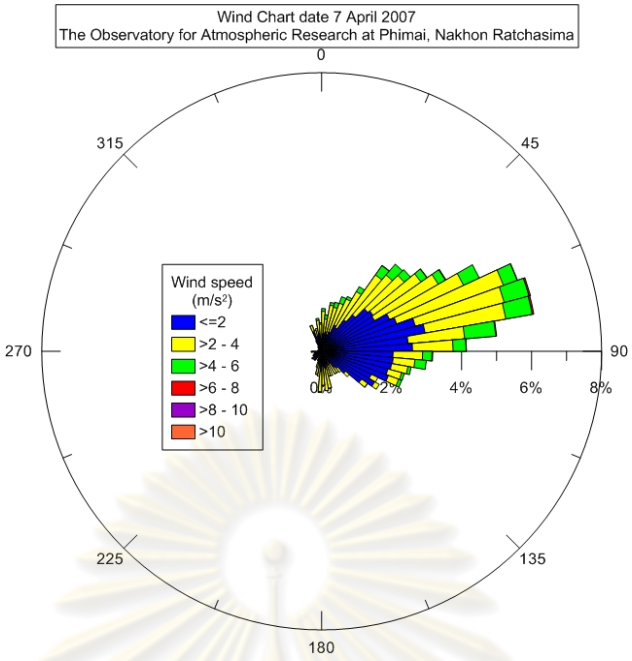

Figure 4.49 Wind chart on a typical day in summer.

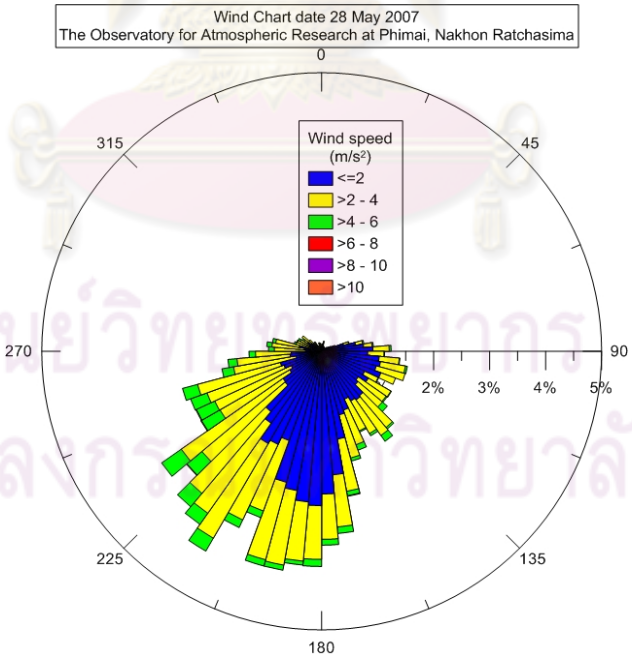

Figure 4.50 Wind chart on a typical day in rainy season.

The day that has high aerosol optical depth and single scattering albedo and mode of the particles can be shown in table 4.3.

Table 4.3 Time events of high AOD in 2006 and 2007, H = high and L = low value.

Event	Date	AOD	SSA	Fine size	Carse size
1	6-Jan-06	H	H	L	L
2	15-Jan-06	H	N	L	H
3	23-Jan-06	H	H	L	L
4	26-Jan-06	H	H	L	H
5	12-Feb-06	H	H	H	H
6	17-Feb-06	H	H	L	H
7	27-Feb-06	H	N	H	H
8	4-Mar-06	H	H	H	L
9	13-Mar-06	H	H	H	L
10	24-Apr-06	H	H	L	H
11	4-May-06	H	N	L	H
12	15-May-06	H	N	L	H
13	16-Jun-06	H	H	L	H
14	26-Jun-06	H	H	L	H
15	8-Jul-06	H	L	L	H
16	9-Sep-06	H	L	L	H
17	24-Sep-06	H	H	L	H
18	5-Oct-06	H	H	L	H
19	20-Oct-06	H	N	H	H
20	30-Oct-06	H	H	L	H
21	7-Nov-06	H	L	H	H
22	13-Nov-06	H	L	H	L
23	23-Nov-06	H	H	H	L
24	26-Nov-06	H	H	H	L
25	17-Dec-06	H	H	H	L
26	28-Dec-06	H	H	L	H
27	14-Jan-07	H	H	L	H
28	22-Jan-07	H	H	H	H
29	28-Jan-07	H	H	L	H
30	2-Feb-07	H	H	H	L
31	6-Feb-07	H	H	H	L
32	12-Feb-07	H	H	H	H
33	22-Feb-07	H	H	H	H
34	26-Feb-07	H	L	H	L
35	2-Mar-07	H	L	H	H
36	15-Mar-07	H	L	H	L
37	24-Mar-07	H	H	L	H
38	29-Mar-07	H	H	L	L
39	11-Apr-07	H	H	L	L
40	25-Apr-07	H	H	L	H
41	9-May-07	H	H	L	L
42	20-May-07	H	H	L	H
43	28-May-07	H	H	L	H
44	30-May-07	H	L	L	H
45	12-Jun-07	H	N	L	L
46	18-Jun-07	H	H	L	H
47	24-Jul-07	H	H	L	H
48	30-Jul-07	H	H	L	H
49	25-Aug-07	H	H	L	H
50	22-Sep-07	H	H	L	L
51	27-Sep-07	H	L	L	H
52	21-Oct-07	H	L	H	L
53	25-Oct-07	H	L	L	H
54	6-Nov-07	H	H	L	L
55	22-Nov-07	H	H	L	H
56	1-Dec-07	H	H	L	H
57	6-Dec-07	H	H	L	L
58	18-Dec-07	H	L	L	H
59	22-Dec-07	H	H	L	L

By categorize the value of aerosol optical depth and single scattering albedo to 3 cases of, figure 4.51, high of AOD and SSA, high of AOD and low of SSA, high of AOD and not change of SSA and 3 cases of high of AOD and high of fine mode

particle and high of AOD and high of coarse mode particle, figure 4.52. Most of increase of aerosol optical depth is also effect in increase of single scattering albedo. A large amount of aerosol particle is in coarse mode and non-absorbing aerosols, when it high of aerosol optical depth in study area.

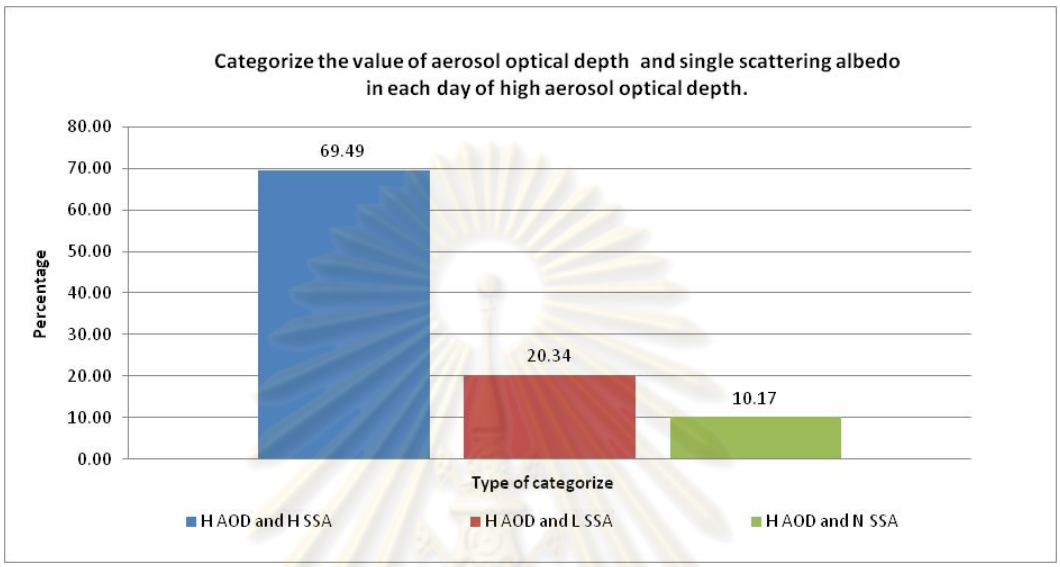

Figure 4.51 Categorize the value of aerosol optical depth and single scattering albedo in each day of high aerosol optical depth.

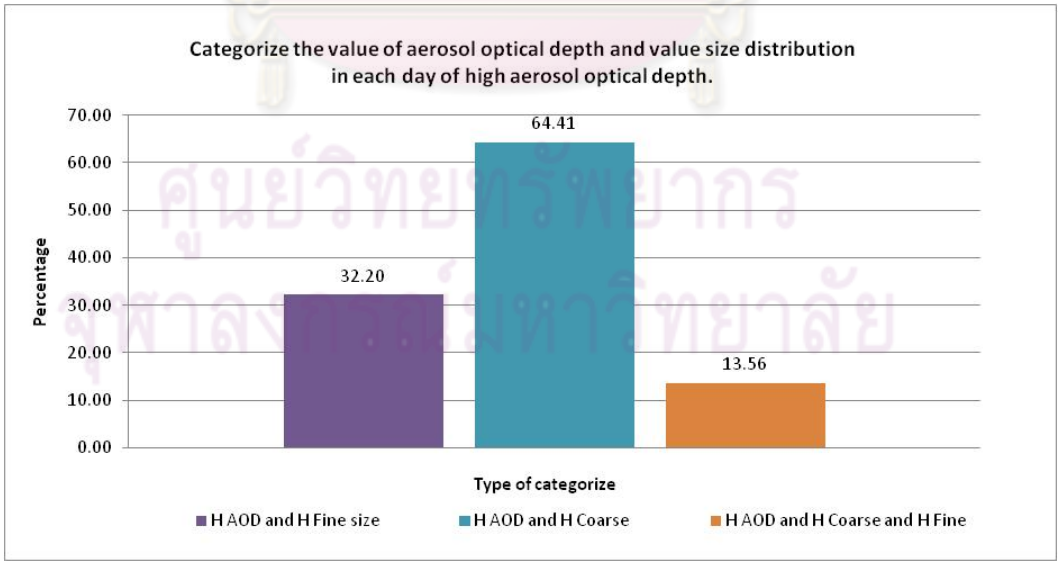

Figure 4.52 Categorize the value of aerosol optical depth and value size distribution in each day of high aerosol optical depth.

In summer, the high aerosol optical depth came of fine and coarse particle. The event of high aerosol optical depth because of coarse particle is more than winter, as shown in figure 4.53.

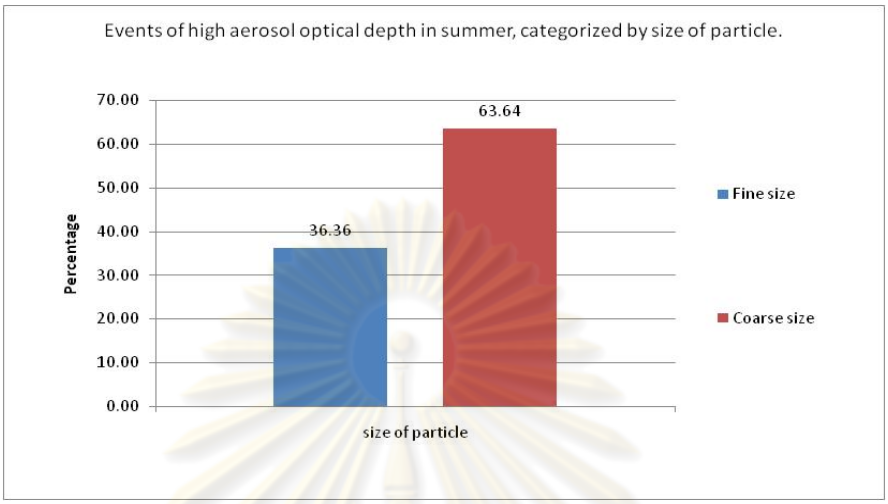

Figure 4.53 Number of event of high aerosol optical depth in summer, categorized by size of particle.

In rainy season, the high aerosol optical depth came from coarse mode particle in every event, as shown in figure 4.54.

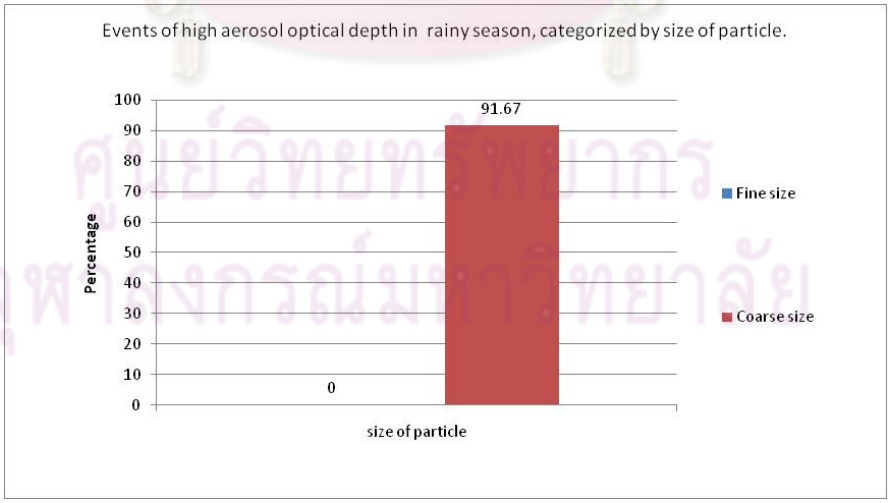

Figure 4.54 Number of event of high aerosol optical depth in rainy season, categorized by size of particle.

In winter, the high aerosol optical depth came from both of fine and coarse mode particles, as shown in figure 4.55.

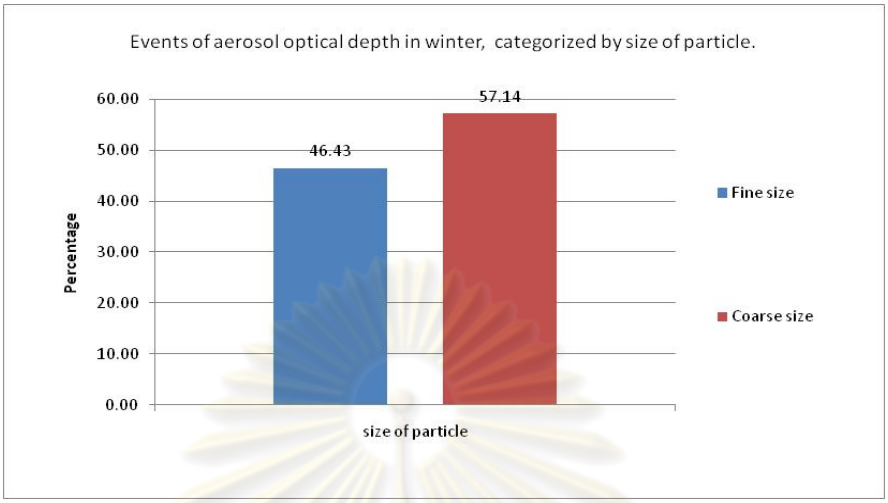

Figure 4.55 Number of event of high aerosol optical depth in winter, categorized by size of particle.

Because of the study is in agriculture and saline area, most of aerosol particles are likely to come from agriculture and saline activity, biomass burning and salt particle respectively. On rainy season most of aerosol particle both of distant source and local source are mostly deposited by precipitation. But the aerosol particles from local sources are dominated. It is clear that majority aerosol particles come from local source, large and non-absorbing aerosol; it may contain of biomass burning and salt particle from saline.

For distance source, aerosol is control by wind direction. We can use this fact to categorize type of aerosol particles. In winter, the wind brings aerosol particles from China area, Northern Thailand. It is likely to contain a lot of soot particles, more absorbing aerosol in fine mode particles. However, aerosols from local source still have an effect because we can find aerosol in coarse mode particle. When wind passes through the ocean area such as India Ocean in rainy season and Pacific Ocean in summer, it brings of sea salt particle of coarse mode which is non-absorbing particle too.

From 2006 to 2007 the average of AOD and SSA are 0.49 and 0.89 respectively. In compare to Do-Hyeong Kim et al, who is study the aerosol in Sri Samrong area, Northern Thailand, he found that the SSA value average from 1997 to 2000 is 0.88 (Kim et al, 2005). Our results are nearly the same. The average of AOD value in two year is much more than Crete-Paris in France (0.26), Greenbelt-MD in United States (0.24), Persian Gulf (0.22), Saudi Arabia (0.17) and Maldives (0.27). The AOD in this study is lower than South America cerrado in Brazil (0.80) and close to Mexico City (0.43) (Dobovik, 2002).

CHAPTER V
CONCLUSIONS AND SUGGESTIONS

5.1 Conclusions

In 2006, on select wavelength: 500 nm, it clears that AOD and SSA value are very high in two periods, March and September. They are lower in June to July and December to January. The highest monthly average of AOD is 0.75 in March and the lowest is 0.28 in June. The highest monthly average of SSA is 0.94 in October and the lowest is 0.87 in May and June.

In 2007, as in 2006, AOD and SSA value is very high in two periods, March and September. They are lower in June to July and December to January. The highest monthly average of AOD is 0.89 in March and the lowest is 0.32 in June. The highest monthly average of SSA is 0.90 in March and October. The lowest monthly of average SSA is 0.83 in December. It is found that the average volume of size of aerosol particle in coarse mode is larger than 16.54 micrometer and the size of aerosol particle in fine mode is 0.17 micrometer both of two years. The backward trajectories in winter season show the source of aerosol particle came from the north-east of Thailand, in continental. In summer season most of the aerosol particle came from the east. And in rainy season, the aerosol particle came from the south-west.

The most of high AOD events in summer come from coarse mode particles more than fine mode particles. In rainy season, the high AOD events come from both of fine and coarse particles. In contrast of winter and summer, rainy season, the high AOD only come from coarse mode particle. The local source of aerosols particle are agriculture and saline activity. The far away source is dominated by wind direction

5.2 Suggestions

This study is only focus on physical properties of aerosol such as aerosol optical depth, single scattering albedo and volume size distribution. It cannot categorize the type of aerosol exactly. For the estimate exact type of aerosol, the chemical properties have to be study. However, this study can estimate some type of aerosol by size of particle, single scattering properties and backward trajectory for estimate source of aerosol. Types of aerosol depend on them. To improving estimate type of aerosol, we can use relation between single scattering albedo in another wavelength to find the pattern form that can identify type of aerosol (Dubovik O. et al., 2002).

If we know about aerosol optical properties in this area, we can find about some aerosol radiative forcing on this area too. Aerosol radiative forcing is very important to predict our climate in the future. From this study, we can find it. By compare between radiative fluxes that have an effect of aerosol and none of aerosol in clear sky day. The result from this study can do it.

Furthermore, one should compare value of aerosol optical properties from this study with satellite data, providing that is available. Because of satellite data can observe data in large area but the correction depends on calibration between ground base data and satellite data. If we use data of this study to calibrate satellite data, the large area data can be analyse. The effect of aerosol particle on climate is an active branch of advantage research.

REFERENCES

Aoki K. and Fujiyoshi Y.. 2003. Sky Radiometer Measurements of Aerosol Optical Properties over Sapporo, Japan. Journal of the Meteorological Society of Japan, Vol. 81, No. 3.

Charlson R.J. and Heintzenberg J.. 1995. Aerosol Forcing of Climate. Great Britain : Biddles Ltd,.

Donald Ahrens C.. 2007. Essentials of Meteorology. Brooks Cole; 5 edition (February 5, 2007).

Corrigan C. E., Ramanathan V., Schauer J. J.. 2006. Impact of monsoon transitions on the physical and optical properties of aerosols, Journal of Geophysical Research, Vol. 111 (2005), D18208, doi:10.1029/2005JD006370.

Dubovik Oleg, Holben Brent, Eck Thomas F., Smirnov Alexander, Yoram J. Kaufman, King Michael D., Tanre Didier, and Slutsker Ilya. 2002. Variability of Absorption and Optical Properties of Key Aerosol Types Observed in Worldwide Locations. American Meterorological Society, Vol 59 (February 2002) : 590.

Duce R. A..1995. Sources, distributions, and fluxes of mineral aerosols and their relationship to climate, in: R.J. Charlson / J. Heintzenberg (eds.), Aerosol forcing of climate, John Wiley & Sons, Chichester 1995.

Flossmann I. Andrea. 1998. Interaction of Aerosol Particles and Clouds. American Meteorological Society, Vol. 55 (March 1998) : 879.

James Haywood and Olivier Boucher. 2000. Estimates of the Direct and Indirect Radiative Forcing Due to Tropospheric Aerosols : A Review. Reviews of Geophysics, Vol. 38 (November 2000) : 513.

Johnson B. T.. 2003. The Semi-Direct Aerosol Effect : The University of Reading, Department of Meteorology.

Kiehl J.T., and Trenberth K.E., 1997: Earth's annual global mean energy budget. Bull. Amer. Meteor. Soc., 78, 197-208.

Kikuchi Nobuyuki. 2007. Comparing results between example, single precision, SGI supercomputer and double precision results. Center for Global Environmental Research National Institute for Environmental Studies. 2007.

Kim Do-Hyeong, Sohn B.J., Nakajima T., and Takamura T.. 2005. Aerosol radiative forcing over East Asia determined from ground-based solar radiation measurements. Journal of Geophysical Research, Vol. 110 (2005).

Krishna Moorthy K., Satheesh S.K., and Krishna Murthy B. V.. 1998. Characteristics of spectral optical depths and size distributions of aerosols over tropical oceanic regions. Journal of Atmospheric and Solar-Terrestrial Physics, Vol. 60 (1998) 981-992.

Nakajima Teruyuki, Tonna Glauco, Rao Ruizhong, Boi Paolo, Kaufman Yoram, and Holben Brent. 1996. Use of sky brightness measurements from ground for remote sensing of particulate polydispersions. Applied Optics Vol. 35, No. 15 (May 1996) : 2672.

Prede co., Ltd. Skyradiometer (POM-02L) version 4.50 Operation Manual, Sasamoto Blg. 1-26-8, Kamidaira, Fussa-shi, Tokyo, 197-0012, Japan.

Reist C. Parker. 1993. Aerosol Science and Technology. 2nd edition. Singapore : McGraw-Hill, Inc,.

Ramanathan V., Crutzen P. J., Lelieveld J., Mitra A. P., Althausen D., Anderson J., Andreae M.O., Cantrell W., Cass G.R., Chung C.E., Clarke A.D., Coakley J. A., Collins W. D., Conant W. C., Dulac F., Heintzenberg J., Heymesfield A. J., Holben B., Howell S., Hudson J., Jayaraman A., Kiehl J. T., Krishnamurti T. N., Lubin D., McFarquhar G., Novakov T., Ogren J. A., Podgorny I. A., Prather K., Priestley K., Prospero J. M., Quinn P. K., Rajeev K., Rasch P., Rupert S., Sadourny R., Satheesh S. K., Shaw G. E., Sheridan P., and Valero F. P. J.. 2001. Indain Ocean Experiment : An integrated analysis of the climate forcing and effects of the great Indo-Asian haze. Journal of Geophysical Research, Vol. 106 No. D22 : (November 2001) : 28371.

Ramanathan V., Crutzen P. J., Kiehl J. T., and Rosenfeld D.. 2001. Aerosols, Climate, and the Hydrological Cycle. Science, Vol. 294 (December 2001) : 2119.

Ramachandran S. and Cherian R.. 2008. Regional and seasonal variations in aerosol optical characteristics and their frequency distributions over India during 2001-2005. Journal of Geophysical Research, Vol. 113 (April 2008) : D08207.

Satheesh S.K. and Ramanathan V., (2000). Large Differences in Tropical Aerosol Forcing at the Top of the Atmosphere and Earth's surface. Nature, 405: 60-63.

Solomon S., Qin D., Manning M., Chen Z. , Marquis M., Averyt K.B., Tignor M. and Miller H.L. (eds.). (2007). IPCC, 2007: Summary for Policymakers. In: Climate Change 2007: The Physical Science Basis. Contribution of Working Group I to the Fourth Assessment Report of the Intergovernmental Panel on Climate Change. Cambridge University Press, Cambridge, United Kingdom and New York, NY, USA.

Stull B. Roland. 2000. Meteorology for Scientists and Engineers. Second Edition. The United States of America : BROOKS/COLE,.

APPENDICES

APPENDIX A

Aerosol optical depth

APPENDIX A

Year 2006 **Month** January

Average value 0.29 **SD** 0.16 **Min** 0.05 **Max** 0.63

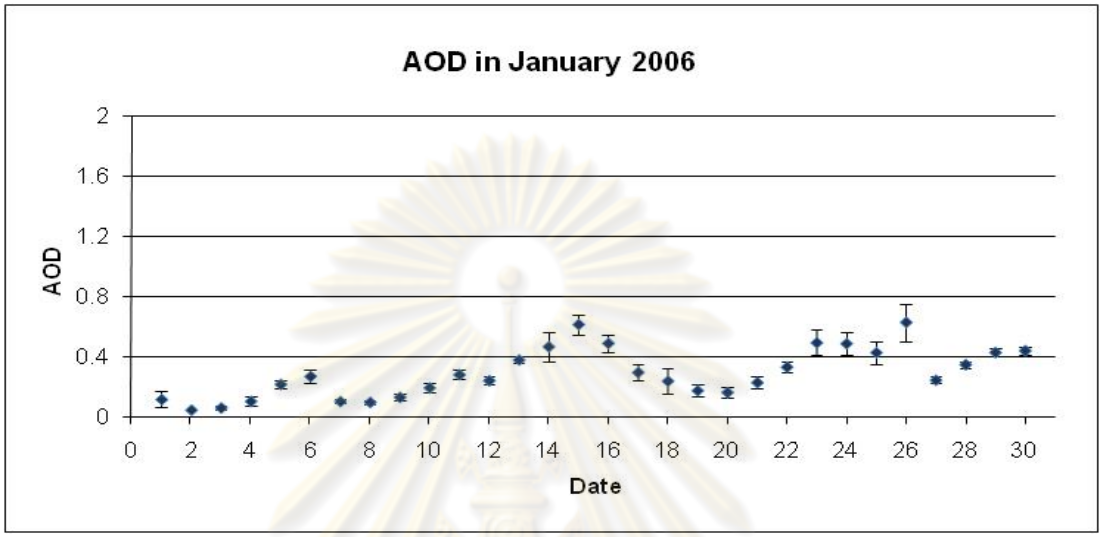

Figure A-1 Aerosol optical depths in January 2006.

Year 2006 **Month** February

Average value 0.50 **SD** 0.30 **Min** 0.25 **Max** 1.43

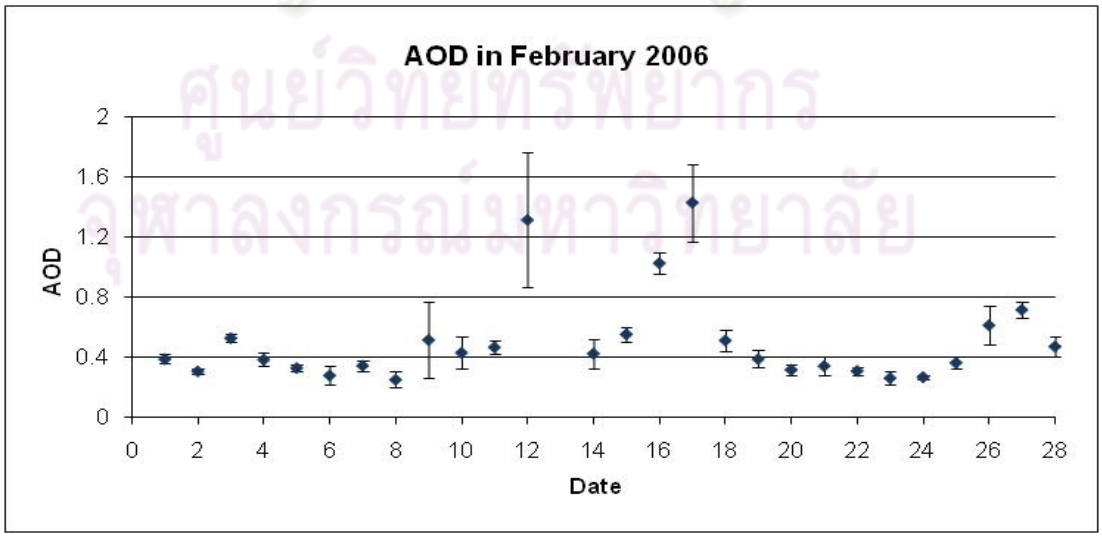

Figure A-2 Aerosol optical depths in February 2006.

Year 2006 **Month** March

Average value 0.75 **SD** 0.23 **Min** 0.43 **Max** 1.25

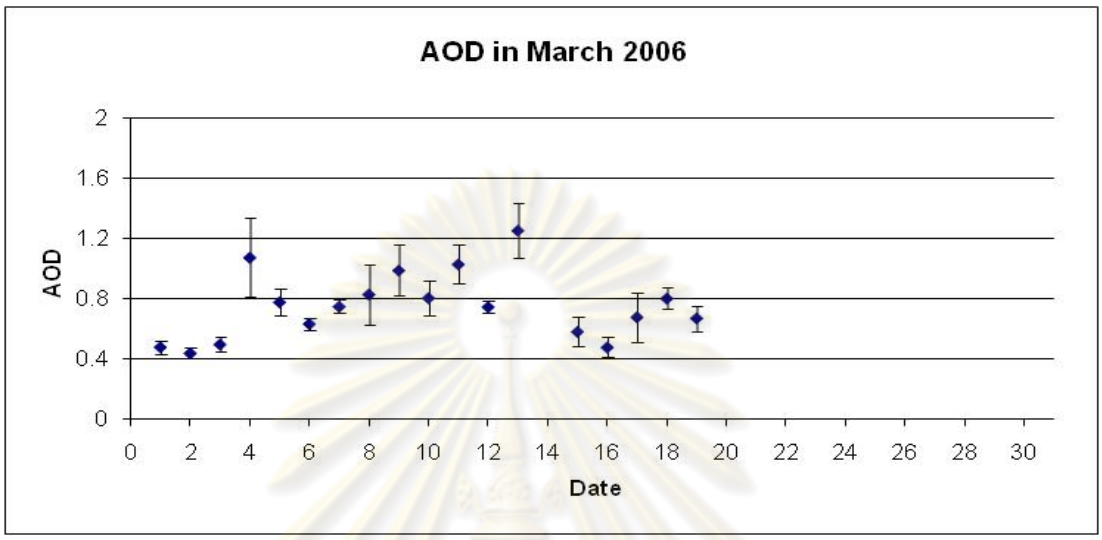

Figure A-3 Aerosol optical depths in March 2006.

Year 2006 **Month** April

Average value 0.50 **SD** 0.30 **Min** 0.19 **Max** 1.05

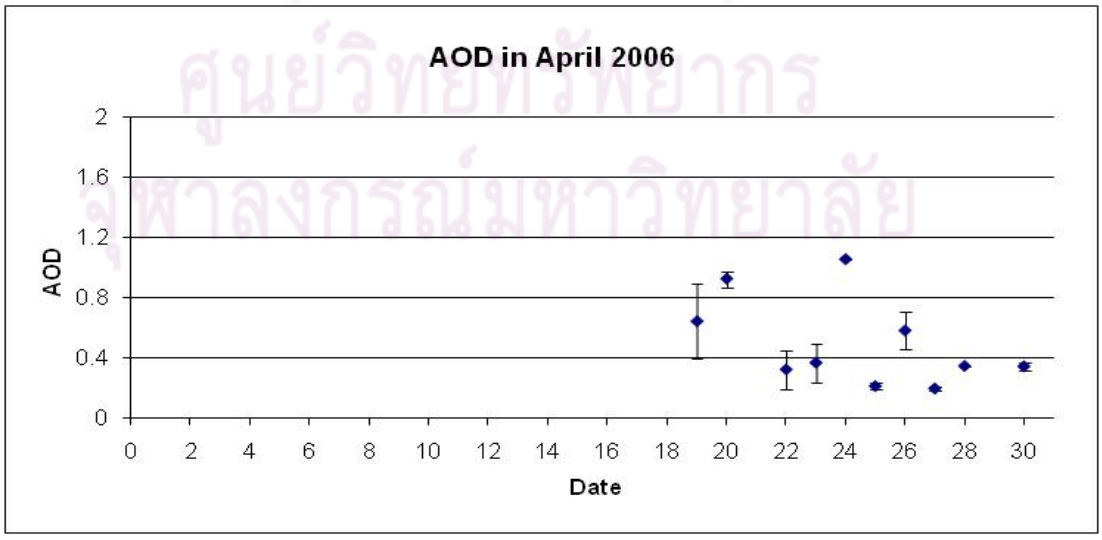

Figure A-4 Aerosol optical depths in April 2006.

Year 2006 **Month** May

Average value 0.50 **SD** 0.18 **Min** 0.24 **Max** 0.84

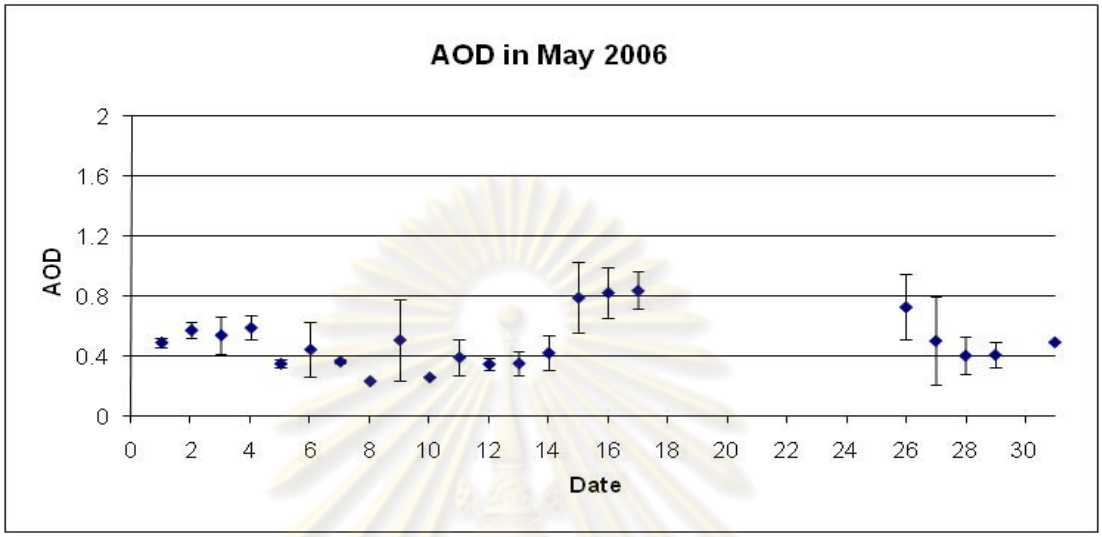

Figure A-5 Aerosol optical depths in May 2006.

Year 2006 **Month** June

Average value 0.28 **SD** 0.15 **Min** 0.21 **Max** 0.75

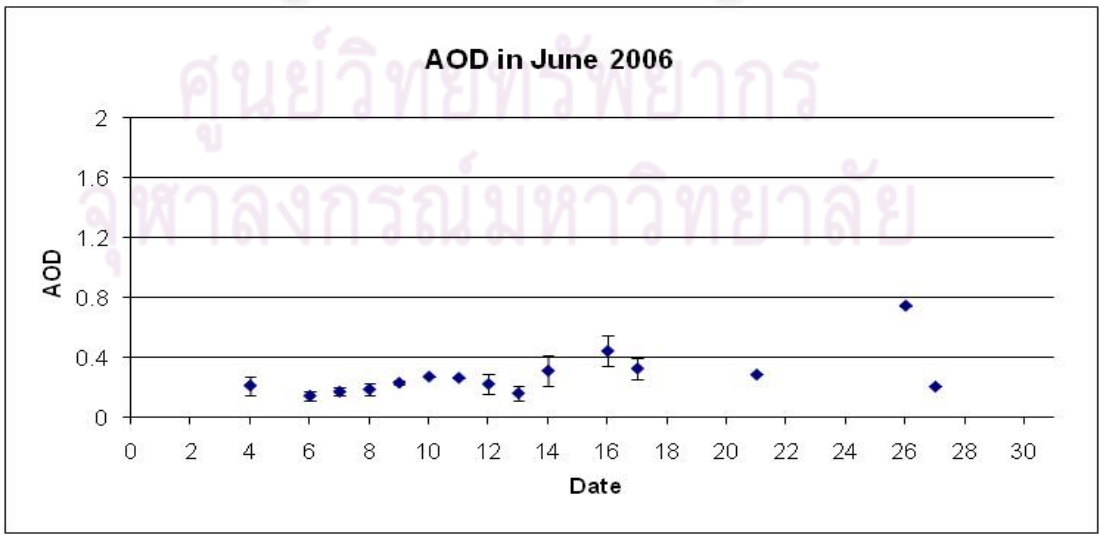

Figure A-6 Aerosol optical depths in June 2006.

Year 2006 **Month** July

Average value 0.34 **SD** 0.15 **Min** 0.21 **Max** 0.58

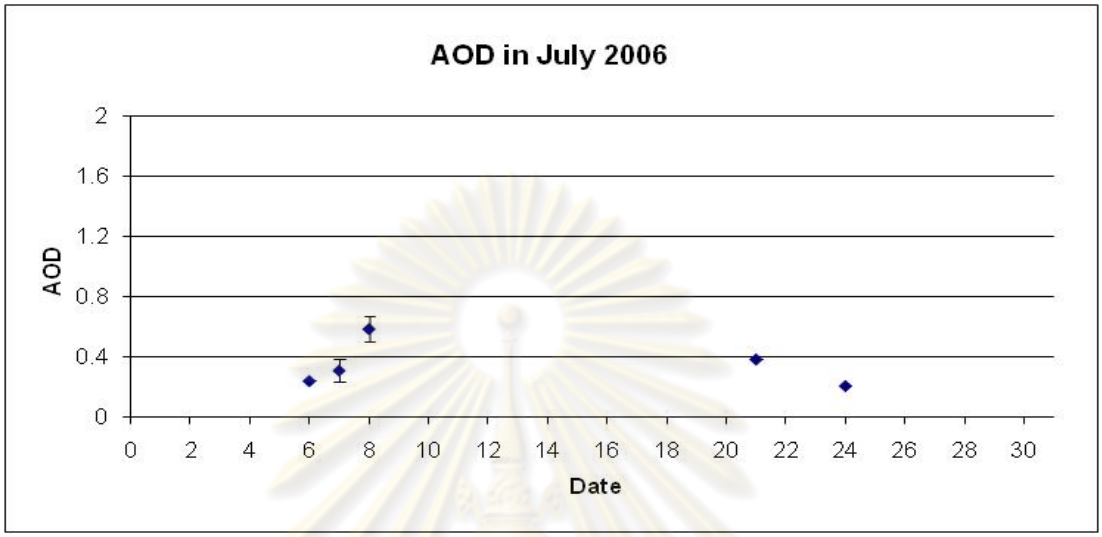

Figure A-7 Aerosol optical depths in July 2006.

Year 2006 **Month** August

Average value 0.50 **SD** - **Min** 0.50 **Max** 0.50

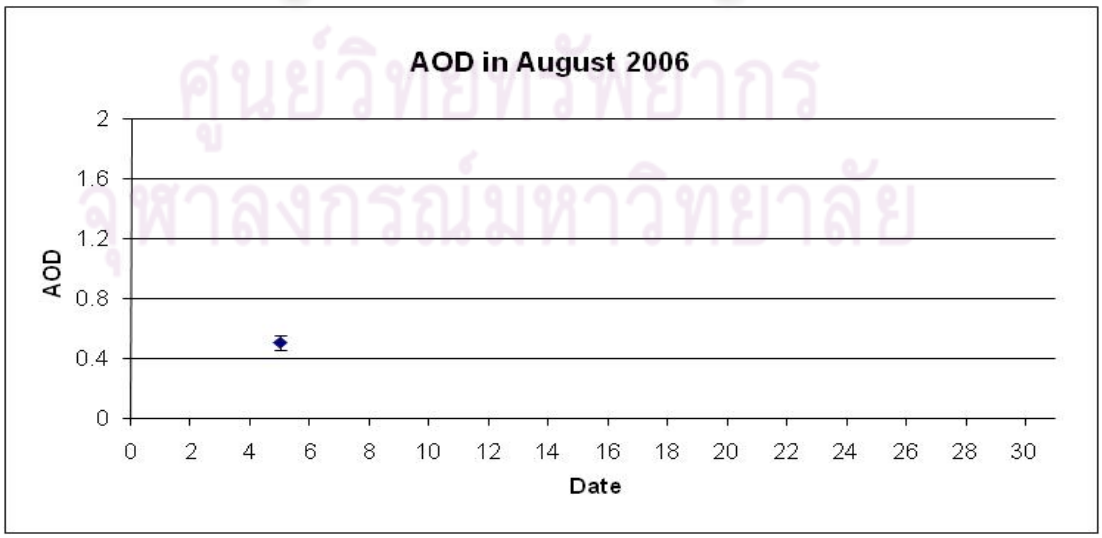

Figure A-8 Aerosol optical depths in August 2006.

Year 2006 **Month** September

Average value 0.60 **SD** 0.61 **Min** 0.13 **Max** 2.10

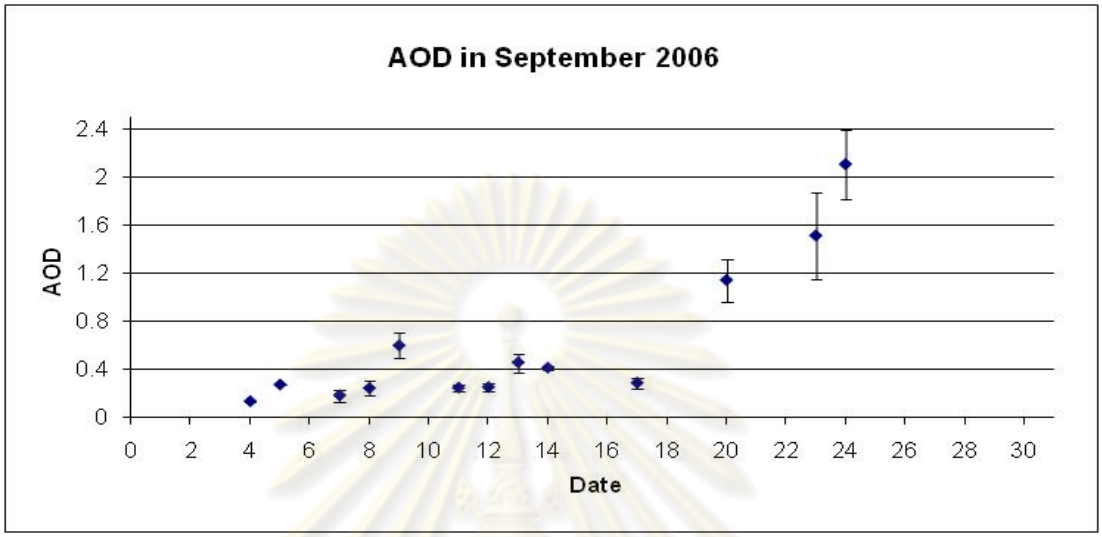

Figure A-9 Aerosol optical depths in September 2006.

Year 2006 **Month** October

Average value 0.37 **SD** 0.19 **Min** 0.14 **Max** 0.75

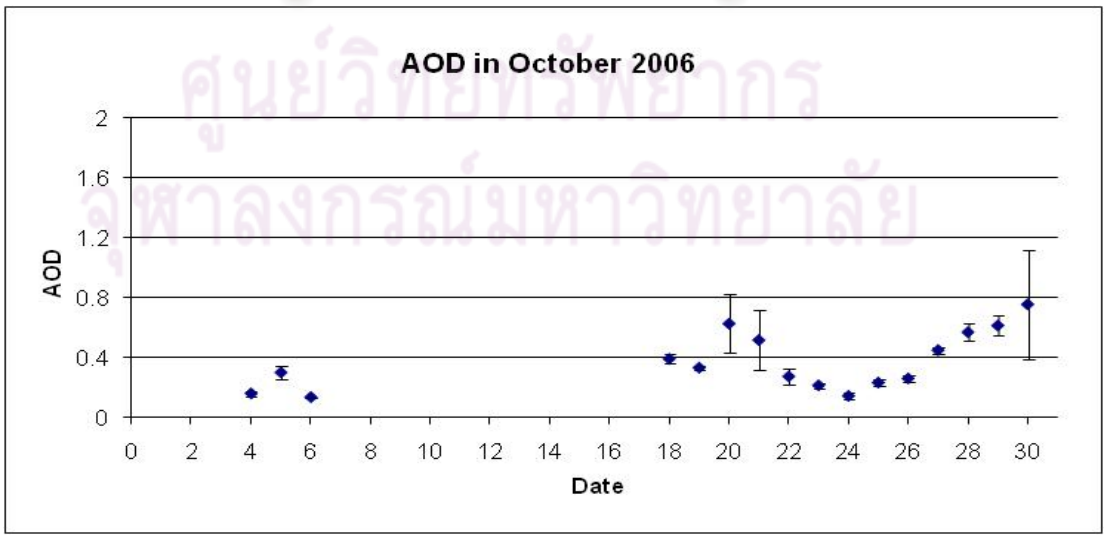

Figure A-10 Aerosol optical depths in October 2006.

Year 2006 **Month** November

Average value 0.41 **SD** 0.22 **Min** 0.15 **Max** 1.06

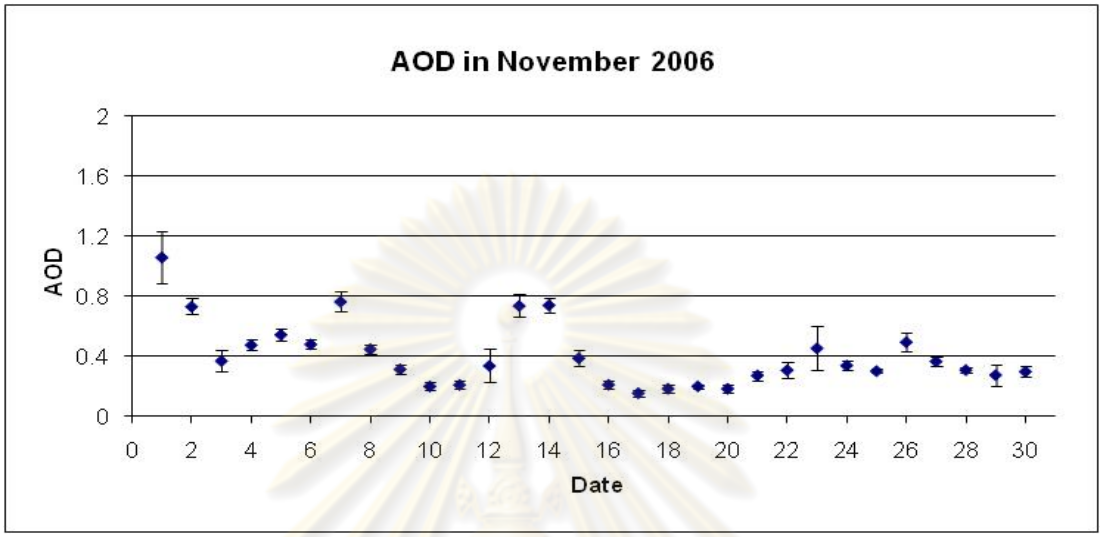

Figure A-11 Aerosol optical depth in November 2006.

Year 2006 **Month** December

Average value 0.34 **SD** 0.14 **Min** 0.11 **Max** 0.72

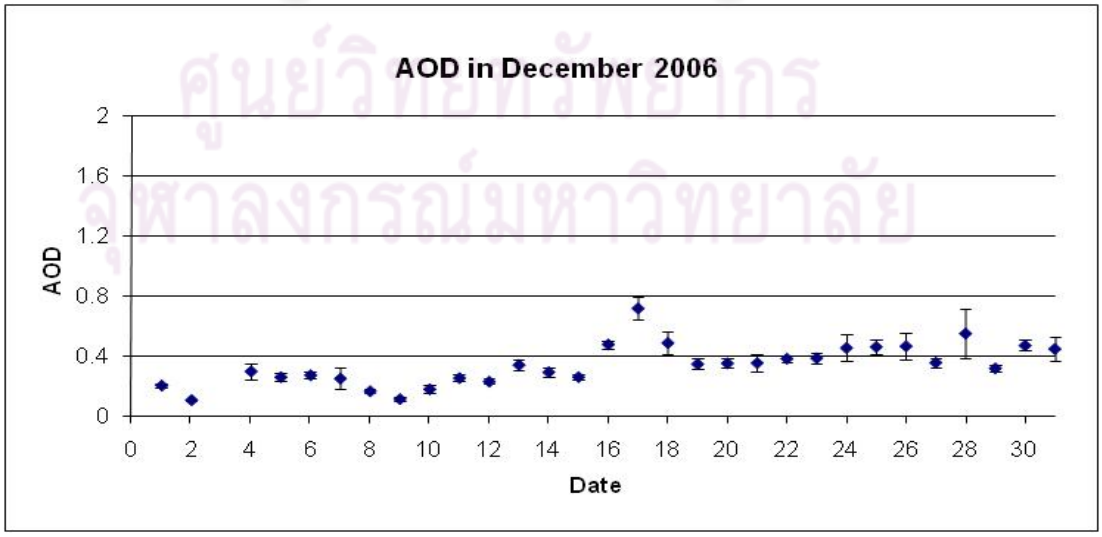

Figure A-12 Aerosol optical depths in December 2006.

Year 2007 **Month** January

Average value 0.42 **SD** 0.24 **Min** 0.15 **Max** 1.22

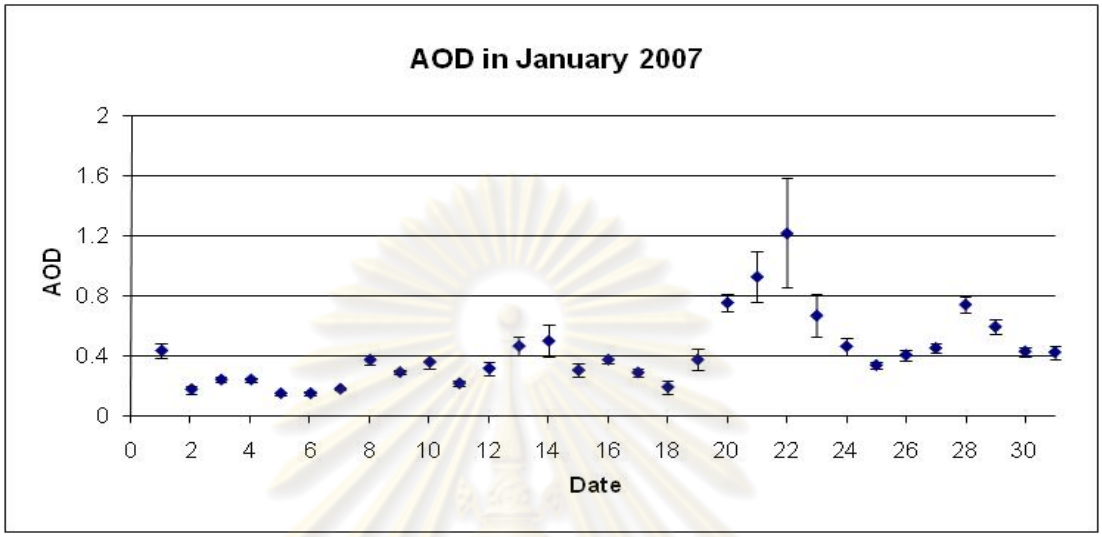

Figure A-13 Aerosol optical depths in January 2007.

Year 2007 **Month** February

Average value 0.74 **SD** 0.25 **Min** 0.31 **Max** 1.26

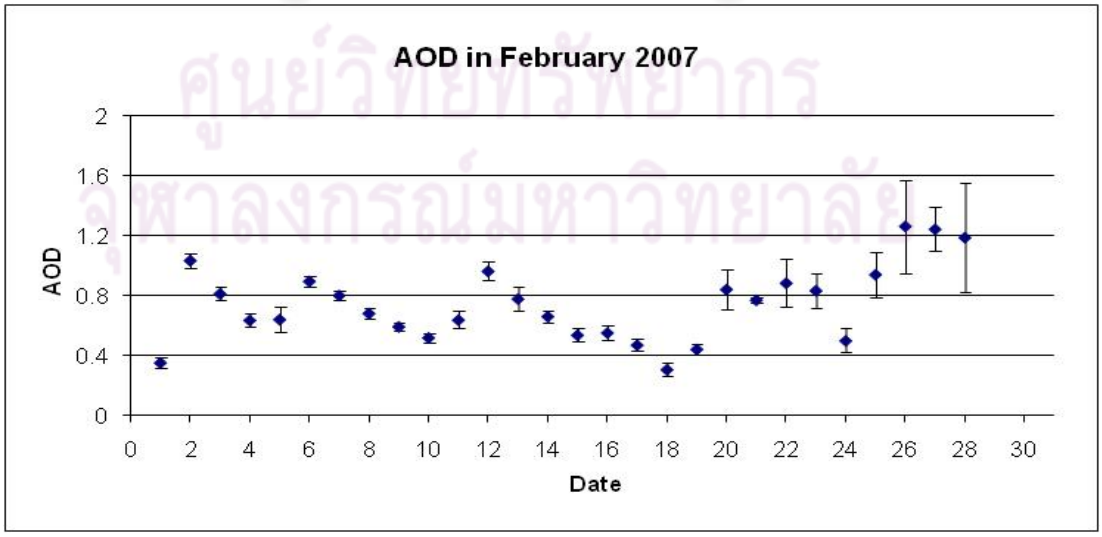

Figure A-14 Aerosol optical depths in February 2007.

Year 2007 **Month** March

Average value 0.89 **SD** 0.30 **Min** 0.42 **Max** 1.63

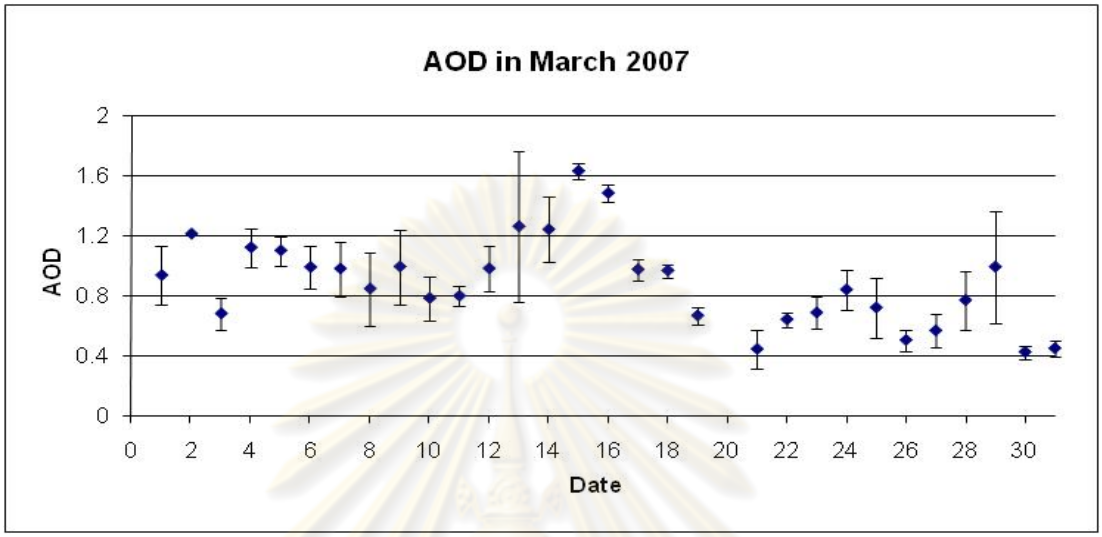

Figure A-15 Aerosol optical depths in March 2007.

Year 2007 **Month** April

Average value 0.59 **SD** 0.28 **Min** 0.20 **Max** 1.31

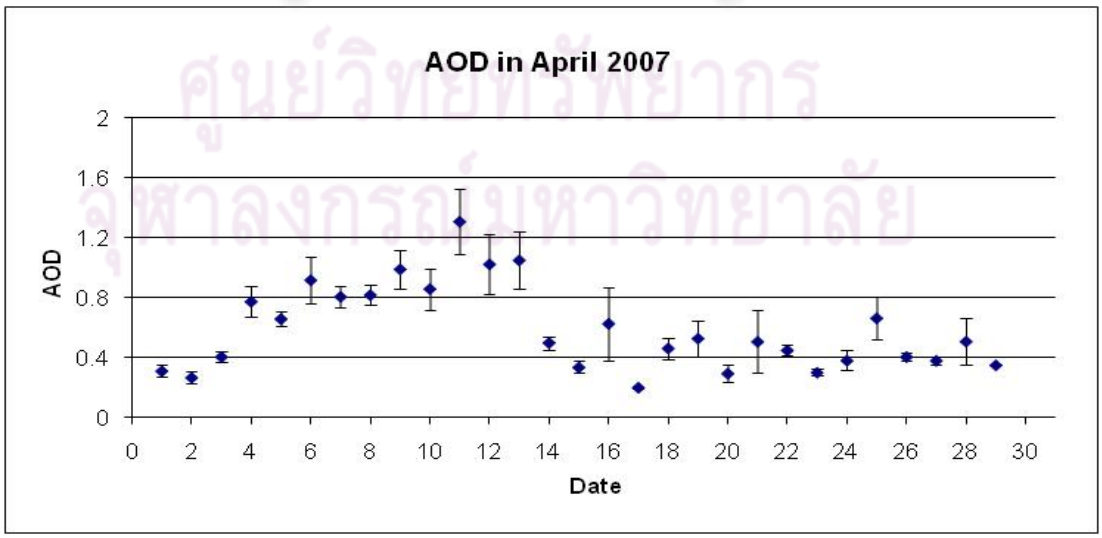

Figure A-16 Aerosol optical depths in April 2007.

Year 2007 **Month** May

Average value 0.46 **SD** 0.31 **Min** 0.22 **Max** 1.44

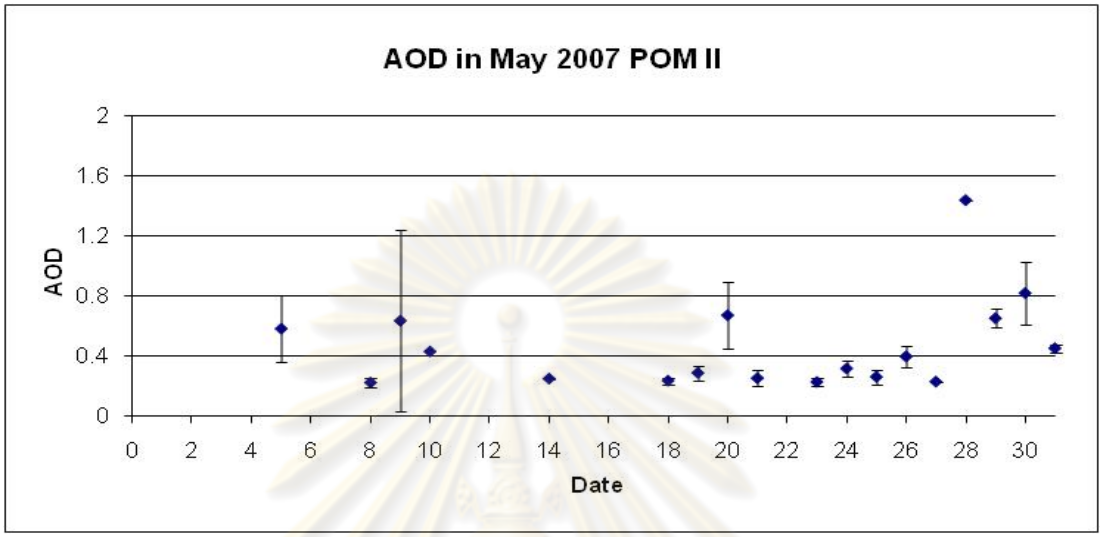

Figure A-17 Aerosol optical depths in May 2007.

Year 2007 **Month** June

Average value 0.32 **SD** 0.14 **Min** 0.12 **Max** 0.66

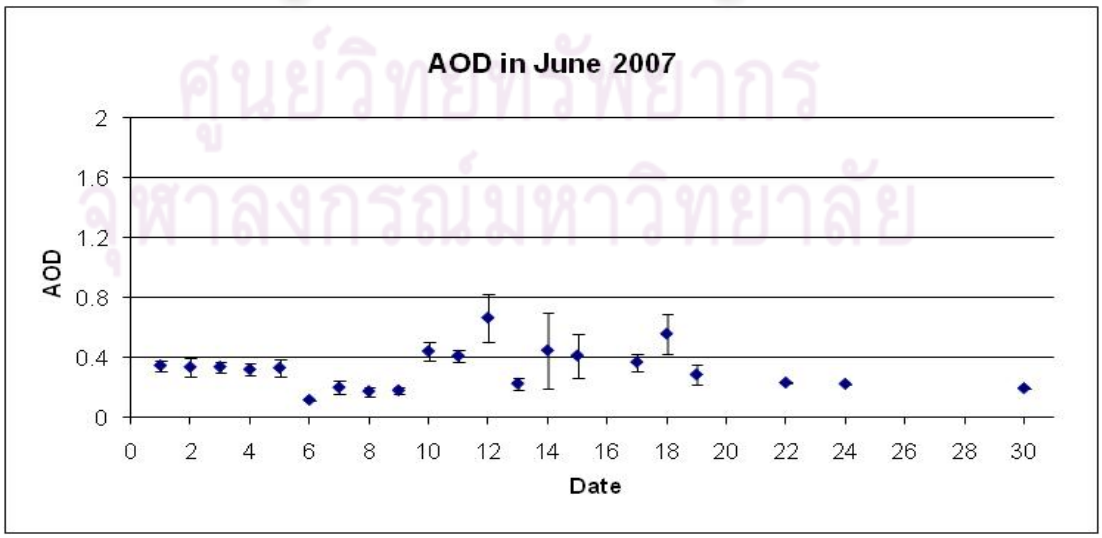

Figure A-18 Aerosol optical depths in June 2007.

Year 2007 **Month** July

Average value 0.38 **SD** 0.30 **Min** 0.11 **Max** 1.35

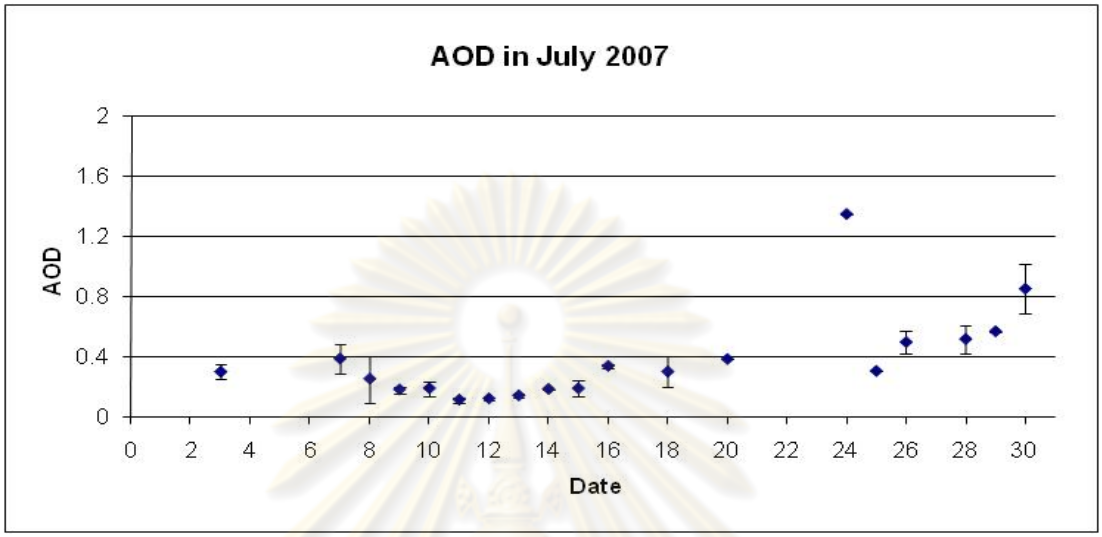

Figure A-19 Aerosol optical depths in July 2007.

Year 2007 **Month** August

Average value 0.42 **SD** 0.20 **Min** 0.17 **Max** 0.97

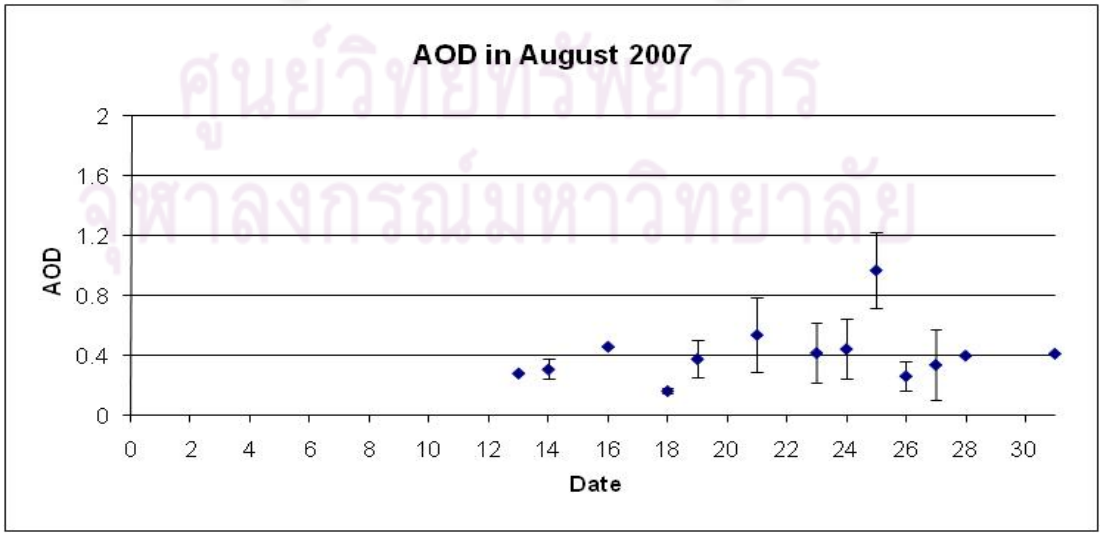

Figure A-20 Aerosol optical depths in August 2007.

Year 2007 **Month** September

Average value 0.65 **SD** 0.34 **Min** 0.26 **Max** 1.44

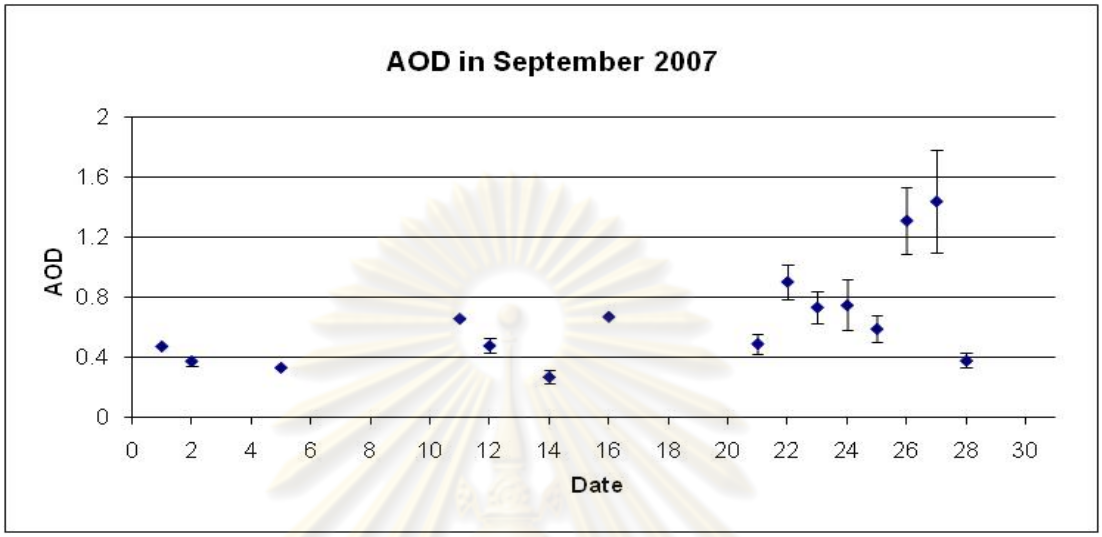

Figure A-21 Aerosol optical depths in September 2007.

Year 2007 **Month** October

Average value 0.60 **SD** 0.28 **Min** 0.37 **Max** 1.20

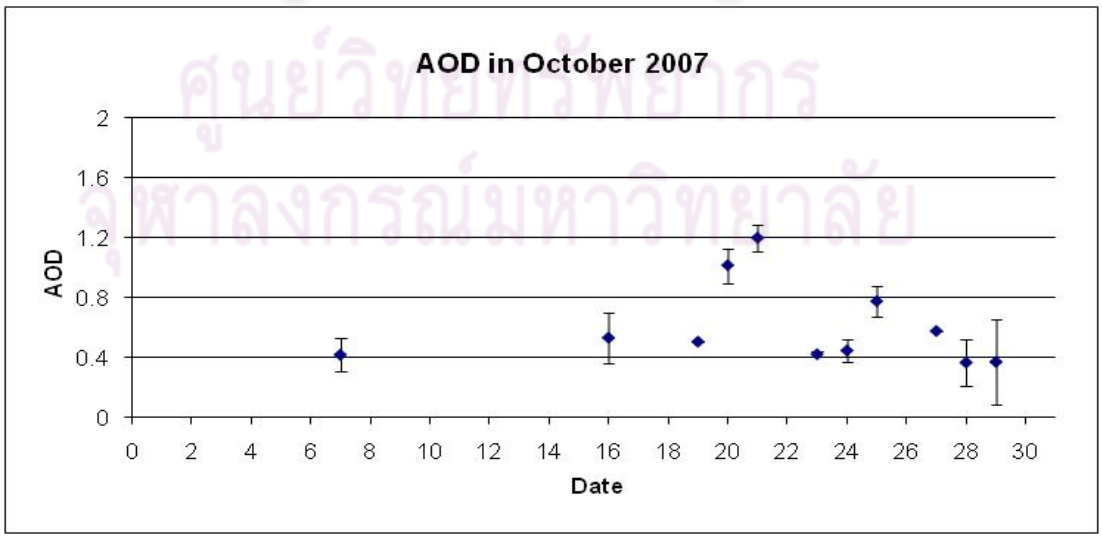

Figure A-22 Aerosol optical depths in October 2007.

Year 2007 **Month** November

Average value 0.45 **SD** 0.16 **Min** 0.22 **Max** 0.94

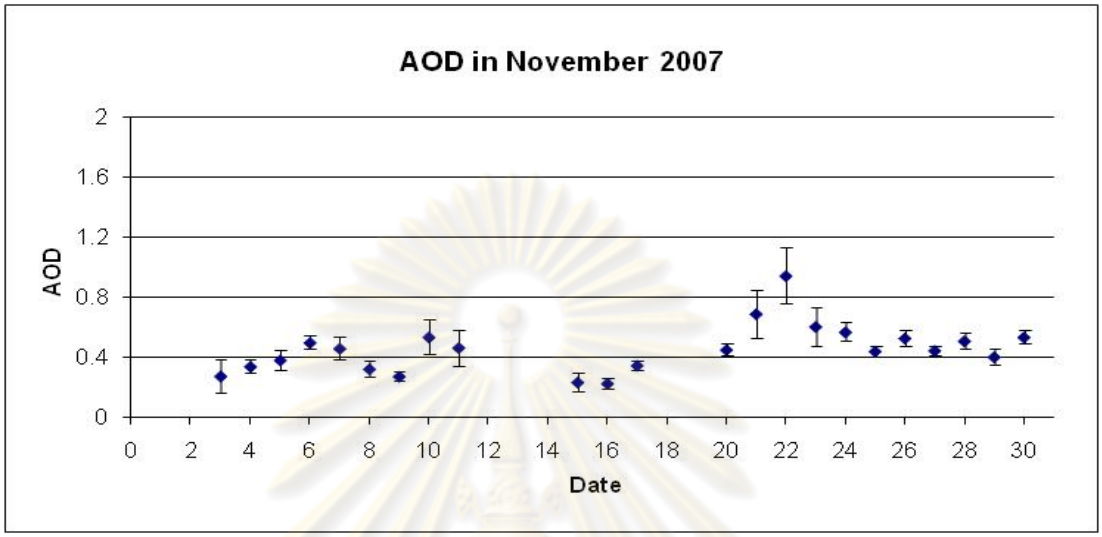

Figure A-23 Aerosol optical depths in November 2007.

Year 2007 **Month** December

Average value 0.34 **SD** 0.10 **Min** 0.16 **Max** 0.53

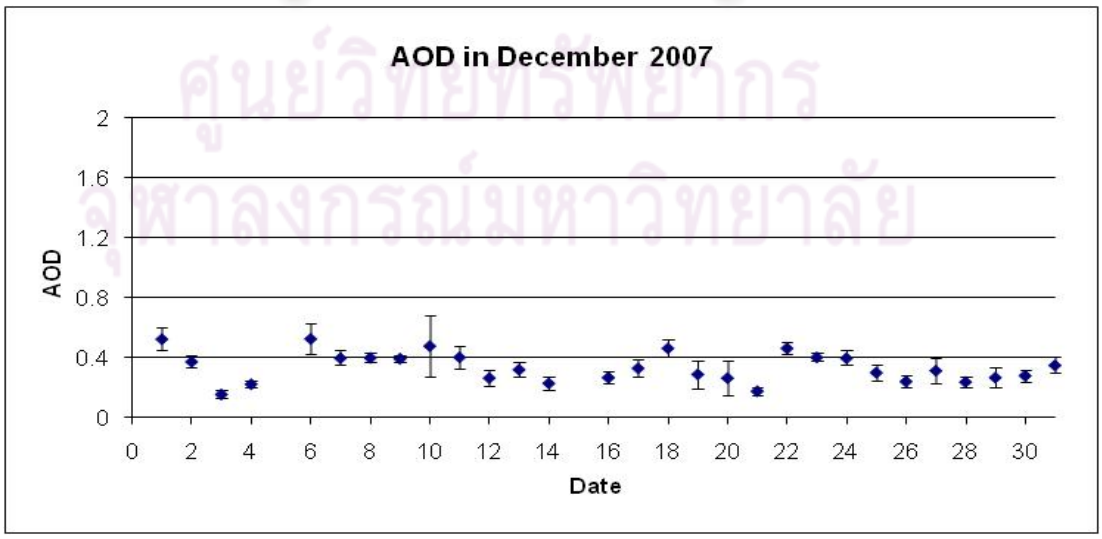

Figure A-24 Aerosol optical depths in December 2007.

APPENDIX B

Single scattering albedo

APPENDIX B

Year 2006 **Month** January

Average value 0.91 **SD** 0.03 **Min** 0.86 **Max** 0.99

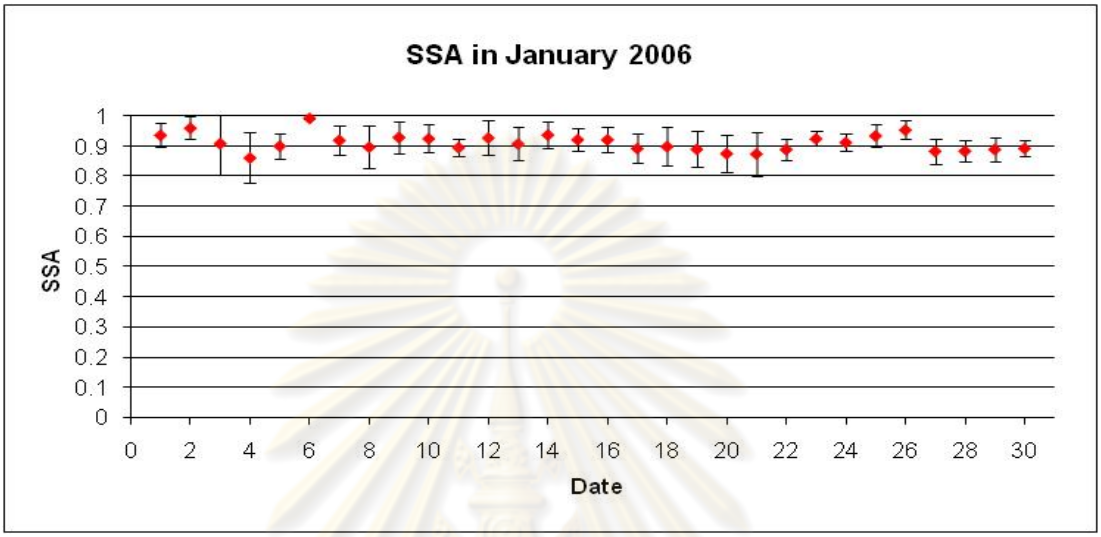

Figure B-1 Single scattering albedo in January 2006.

Year 2006 **Month** February

Average value 0.90 **SD** 0.02 **Min** 0.89 **Max** 0.97

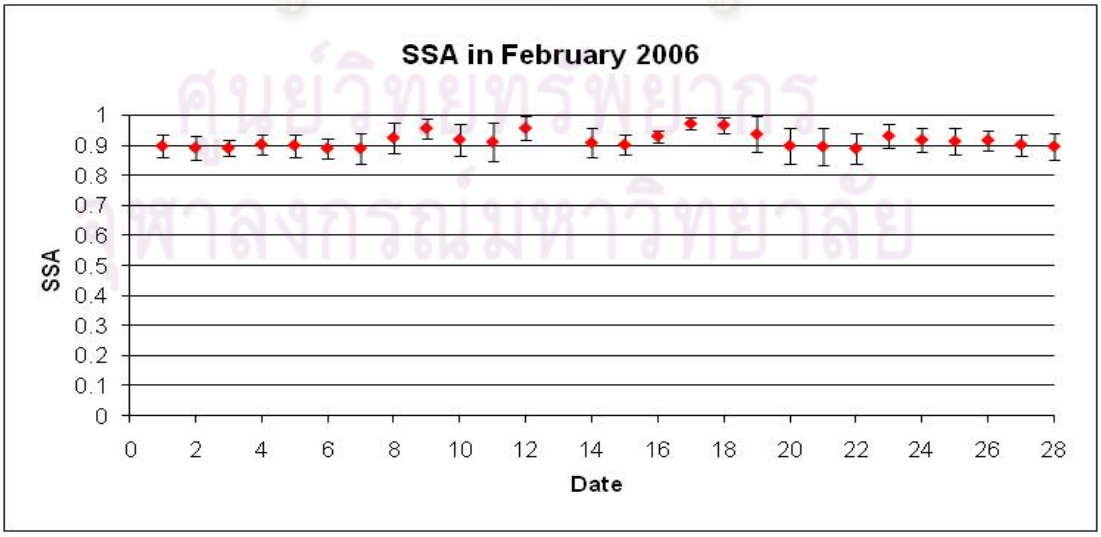

Figure B-2 Single scattering albedo in February 2006.

Year 2006 **Month** March

Average value 0.93 **SD** 0.02 **Min** 0.89 **Max** 0.95

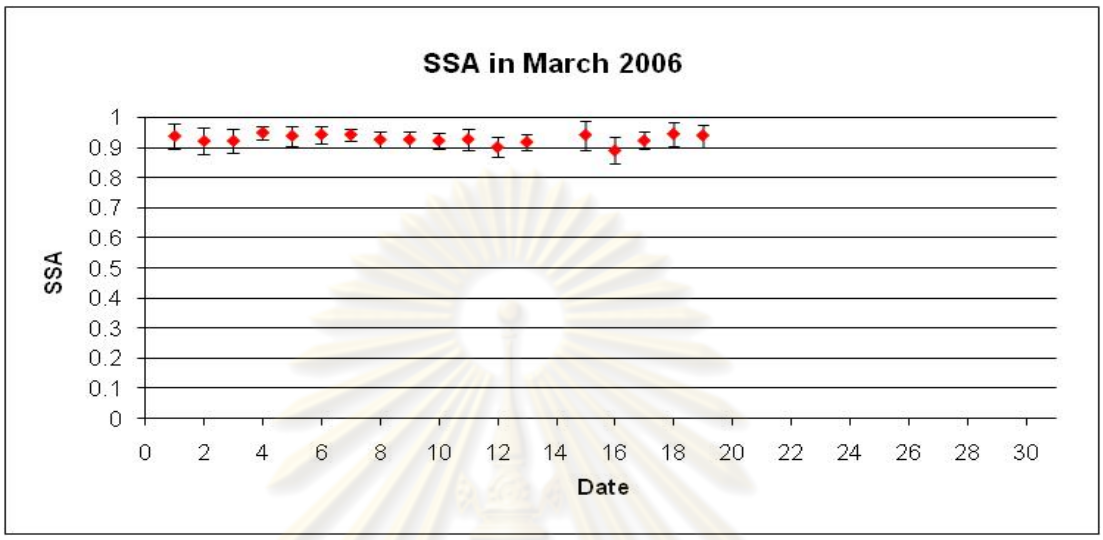

Figure B-3 Single scattering albedo in March 2006.

Year 2006 **Month** April

Average value 0.86 **SD** 0.07 **Min** 0.79 **Max** 0.96

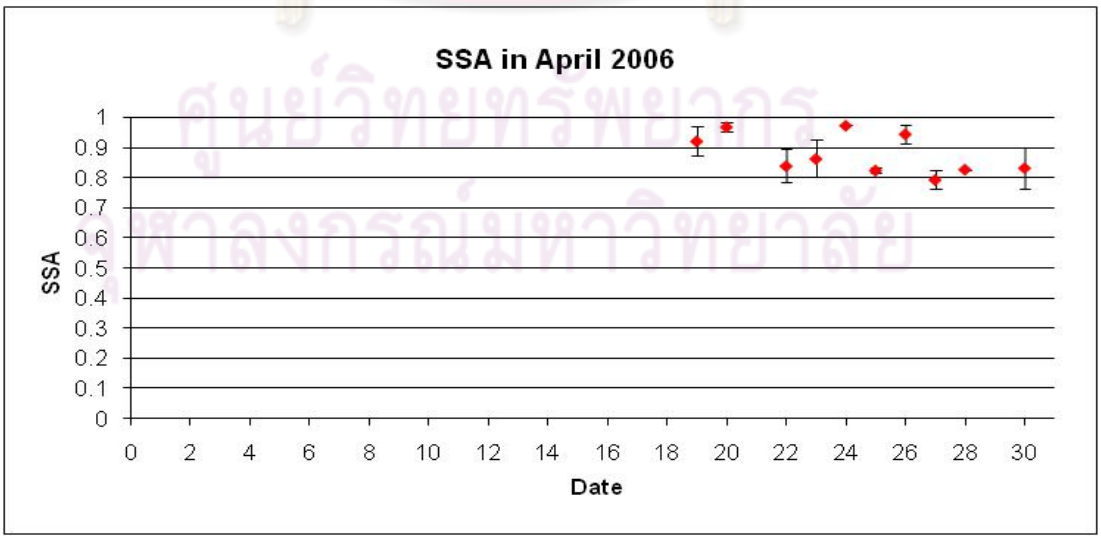

Figure B-4 Single scattering albedo in April 2006.

Year 2006 **Month** May

Average value 0.87 **SD** 0.04 **Min** 0.79 **Max** 0.96

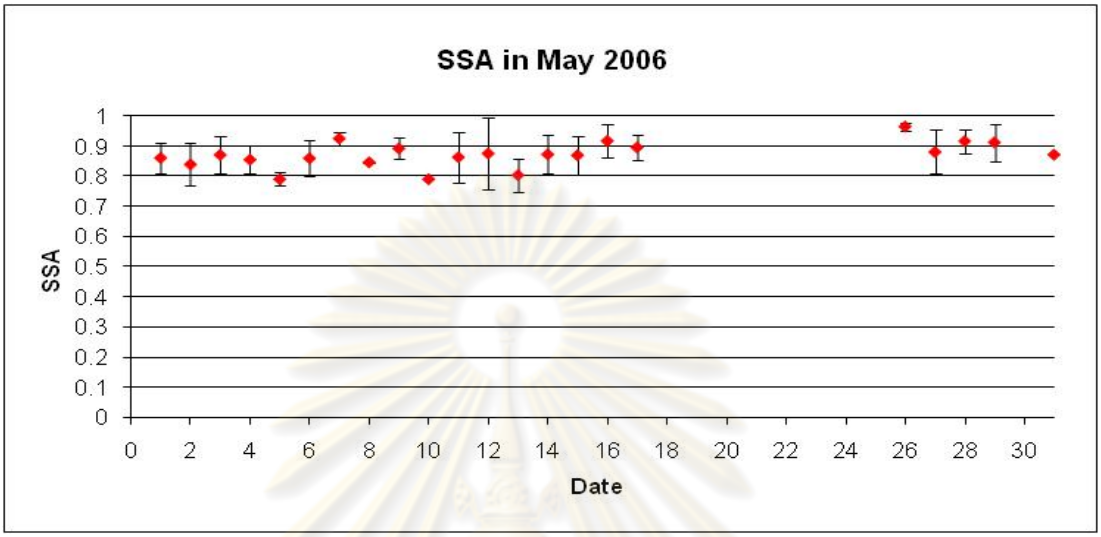

Figure B-5 Single scattering albedo in May 2006.

Year 2006 **Month** June

Average value 0.87 **SD** 0.05 **Min** 0.79 **Max** 0.93

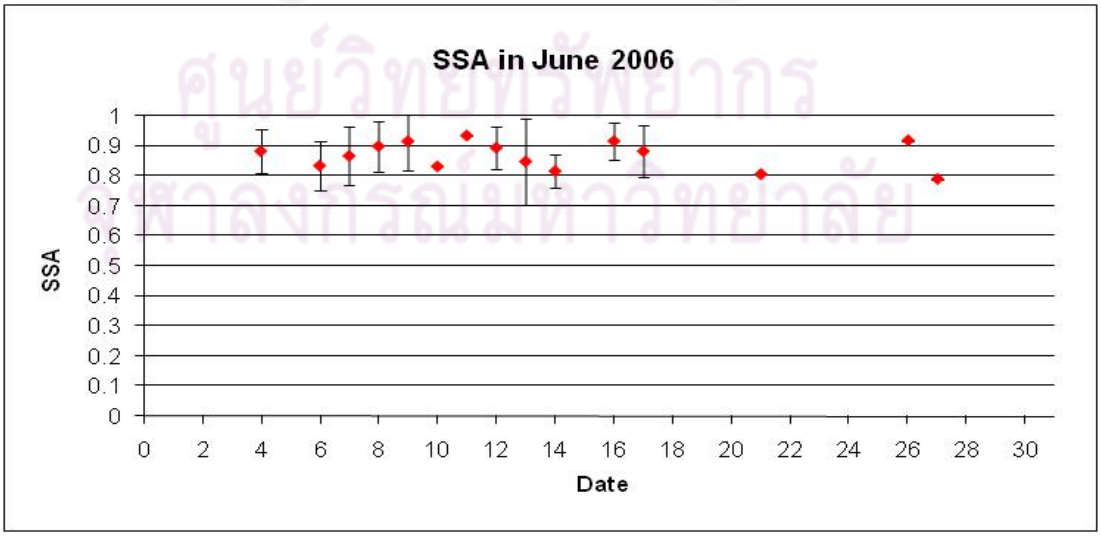

Figure B-6 Single scattering albedo in June 2006.

Year 2006 **Month** July

Average value 0.90 **SD** 0.06 **Min** 0.82 **Max** 0.96

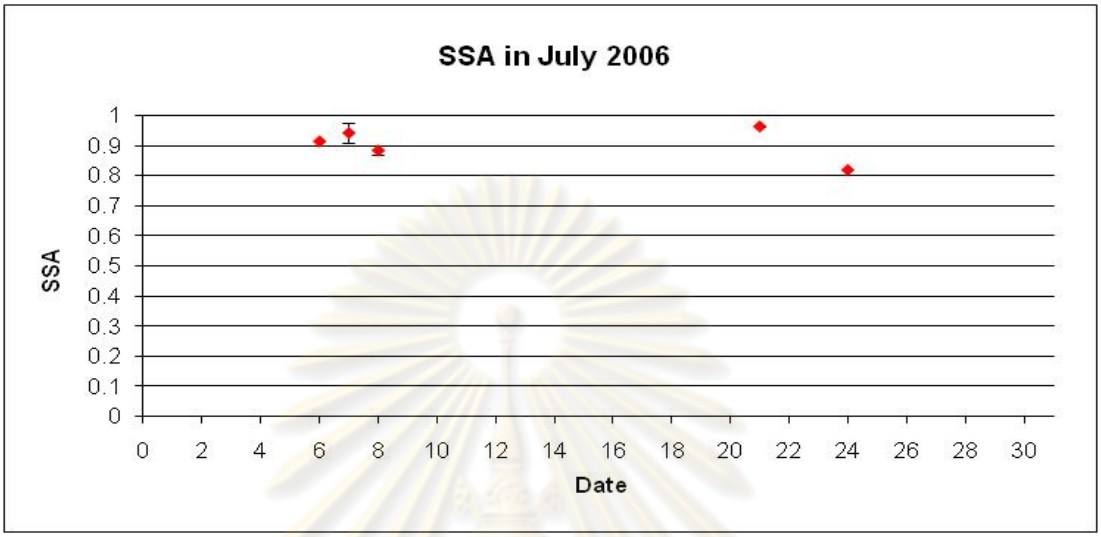

Figure B-7 Single scattering albedo in July 2006.

Year 2006 **Month** August

Average value 0.92 **SD** - **Min** 0.92 **Max** 0.92

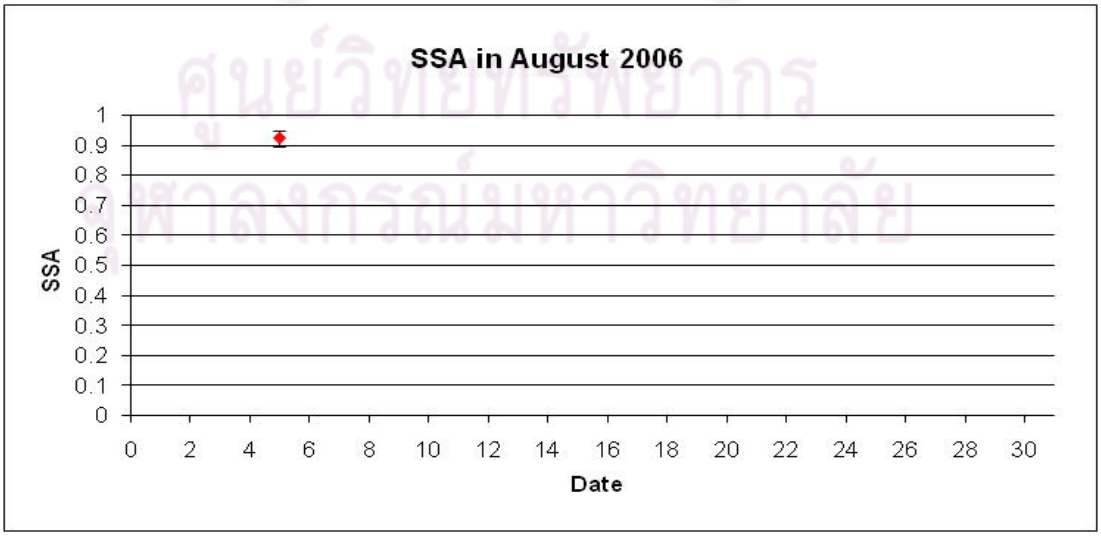

Figure B-8 Single scattering albedo in August 2006.

Year 2006 **Month** September

Average value 0.91 **SD** 0.08 **Min** 0.73 **Max** 1.00

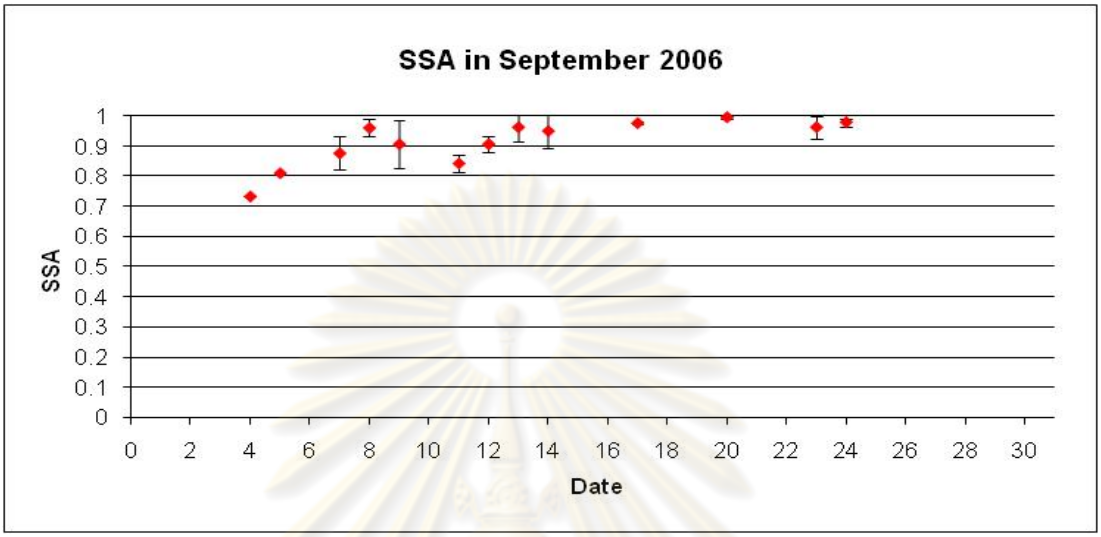

Figure B-9 Single scattering albedo in September 2006.

Year 2006 **Month** October

Average value 0.94 **SD** 0.04 **Min** 0.87 **Max** 1.00

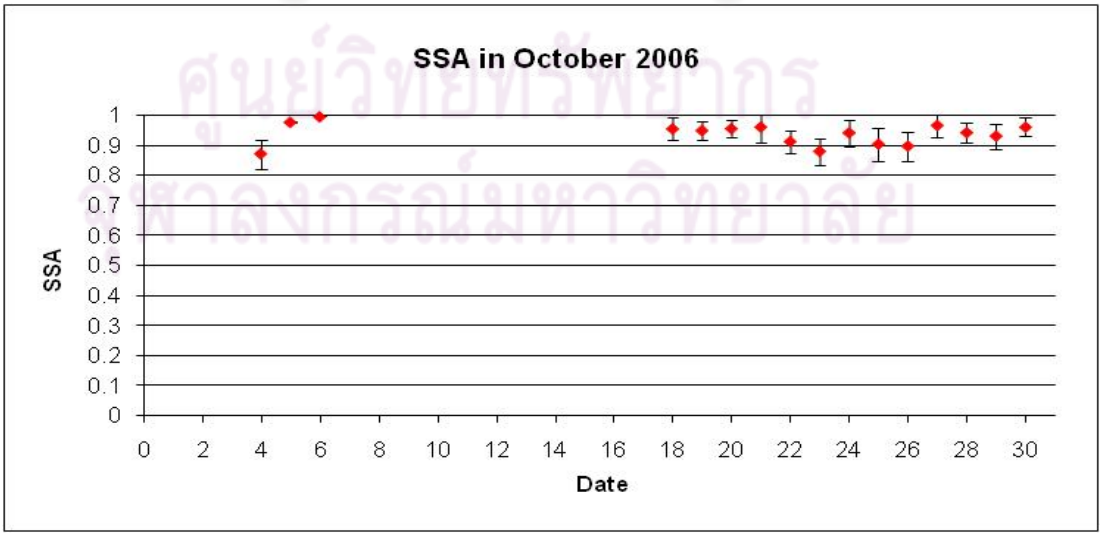

Figure B-10 Single scattering albedo in October 2006.

Year 2006 **Month** November

Average value 0.91 **SD** 0.03 **Min** 0.85 **Max** 0.98

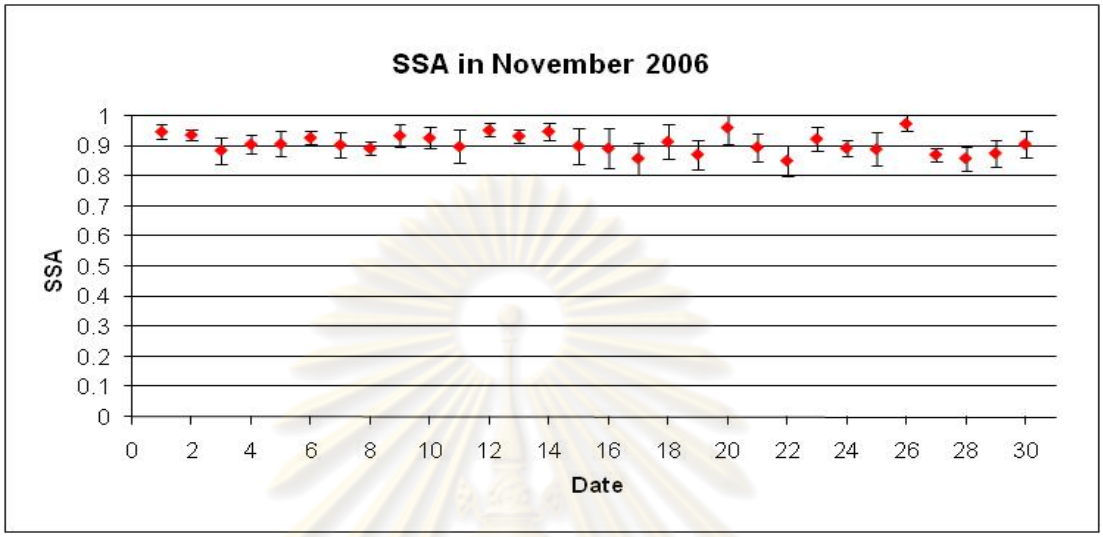

Figure B-11 Single scattering albedo in November 2006.

Year 2006 **Month** December

Average value 0.90 **SD** 0.03 **Min** 0.83 **Max** 0.96

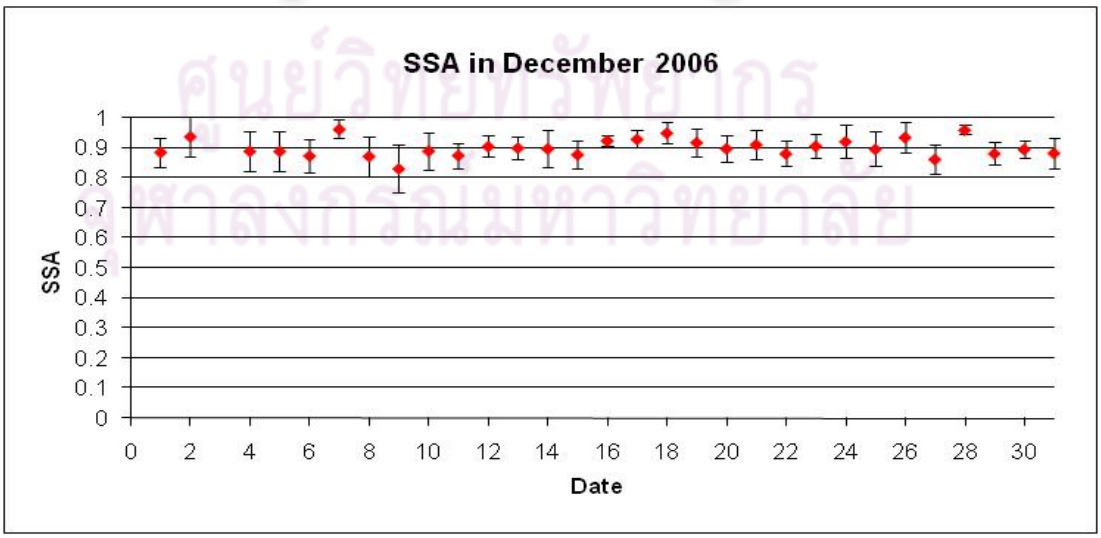

Figure B-12 Single scattering albedo in December 2006.

Year 2007 **Month** January

Average value 0.87 **SD** 0.04 **Min** 0.80 **Max** 0.96

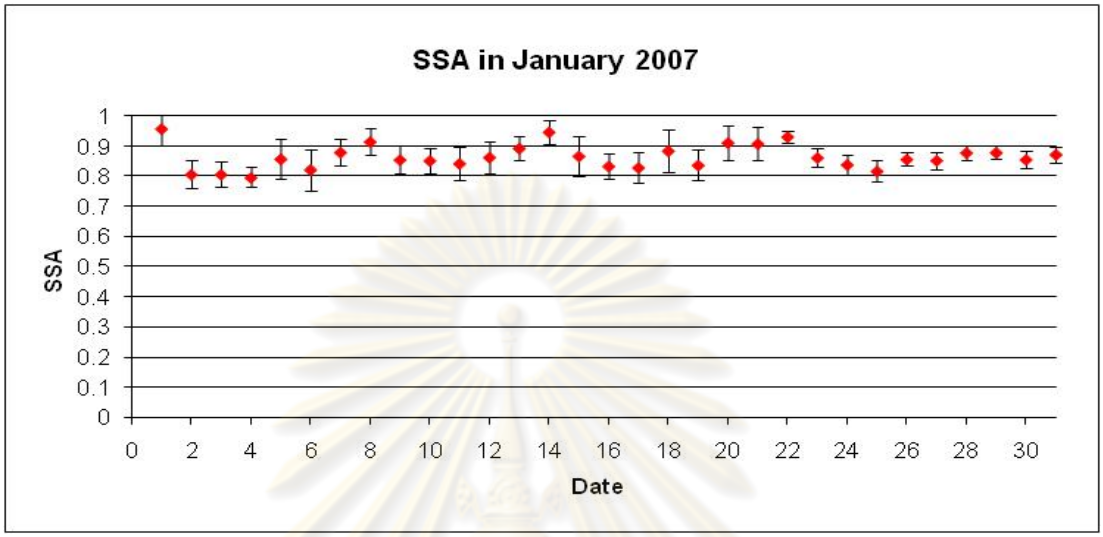

Figure B-13 Single scattering albedo in Januray 2007.

Year 2007 **Month** February

Average value 0.88 **SD** 0.03 **Min** 0.83 **Max** 0.94

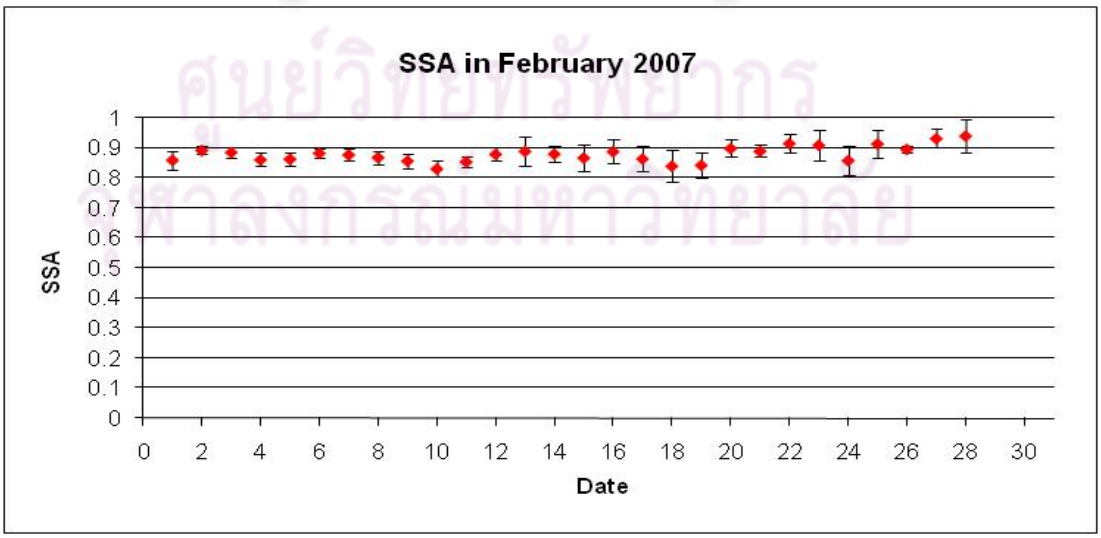

Figure B-14 Single scattering albedo in February 2007.

Year 2007 **Month** March

Average value 0.90 **SD** 0.02 **Min** 0.84 **Max** 0.95

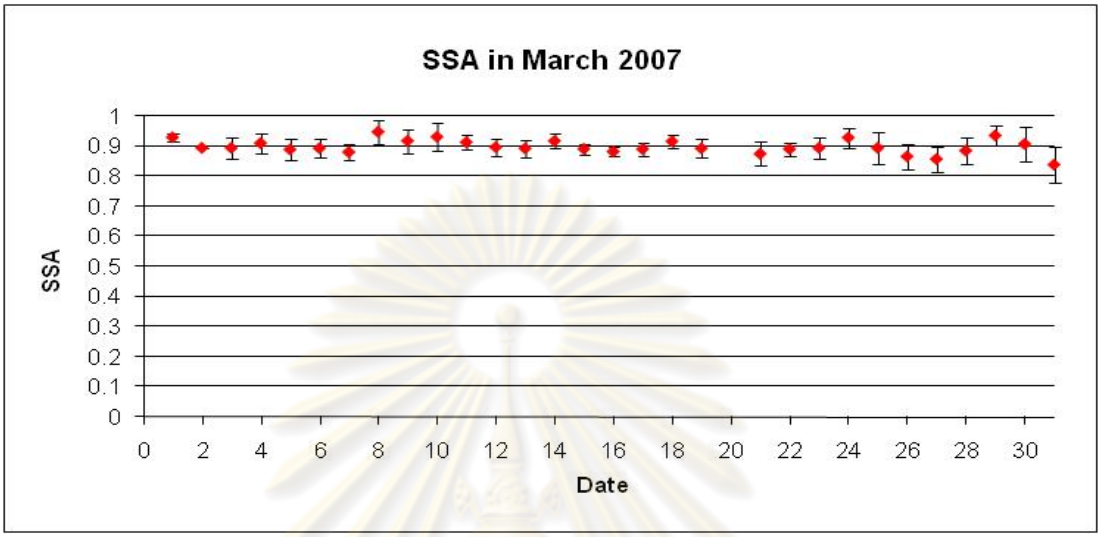

Figure B-15 Single scattering albedo in March 2007.

Year 2007 **Month** April

Average value 0.88 **SD** 0.04 **Min** 0.80 **Max** 0.95

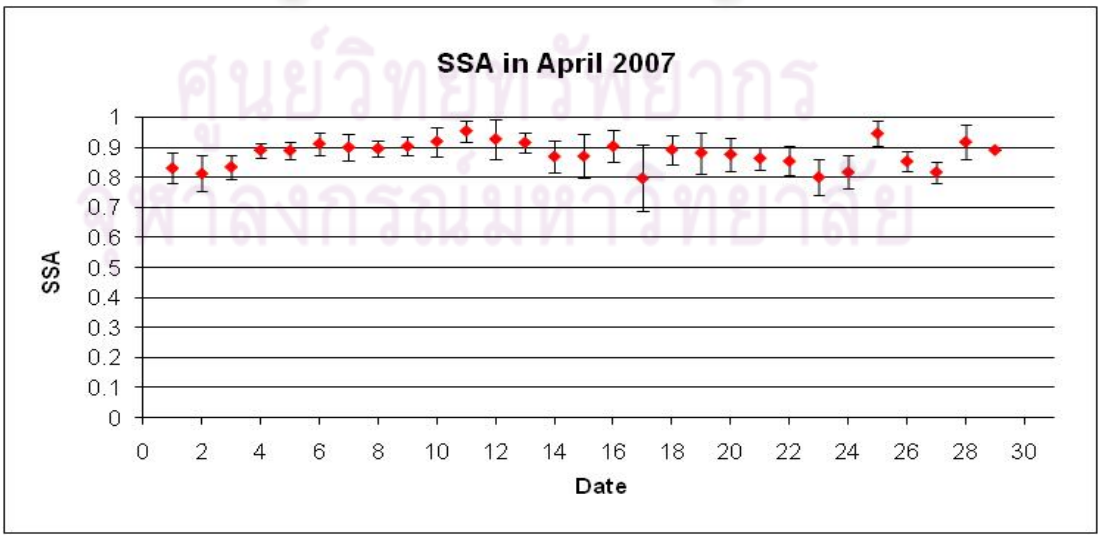

Figure B-16 Single scattering albedo in April 2007.

Year 2007 **Month** May

Average value 0.86 **SD** 0.07 **Min** 0.67 **Max** 0.98

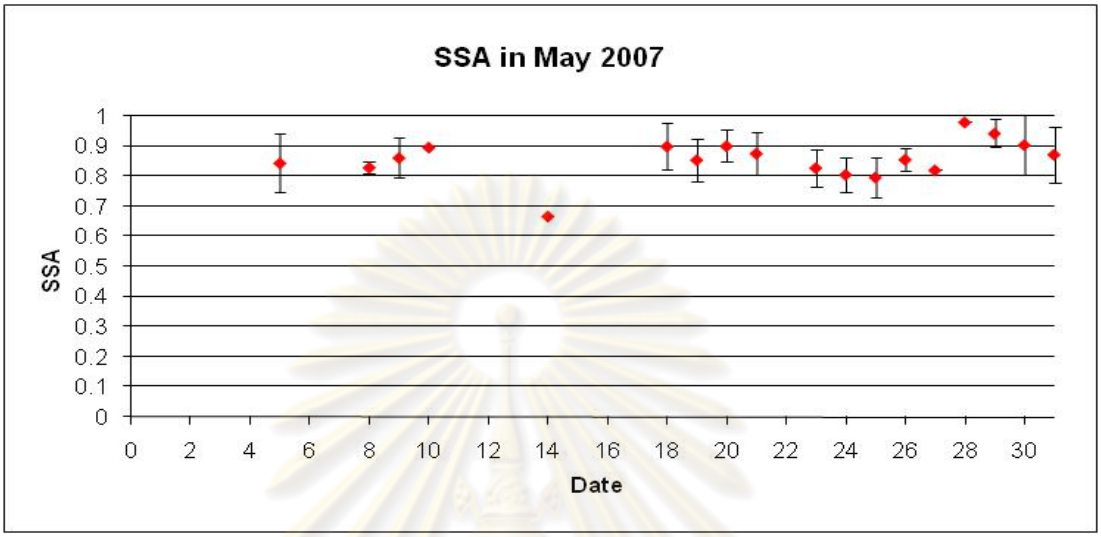

Figure B-17 Single scattering albedo in May 2007.

Year 2007 **Month** June

Average value 0.86 **SD** 0.04 **Min** 0.80 **Max** 0.93

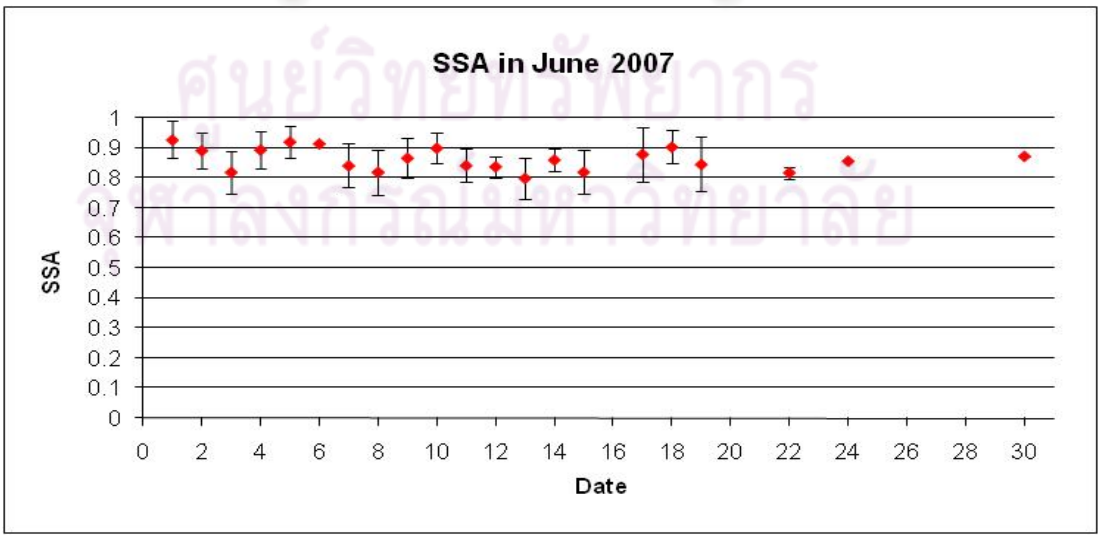

Figure B-18 Single scattering albedo in June 2007.

Year 2007 **Month** July

Average value 0.85 **SD** 0.07 **Min** 0.70 **Max** 0.96

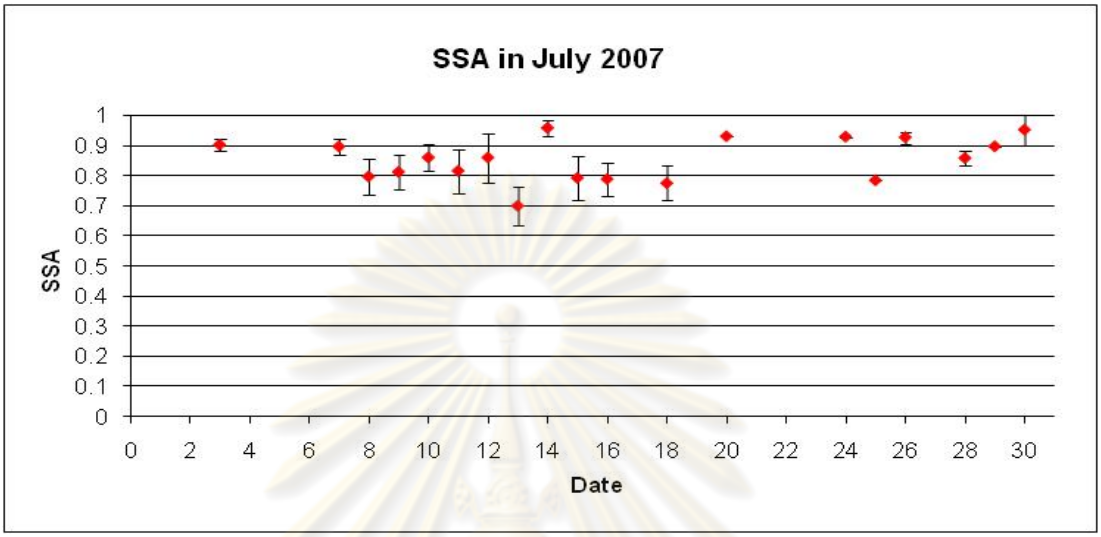

Figure B-19 Single scattering albedo in July 2007.

Year 2007 **Month** August

Average value 0.84 **SD** 0.08 **Min** 0.64 **Max** 0.93

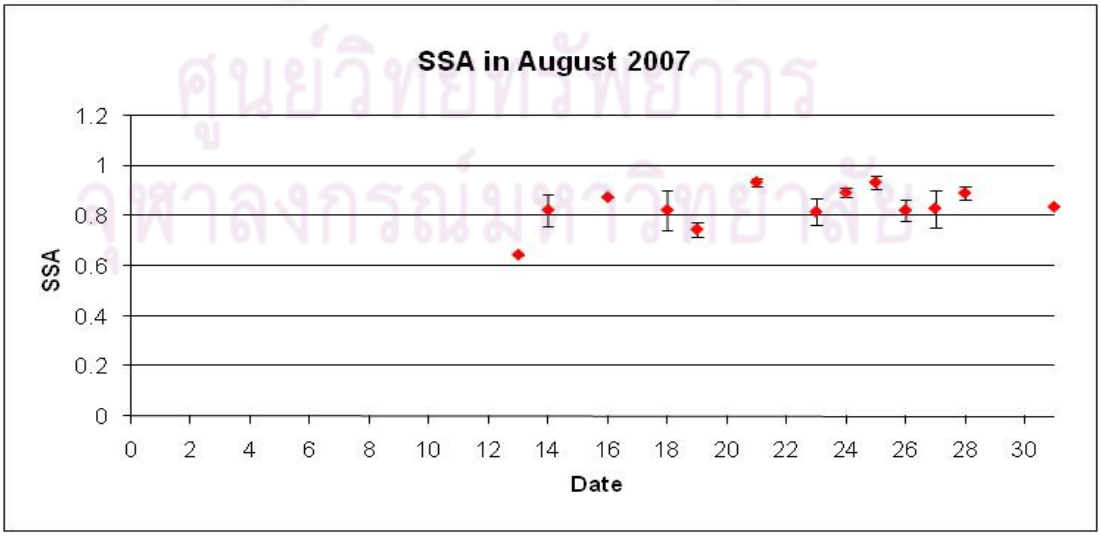

Figure B-20 Single scattering albedo in August 2007.

Year 2007 **Month** September

Average value 0.87 **SD** 0.06 **Min** 0.80 **Max** 0.99

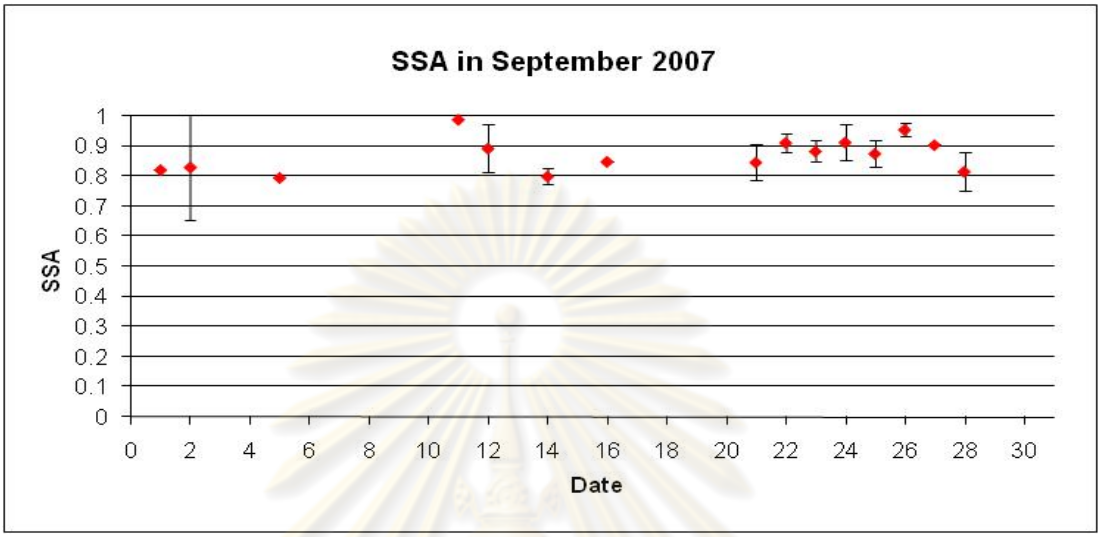

Figure B-21 Single scattering albedo in September 2007.

Year 2007 **Month** October

Average value 0.90 **SD** 0.04 **Min** 0.84 **Max** 1.00

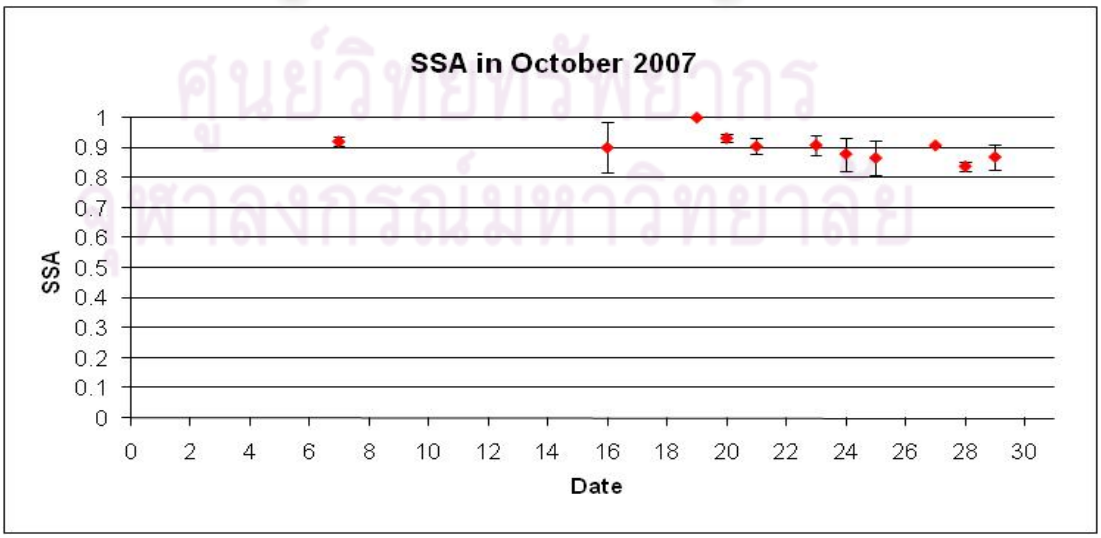

Figure B-22 Single scattering albedo in October 2007.

Year 2007 **Month** November

Average value 0.84 **SD** 0.03 **Min** 0.79 **Max** 0.92

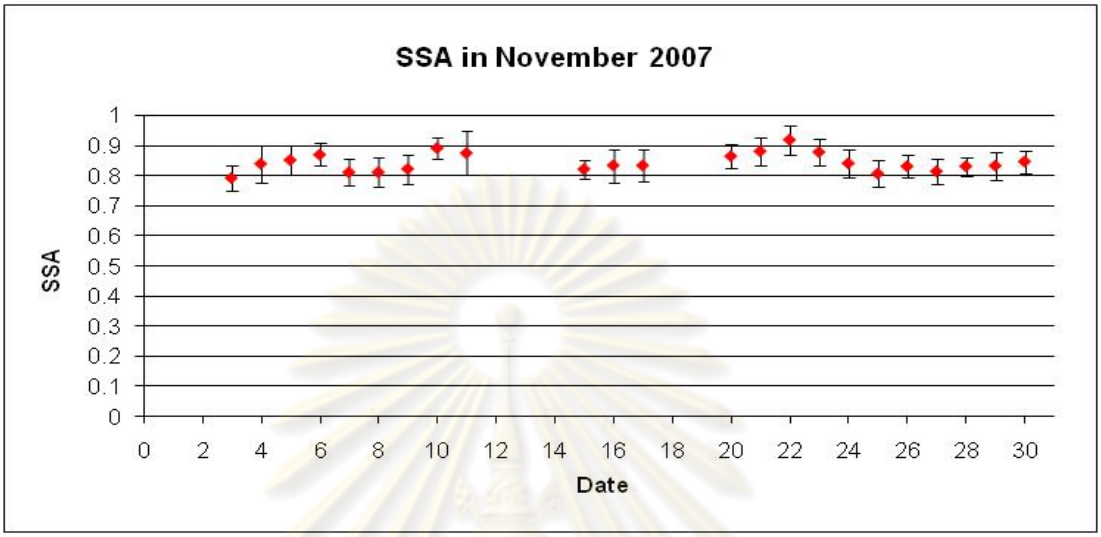

Figure B-23 Single scattering albedo in November 2007.

Year 2007 **Month** December

Average value 0.83 **SD** 0.03 **Min** 0.77 **Max** 0.87

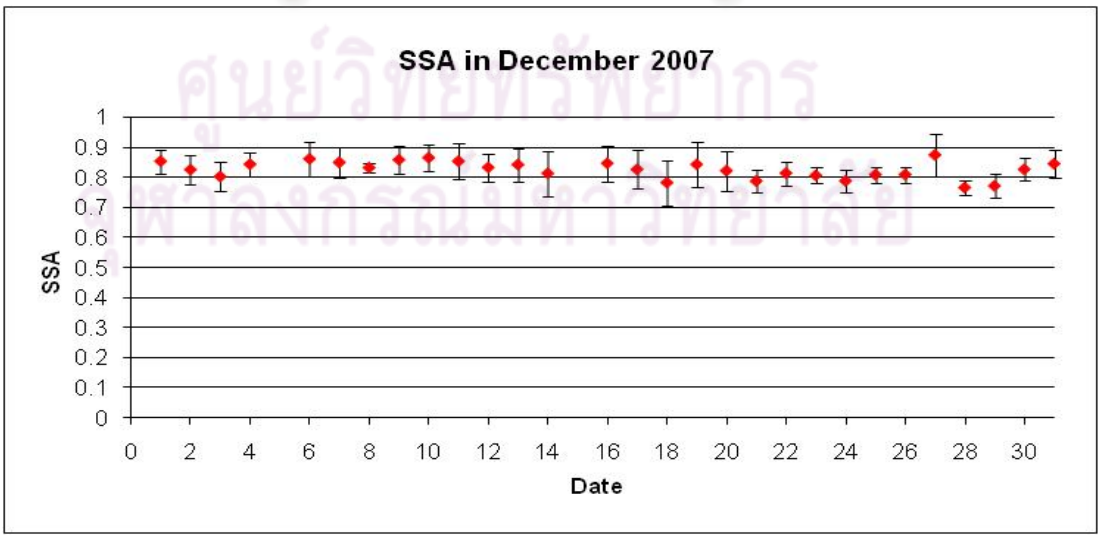

Figure B-24 Single scattering albedo in December 2007.

APPENDIX C

Volume size distribution

APPENDIX C

Year 2006 **Month** January

Fine mode 0.1729 micrometer **Coarse mode** 16.54 micrometer or larger

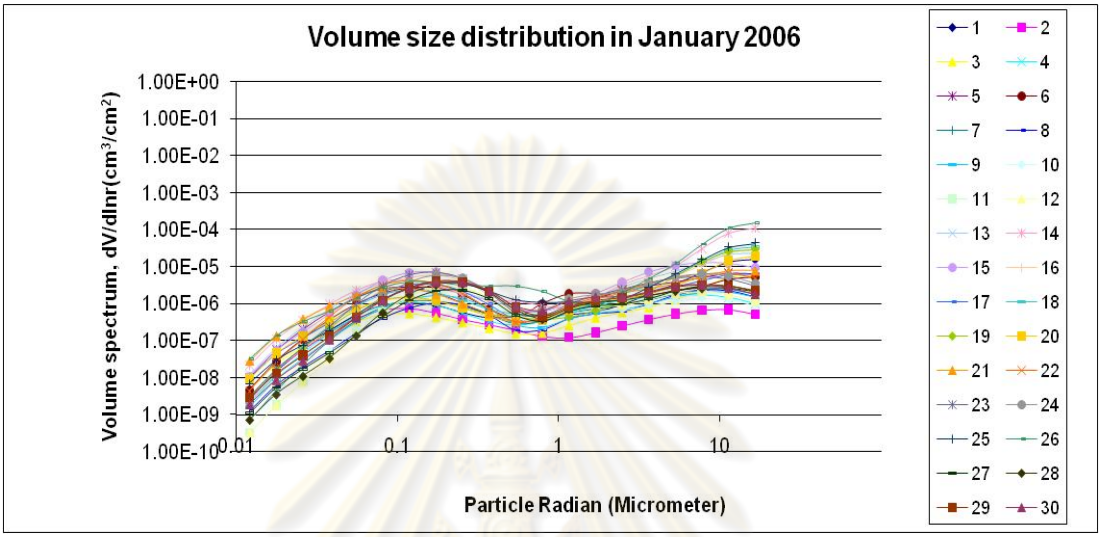

Figure C-1 Volume size distributions in January 2006.

Year 2006 **Month** February

Fine mode 0.1729 micrometer **Coarse mode** 11.31 micrometer

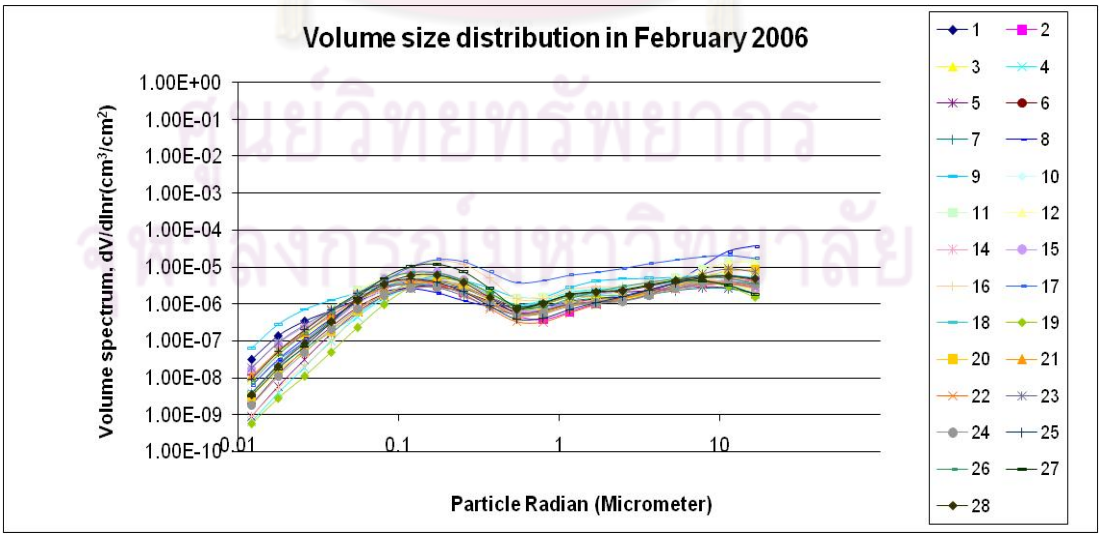

Figure C-2 Volume size distributions in February 2006.

Year	2006	**Month**	March
Fine mode	0.1729 micrometer	**Coarse mode**	16.54 micrometer or larger

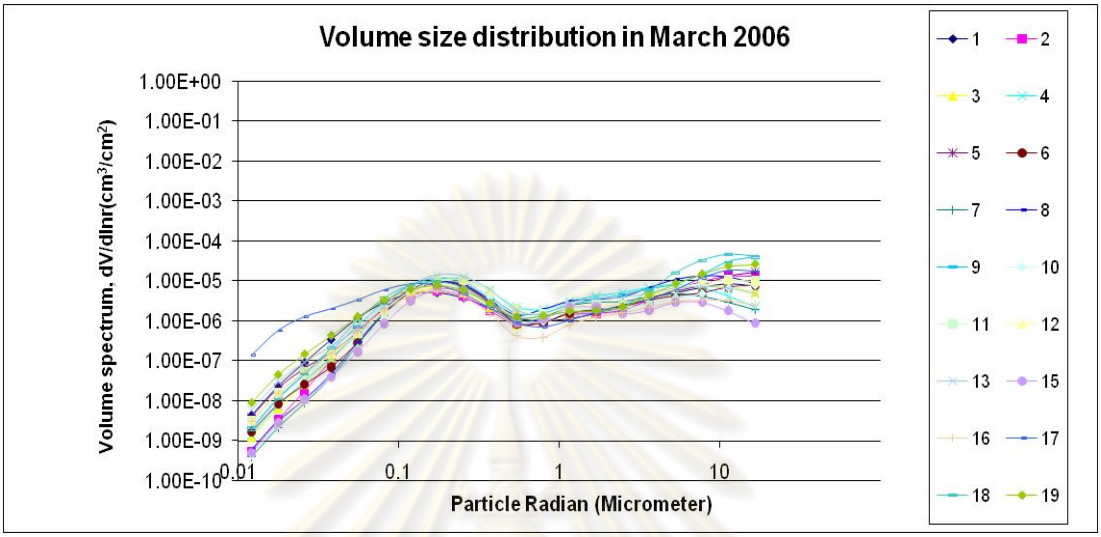

Figure C-3 Volume size distributions in March 2006.

Year	2006	**Month**	April
Fine mode	0.1183 micrometer	**Coarse mode**	16.54 micrometer or larger

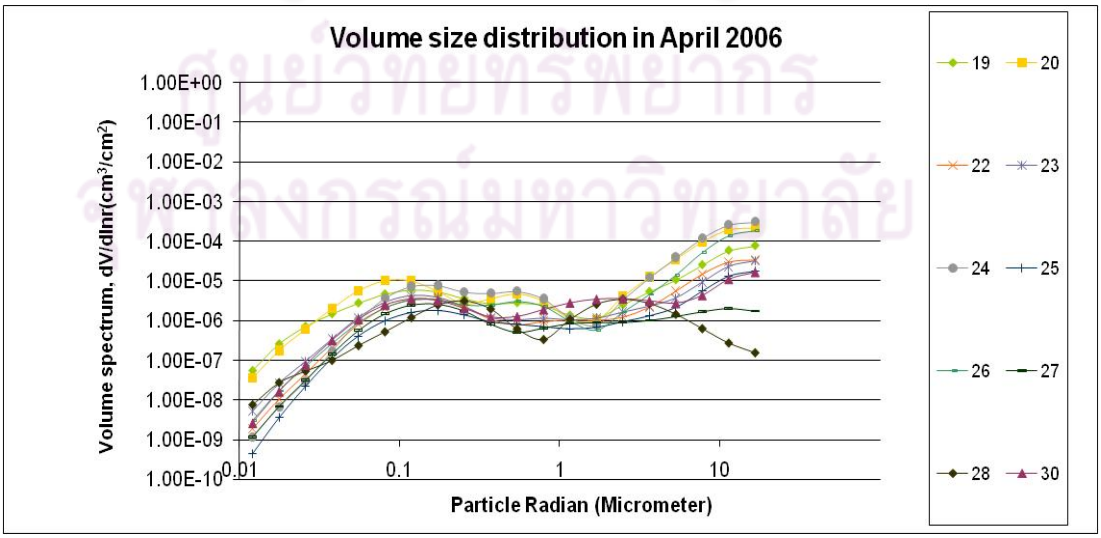

Figure C-4 Volume size distributions in April 2006.

Year	2006	**Month**	May
Fine mode	0.1183 micrometer	**Coarse mode**	16.54 micrometer or larger

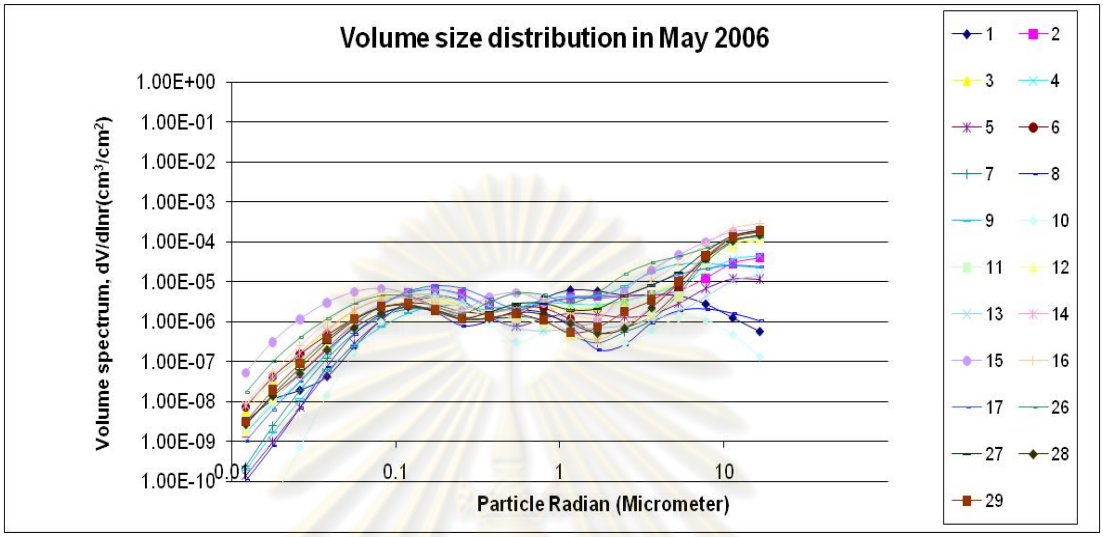

Figure C-5 Volume size distributions in May 2006.

Year	2006	**Month**	June
Fine mode	0.1183 micrometer	**Coarse mode**	16.54 micrometer or larger

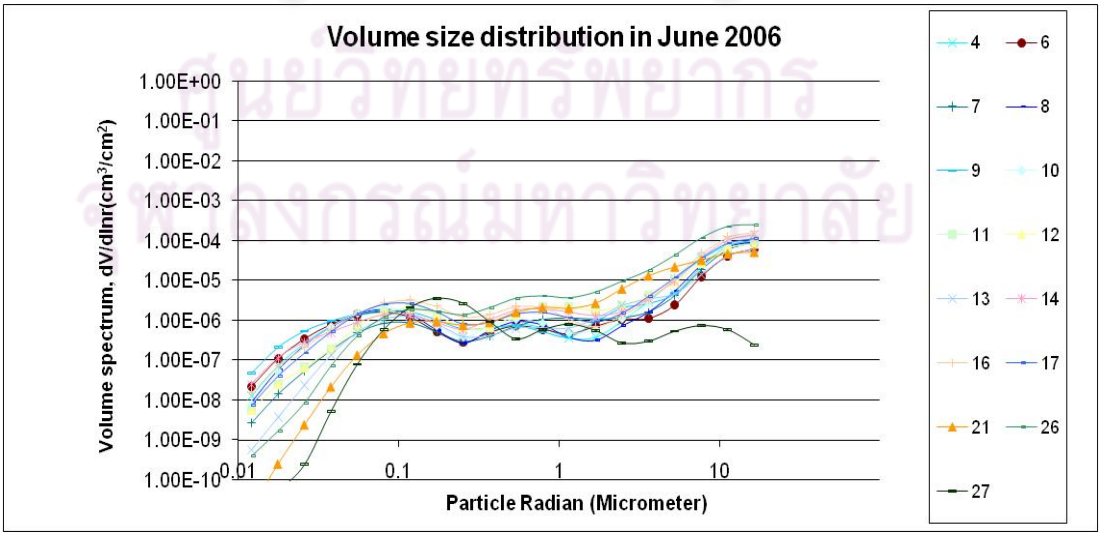

Figure C-6 Volume size distributions in June 2006.

Year	2006	**Month**	July
Fine mode	0.1729 micrometer	**Coarse mode**	16.54 micrometer or larger

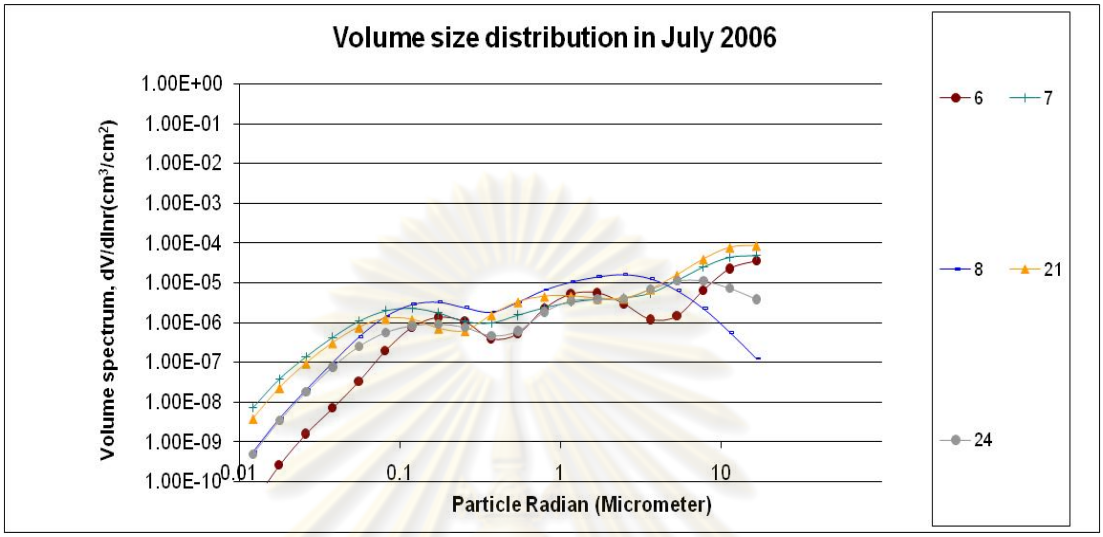

Figure C-7 Volume size distributions in July 2006.

Year	2006	**Month**	August
Fine mode	0.2529 micrometer	**Coarse mode**	11.31 micrometer

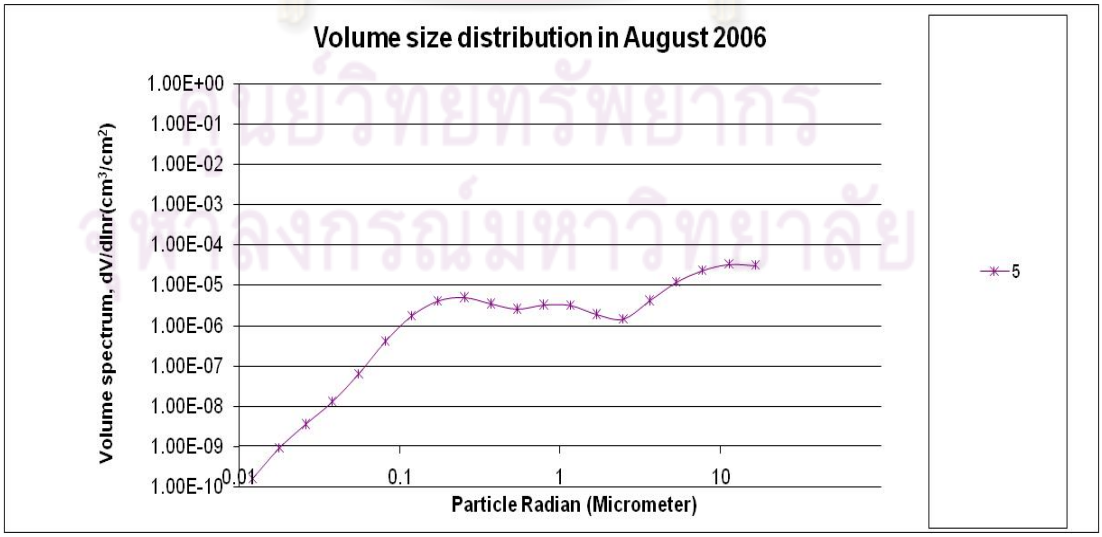

Figure C-8 Volume size distributions in August 2006.

Year	2006	**Month**	September
Fine mode	0.1729 micrometer	**Coarse mode**	16.54 micrometer or larger

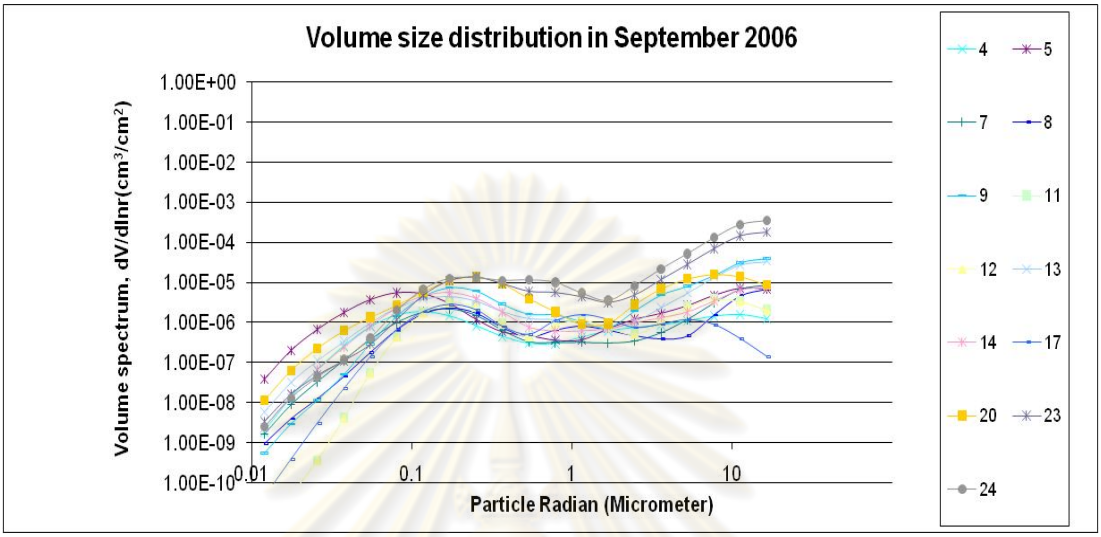

Figure C-9 Volume size distributions in September 2006.

Year	2006	**Month**	October
Fine mode	0.2529 micrometer	**Coarse mode**	16.54 micrometer or larger

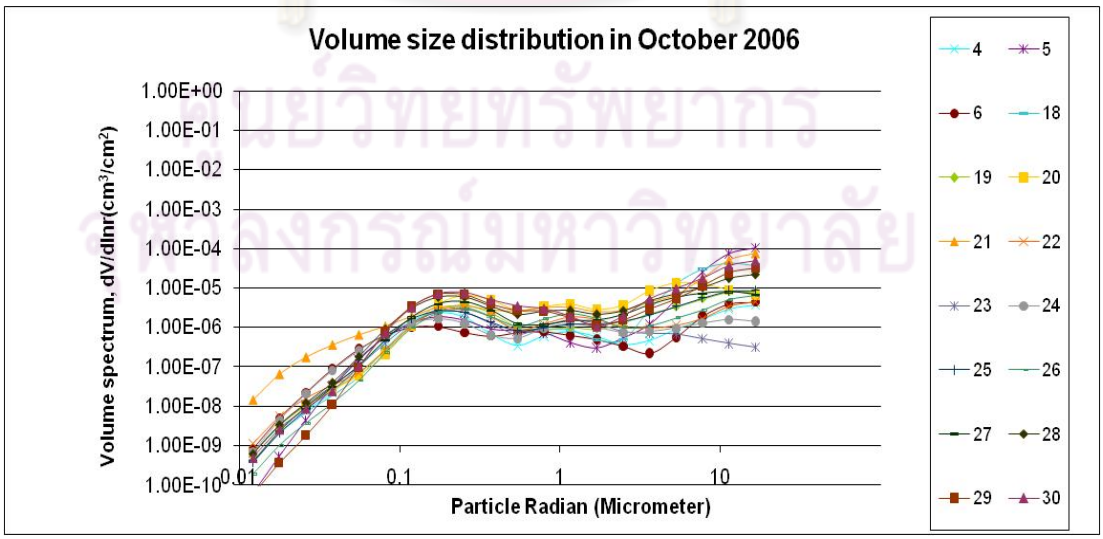

Figure C-10 Volume size distributions in October 2006.

Year	2006	**Month**	November
Fine mode	0.1729 micrometer	**Coarse mode**	16.54 micrometer or larger

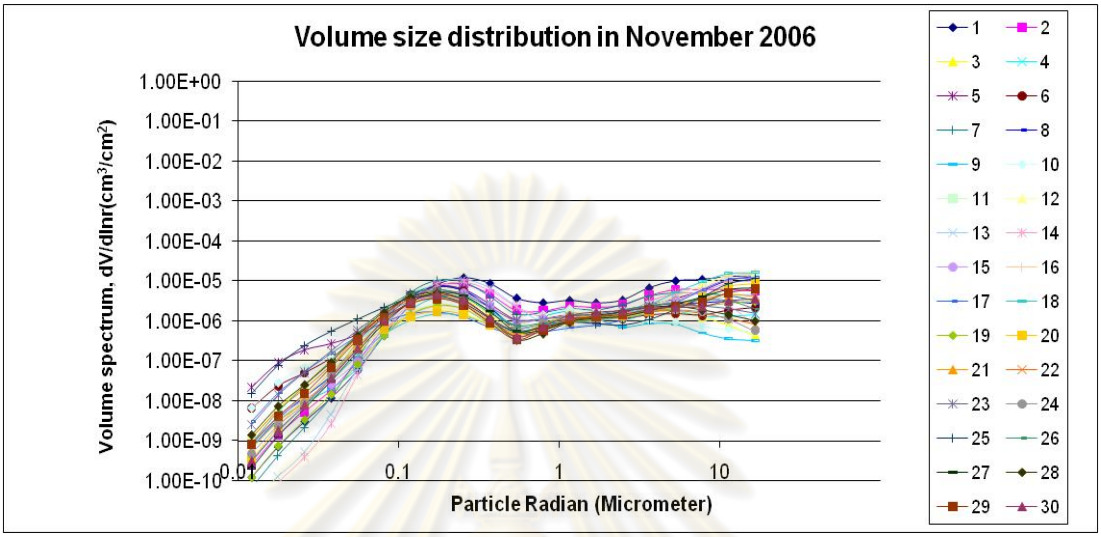

Figure C-11 Volume size distributions in November 2006.

Year	2006	**Month**	December
Fine mode	0.1729 micrometer	**Coarse mode**	16.54 micrometer or larger

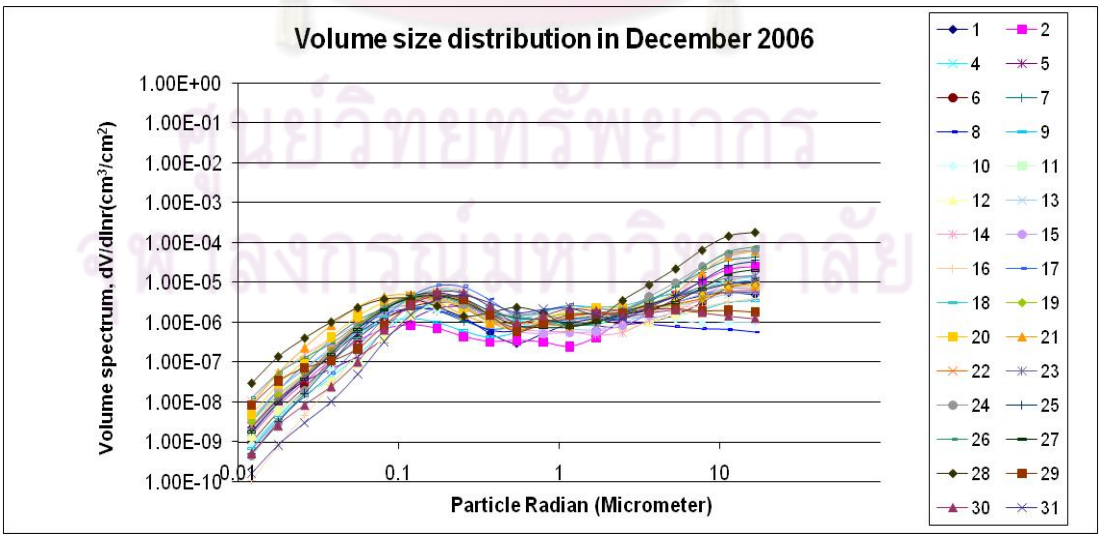

Figure C-12 Volume size distributions in December 2006.

Year 2007 **Month** January

Fine mode 0.1729 micrometer **Coarse mode** 16.54 micrometer or larger

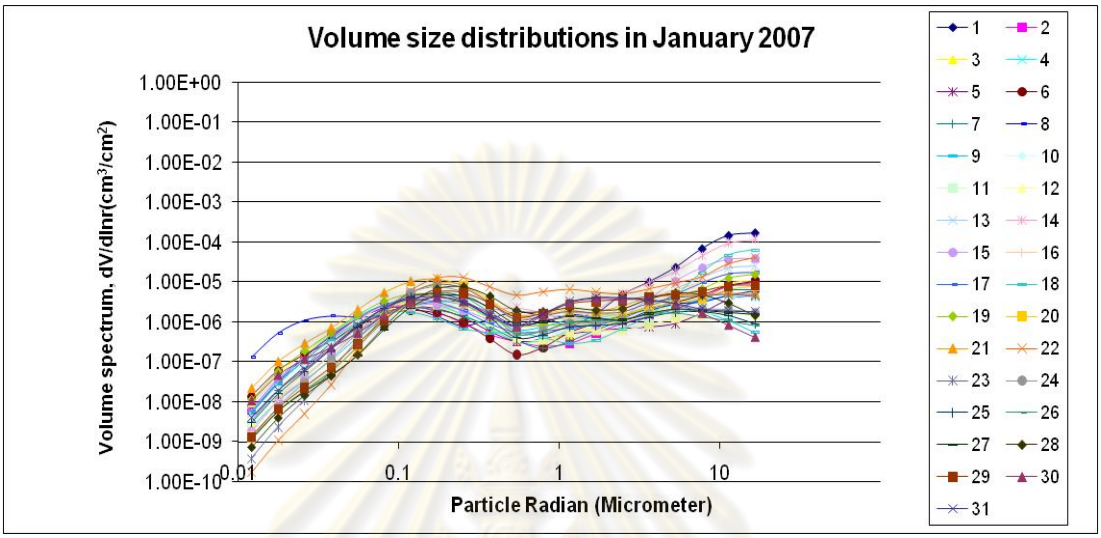

Figure C-13 Volume size distributions in January 2007.

Year 2007 **Month** February

Fine mode 0.1729 micrometer **Coarse mode** 16.54 micrometer or larger

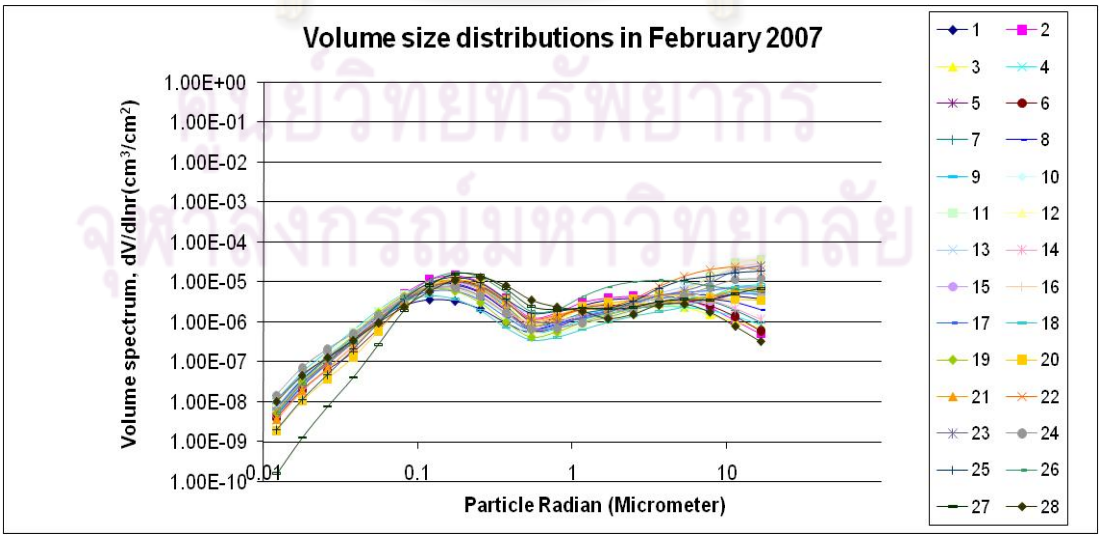

Figure C-14 Volume size distributions in February 2007.

Year	2007	**Month**	March
Fine mode	0.1729 micrometer	**Coarse mode**	16.54 micrometer or larger

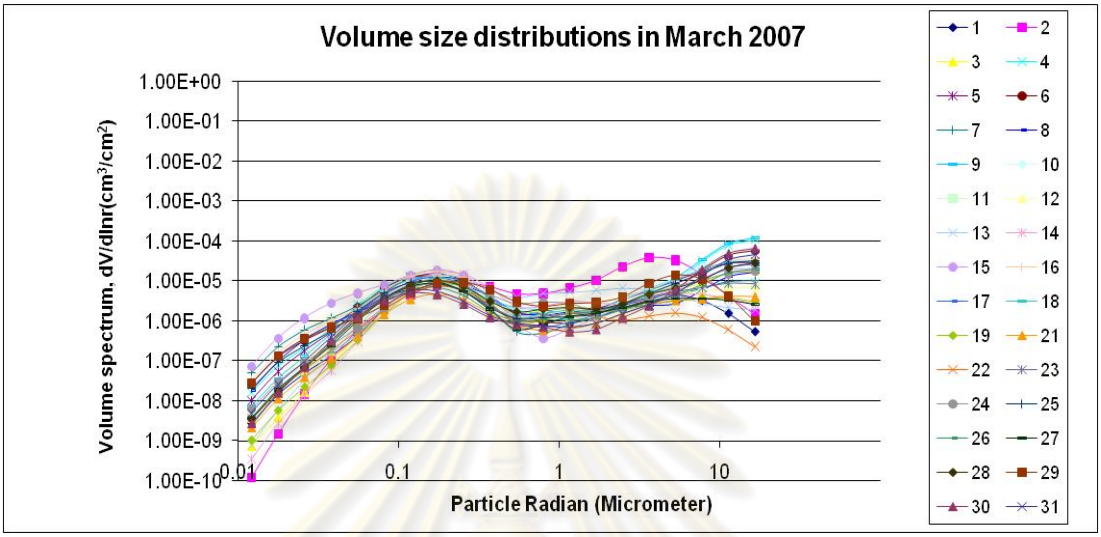

Figure C-15 Volume size distributions in March 2007.

Year	2007	**Month**	April
Fine mode	0.1729 micrometer	**Coarse mode**	16.54 micrometer or larger

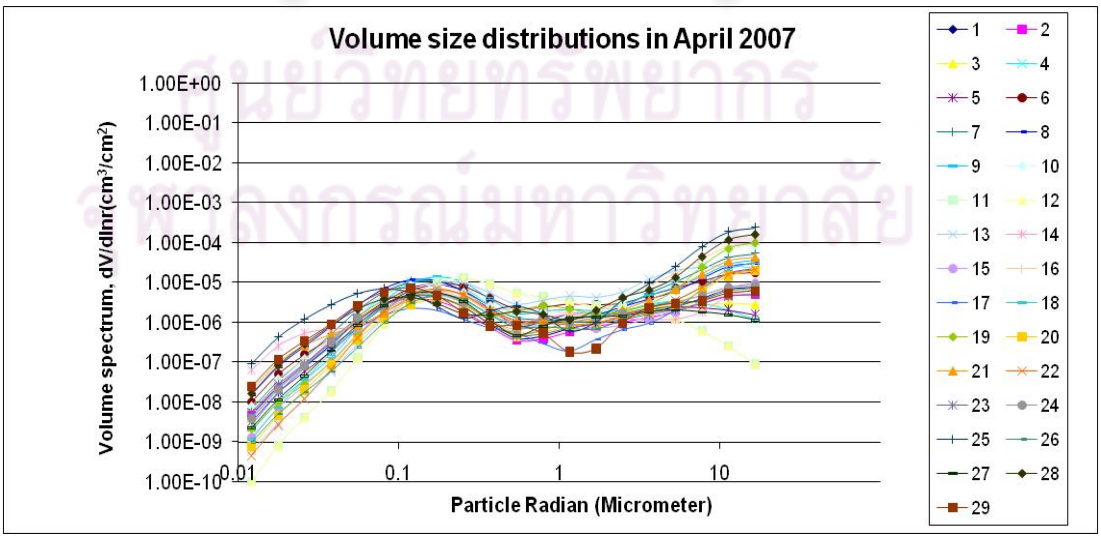

Figure C-16 Volume size distributions in April 2007.

Year	2007	**Month**	May
Fine mode	0.1183 micrometer	**Coarse mode**	16.54 micrometer or larger

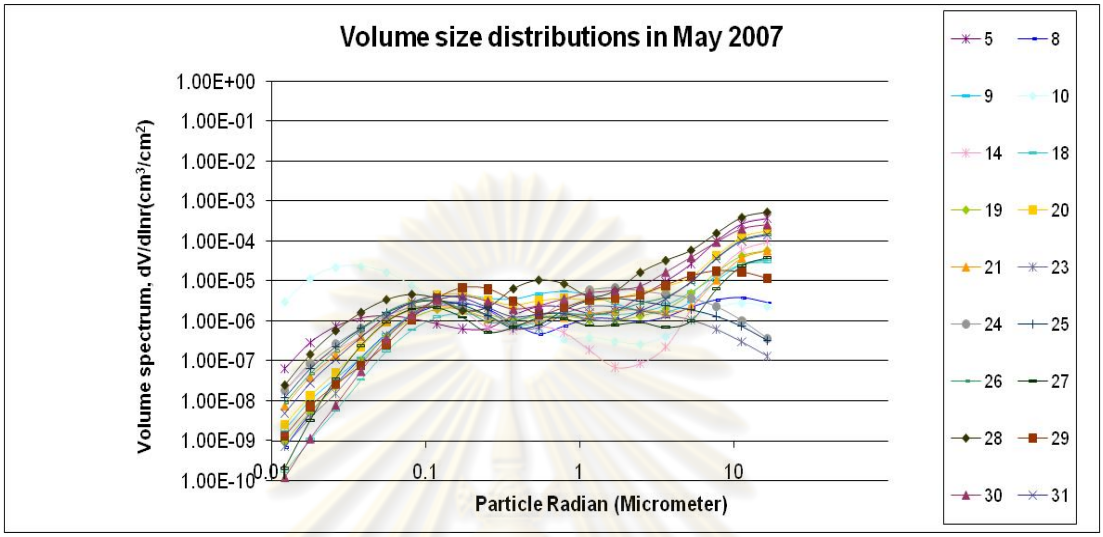

Figure C-17 Volume size distributions in May 2007.

Year	2007	**Month**	June
Fine mode	0.1183 micrometer	**Coarse mode**	16.54 micrometer or larger

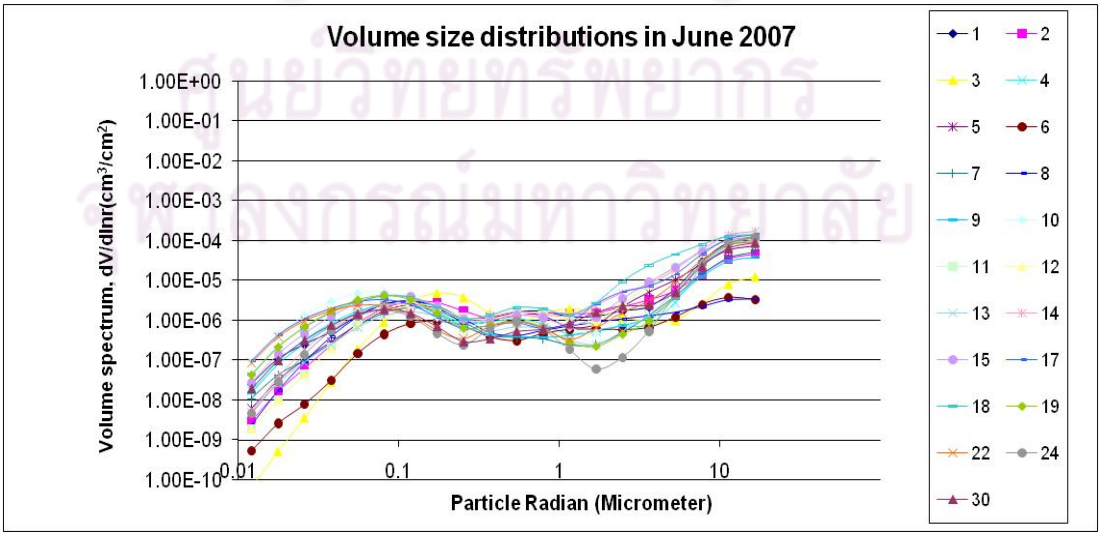

Figure C-18 Volume size distributions in June 2007.

Year	2007	Month	July
Fine mode	0.1183 micrometer	Coarse mode	16.54 micrometer or larger

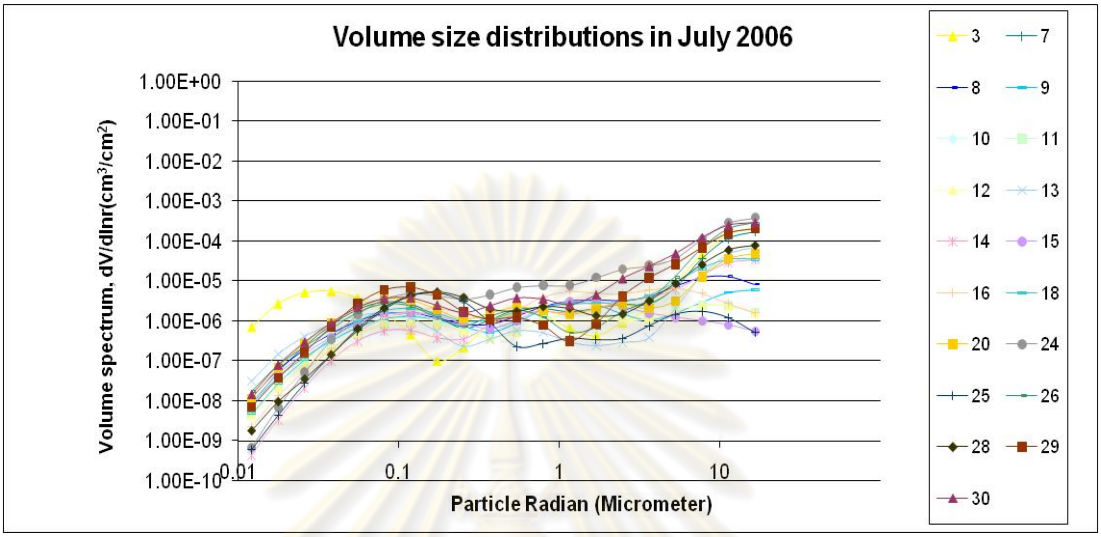

Figure C-19 Volume size distributions in July 2007.

Year	2007	Month	August
Fine mode	0.1183 micrometer	Coarse mode	16.54 micrometer or larger

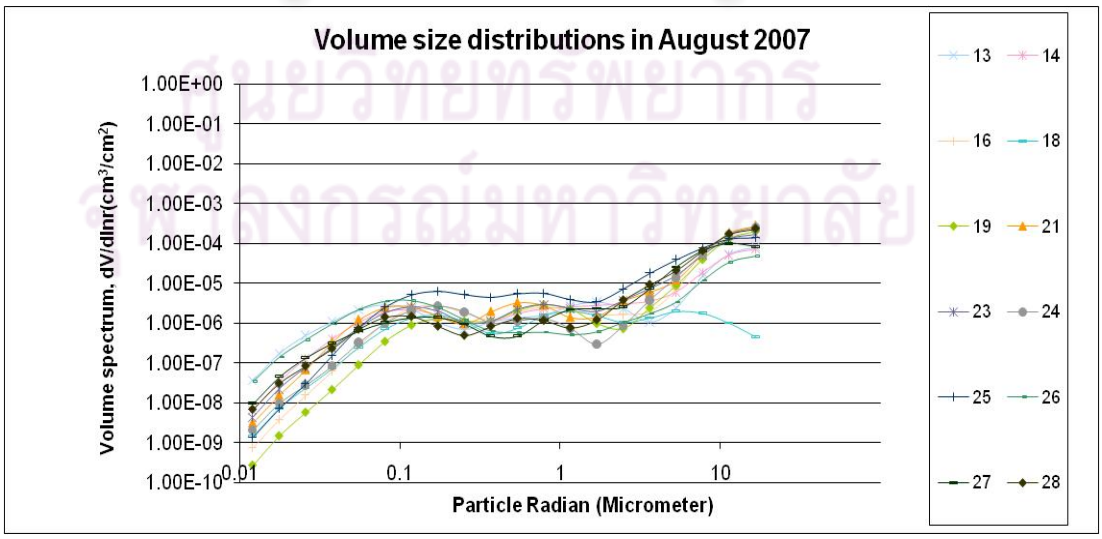

Figure C-20 Volume size distributions in August 2007.

Year	2007	**Month**	September
Fine mode	0.1729 micrometer	**Coarse mode**	16.54 micrometer or larger

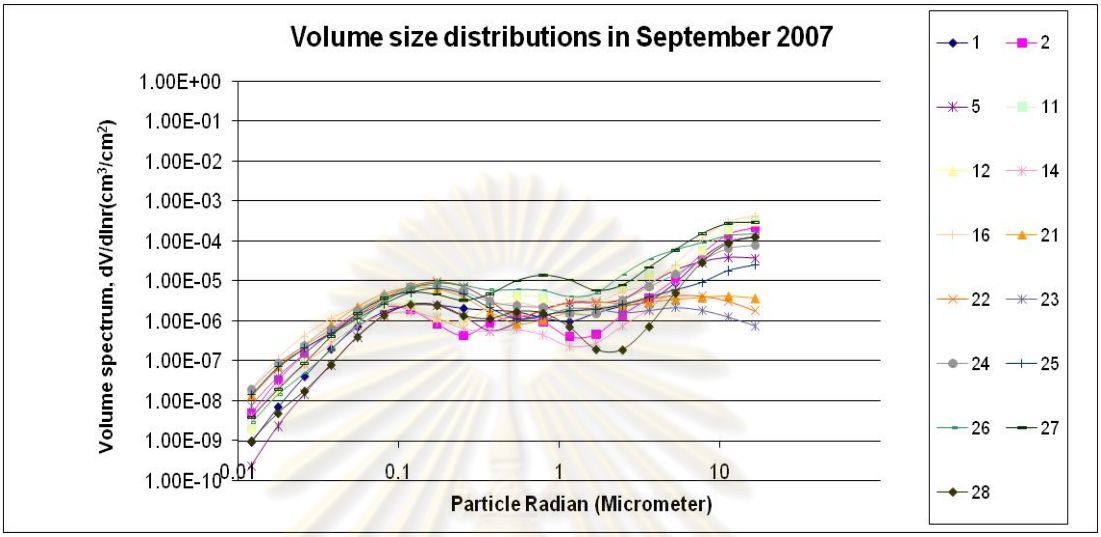

Figure C-21 Volume size distributions in September 2007.

Year	2007	**Month**	October
Fine mode	0.2529 micrometer	**Coarse mode**	16.54 or micrometer larger

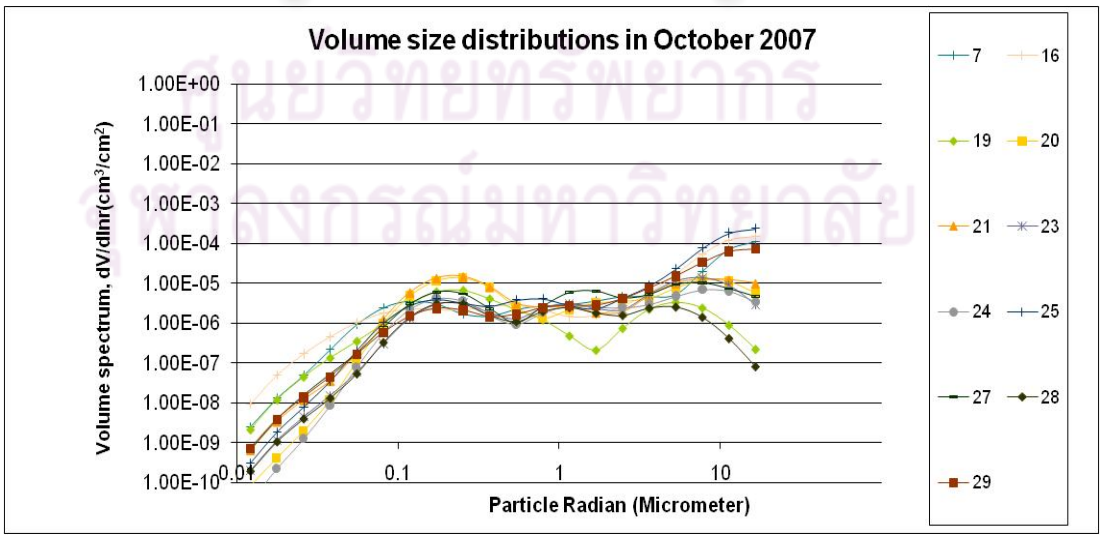

Figure C-22 Volume size distributions in October 2007.

Year	2007	**Month**	November
Fine mode	0.1729 micrometer	**Coarse mode**	16.54 micrometer or larger

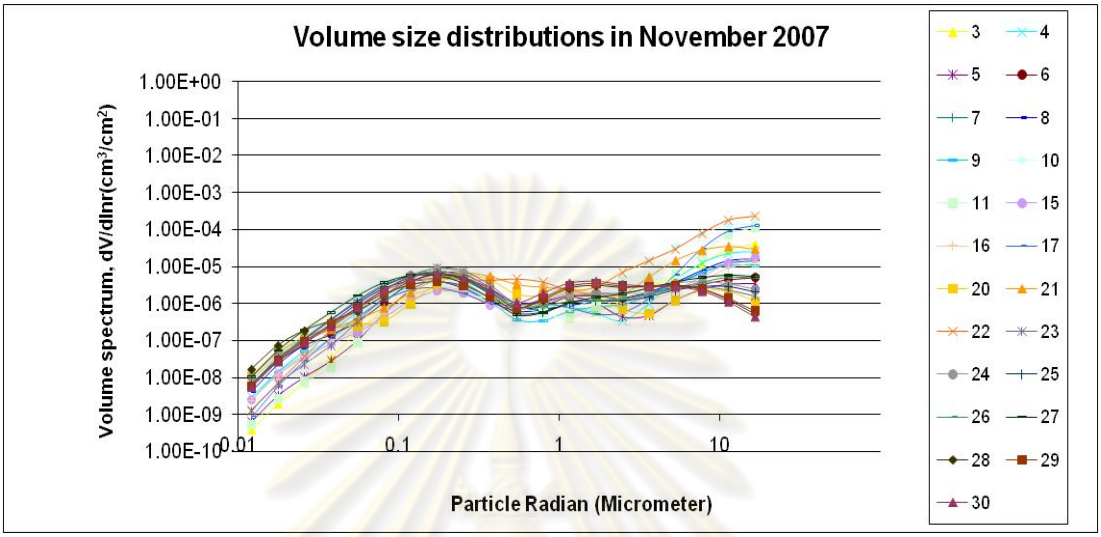

Figure C-23 Volume size distributions in November 2007.

Year	2007	**Month**	December
Fine mode	0.1729 micrometer	**Coarse mode**	16.54 micrometer or larger

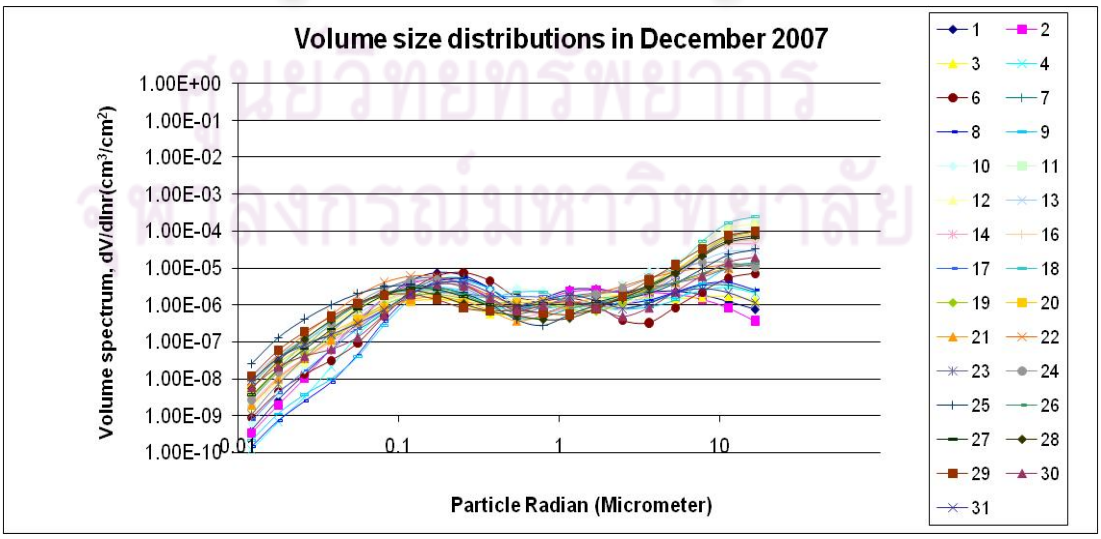

Figure C-24 Volume size distributions in December 2007.

APPENDIX D

Backward trajectory at Phimai

APPENDIX D

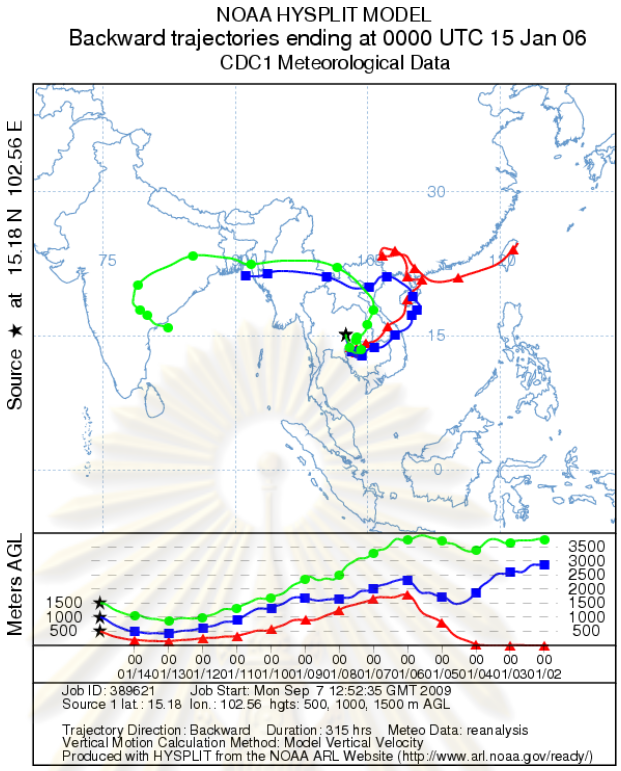

Figure D-1 Backward trajectories on 15 January 2006.

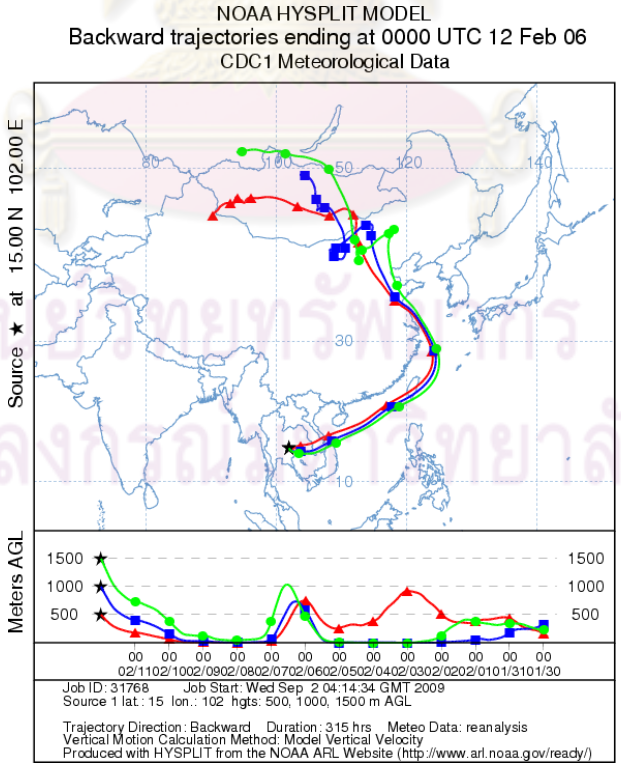

Figure D-2 Backward trajectories on 12 February 2006.

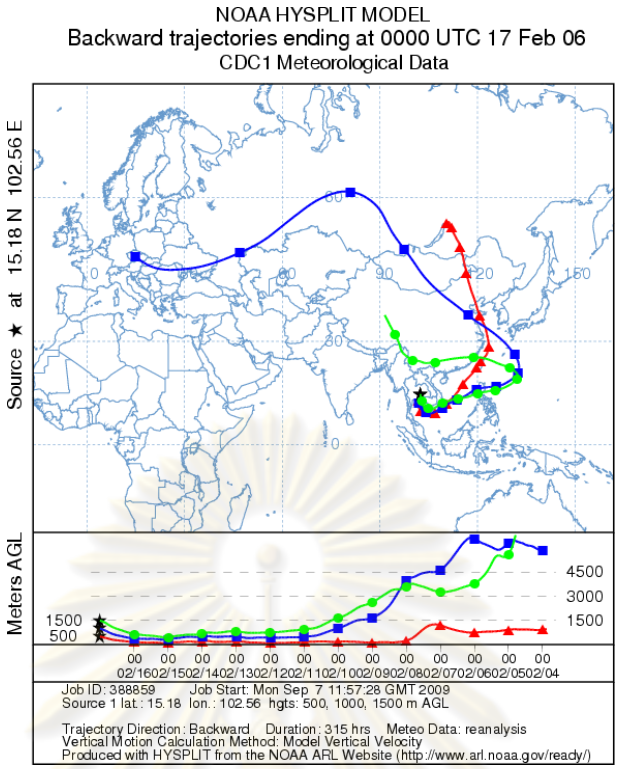

Figure D-3 Backward trajectories on 17 February 2006.

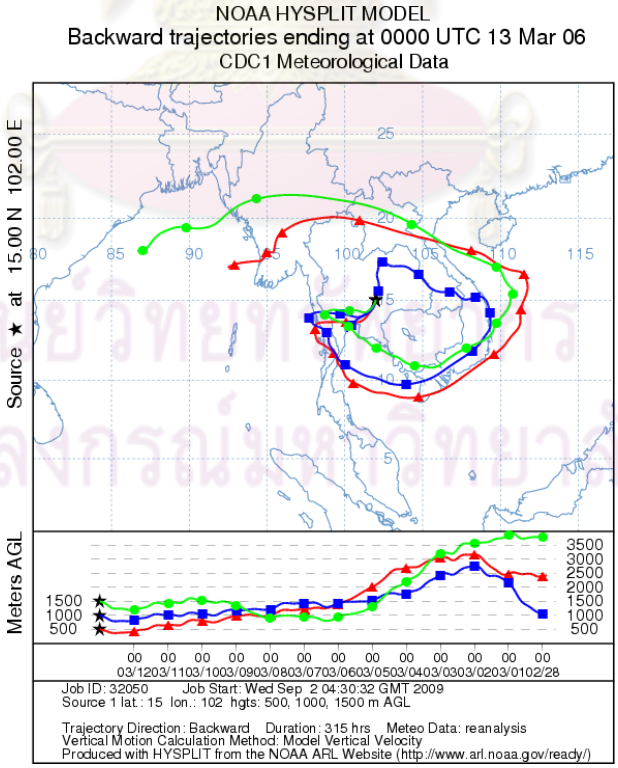

Figure D-4 Backward trajectories on 13 March 2006.

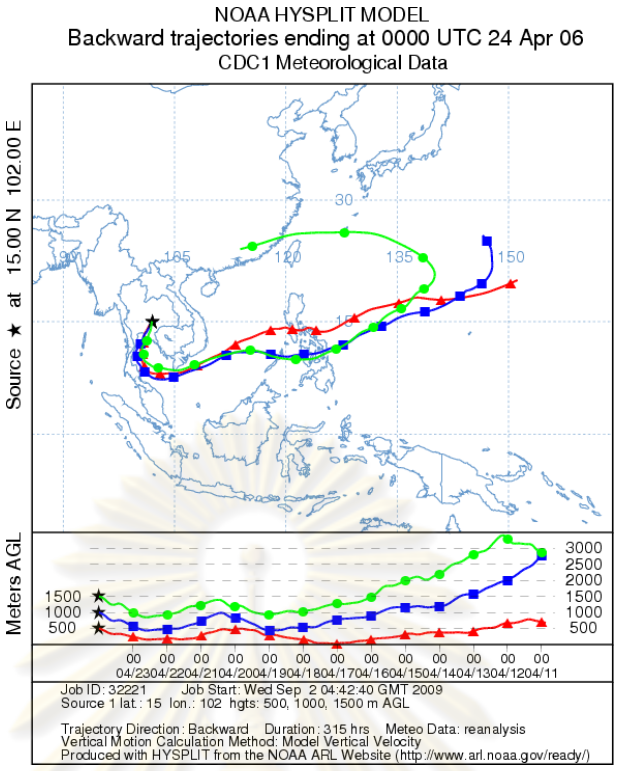

Figure D-5 Backward trajectories on 24 April 2006.

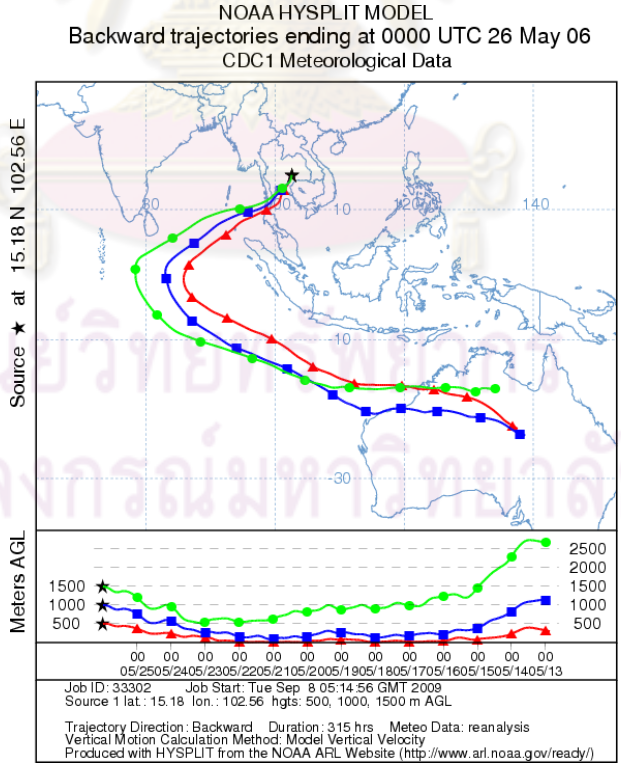

Figure D-6 Backward trajectories on 26 May 2006.

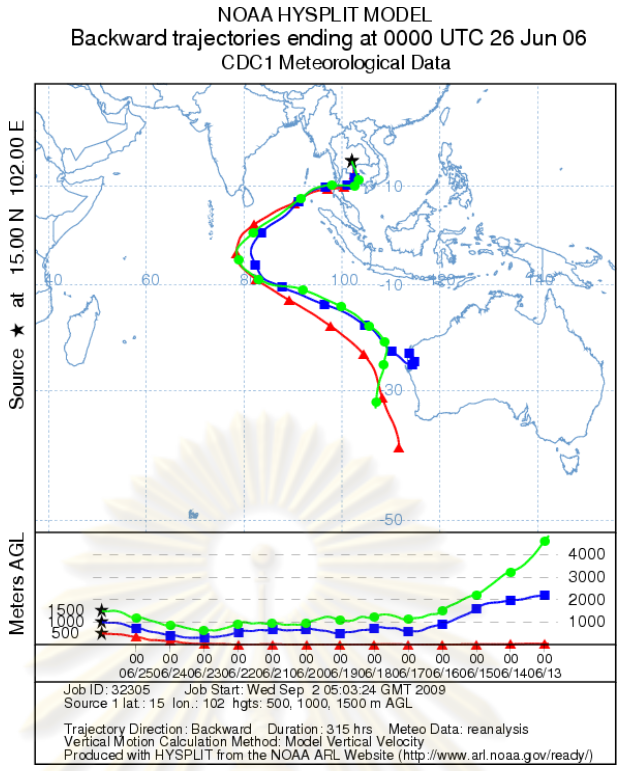

Figure D-7 Backward trajectories on 26 June 2006.

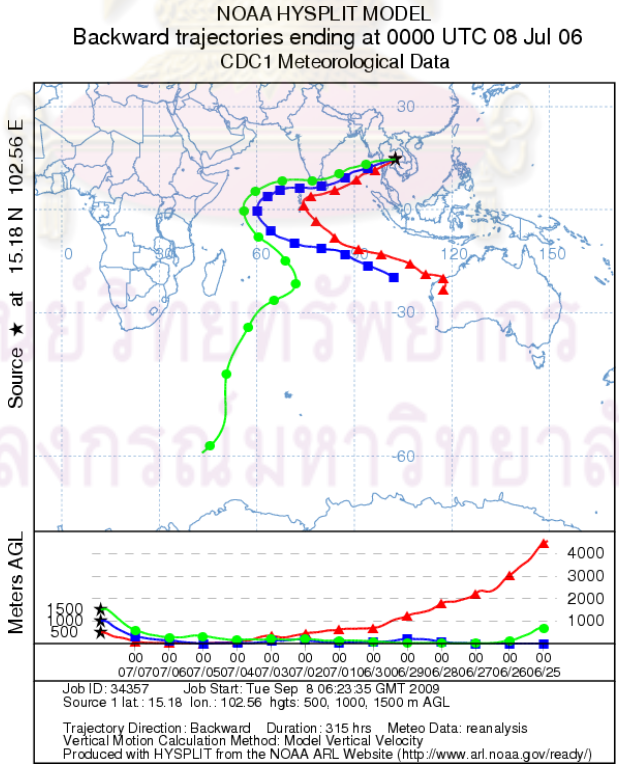

Figure D-8 Backward trajectories on 8 July 2006.

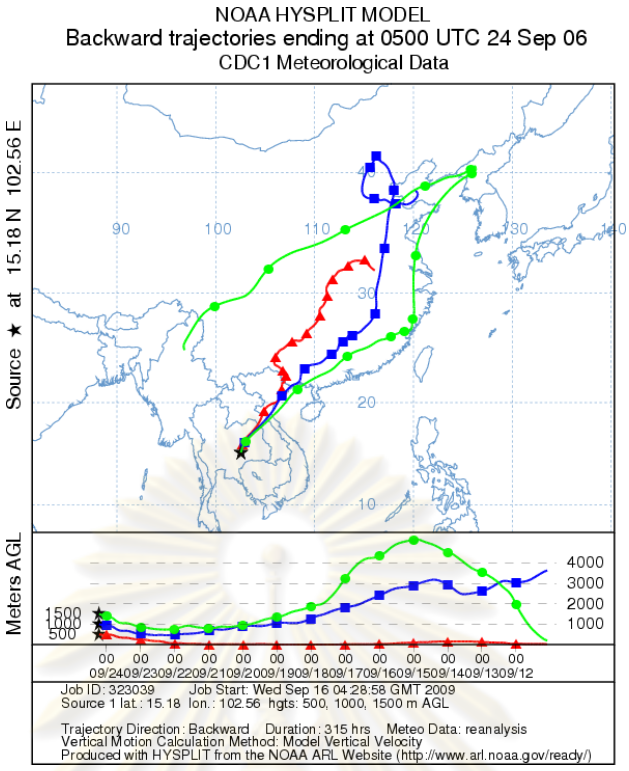

Figure D-9 Backward trajectories on 24 September 2006.

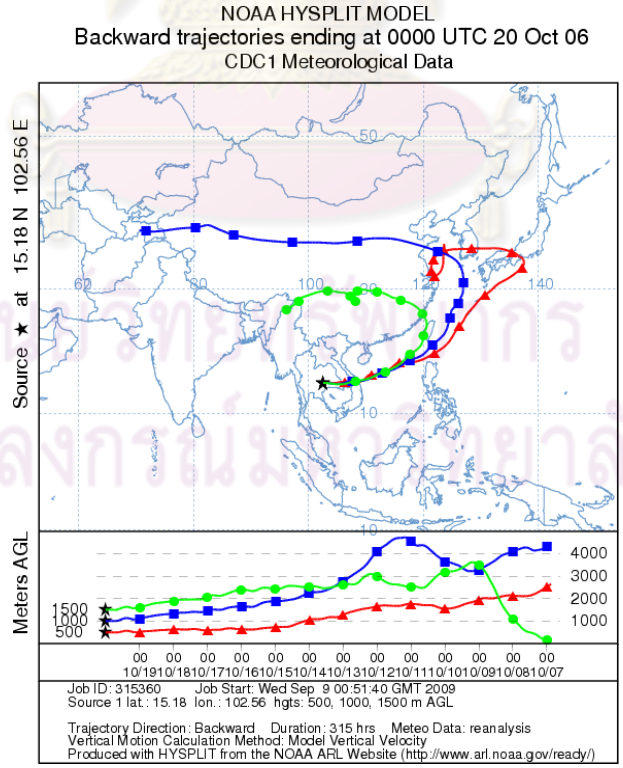

Figure D-10 Backward trajectories on 20 October 2006.

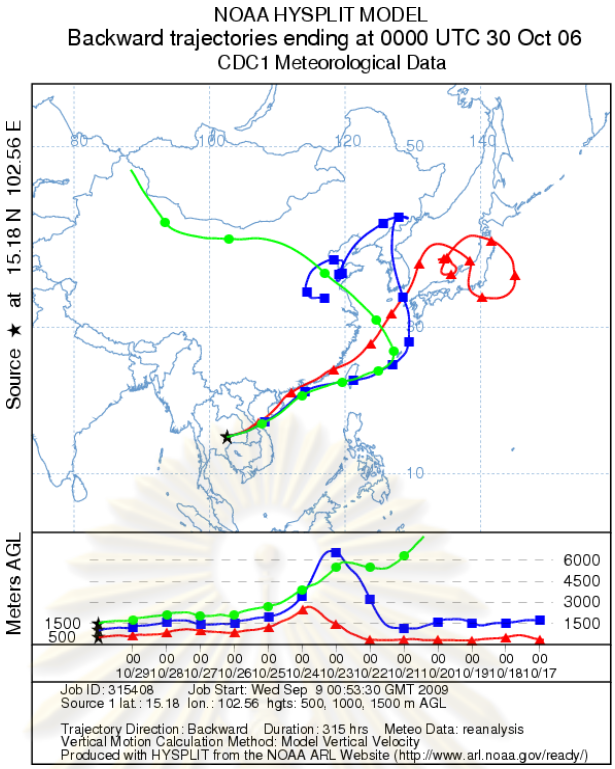

Figure D-11 Backward trajectories on 30 October 2006.

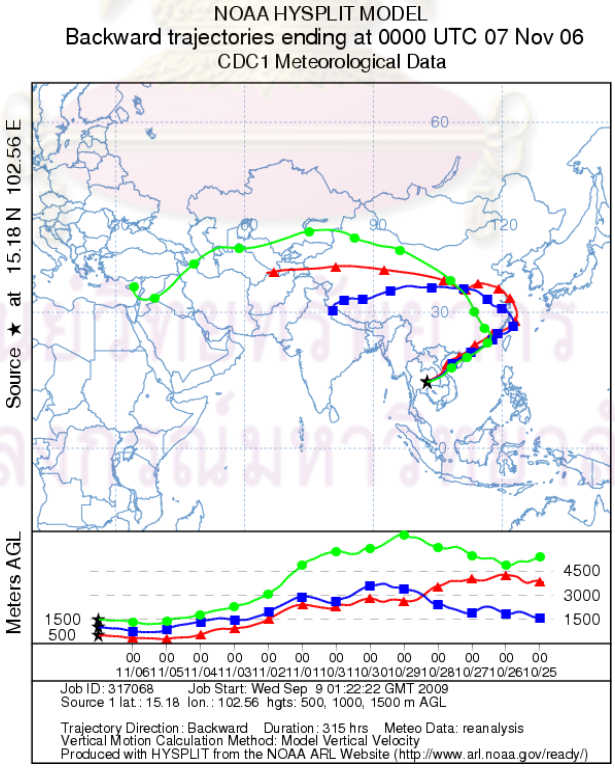

Figure D-12 Backward trajectories on 7 November 2006.

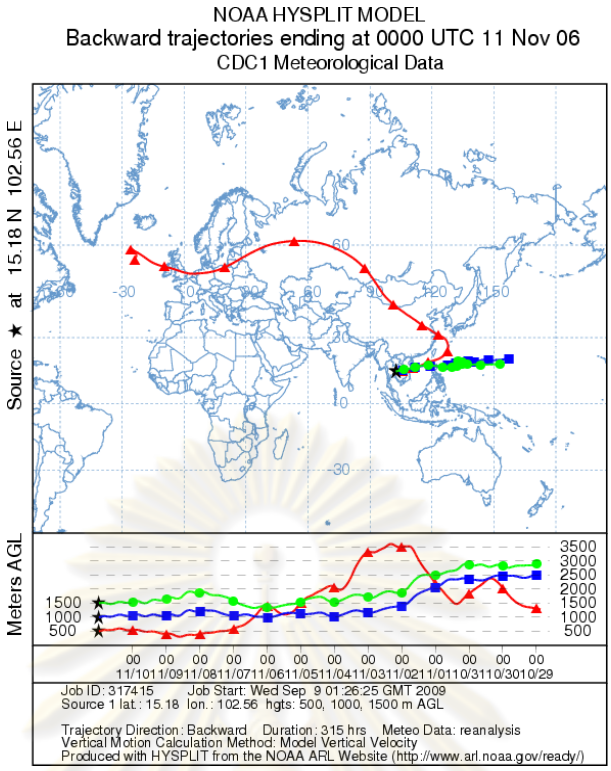

Figure D-13 Backward trajectories on 11 November 2006.

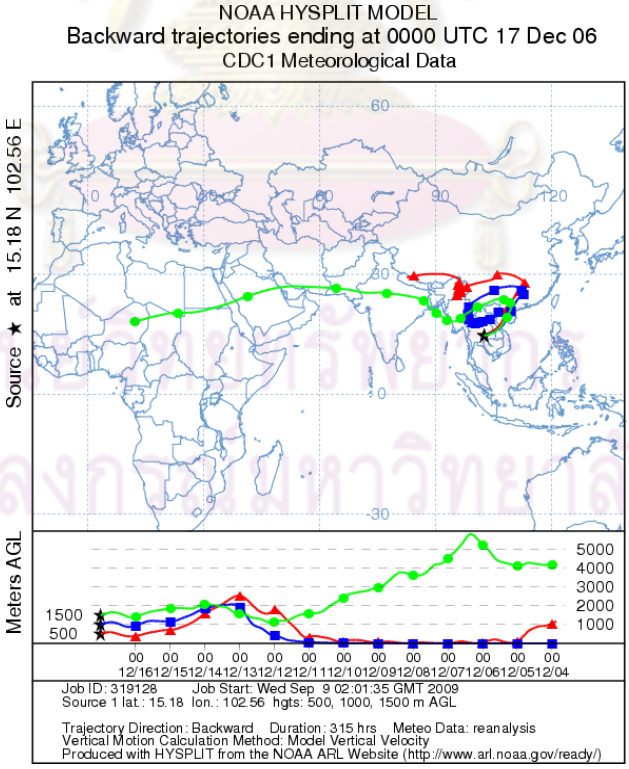

Figure D-14 Backward trajectories on 17 December 2006.

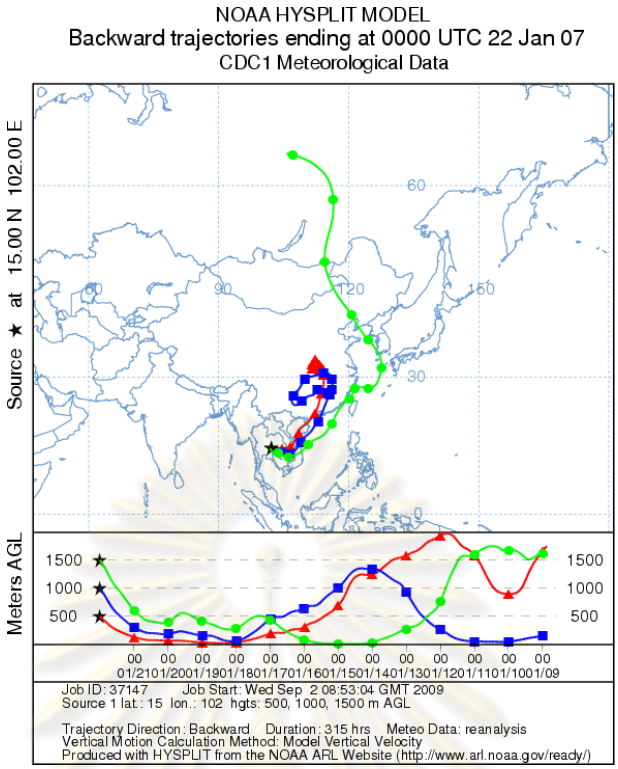

Figure D-15 Backward trajectories on 22 January 2007.

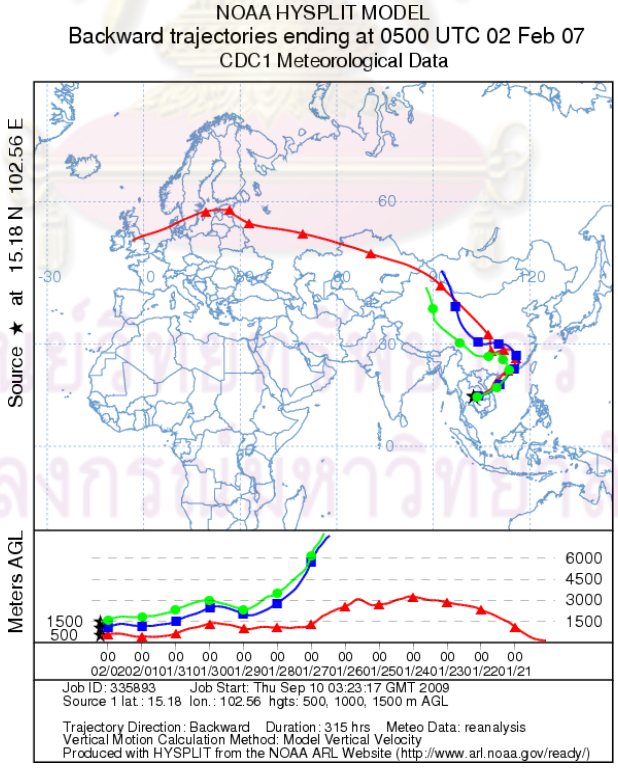

Figure D-16 Backward trajectories on 2 February 2007.

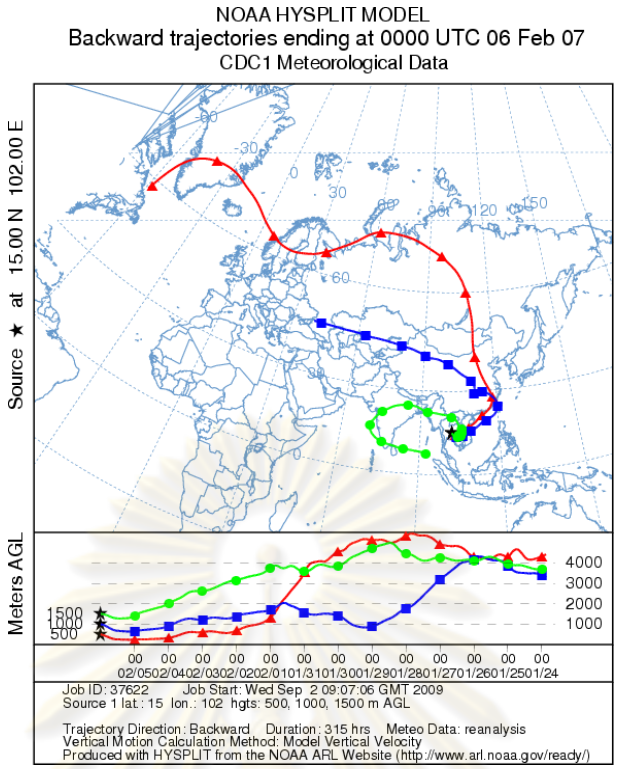

Figure D-17 Backward trajectories on 6 February 2007.

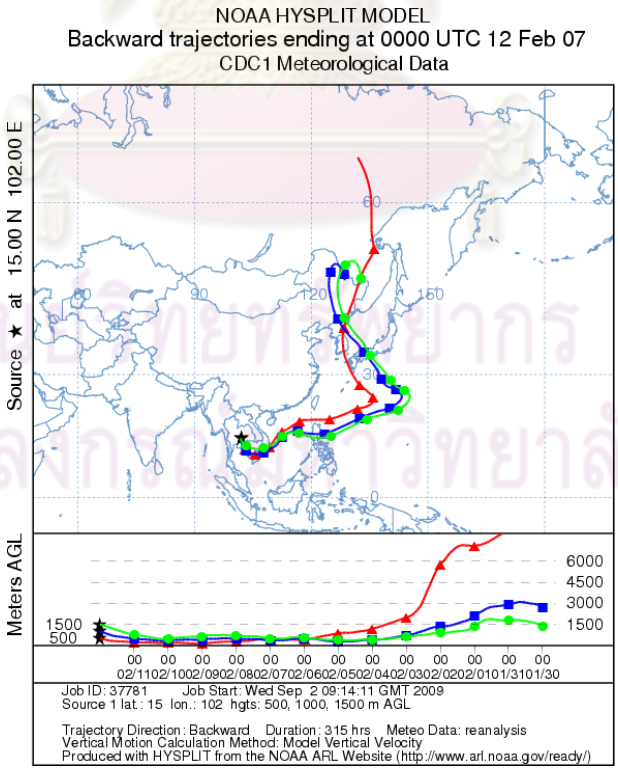

Figure D-18 Backward trajectories on 12 February 2007.

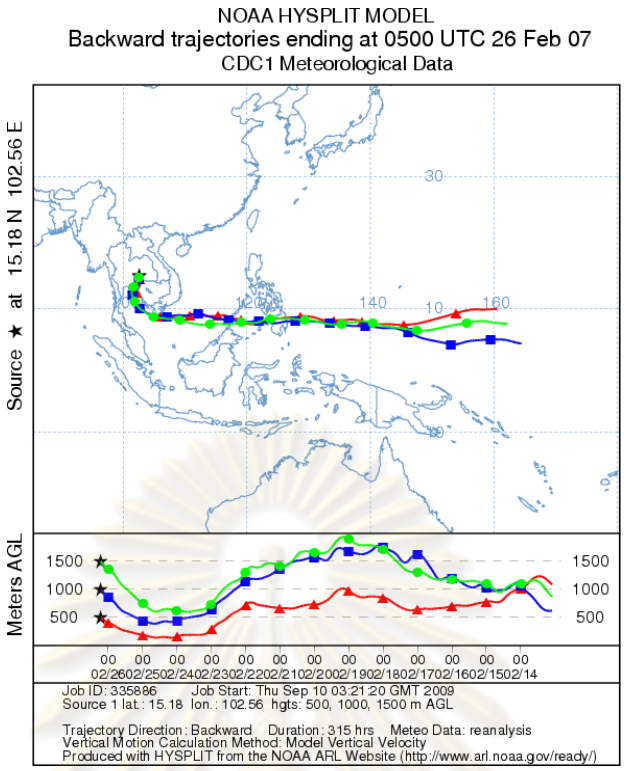

Figure D-19 Backward trajectories on 25 February 2007.

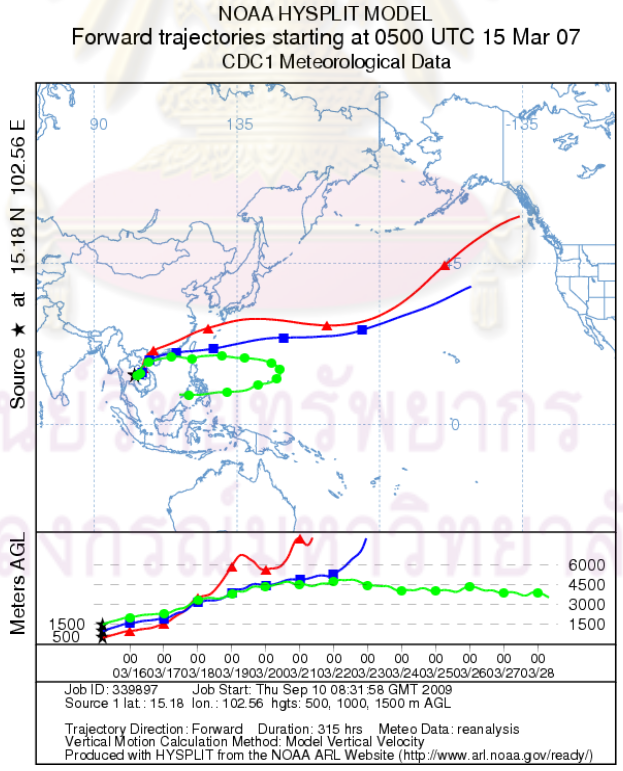

Figure D-20 Backward trajectories on 15 March 2007.

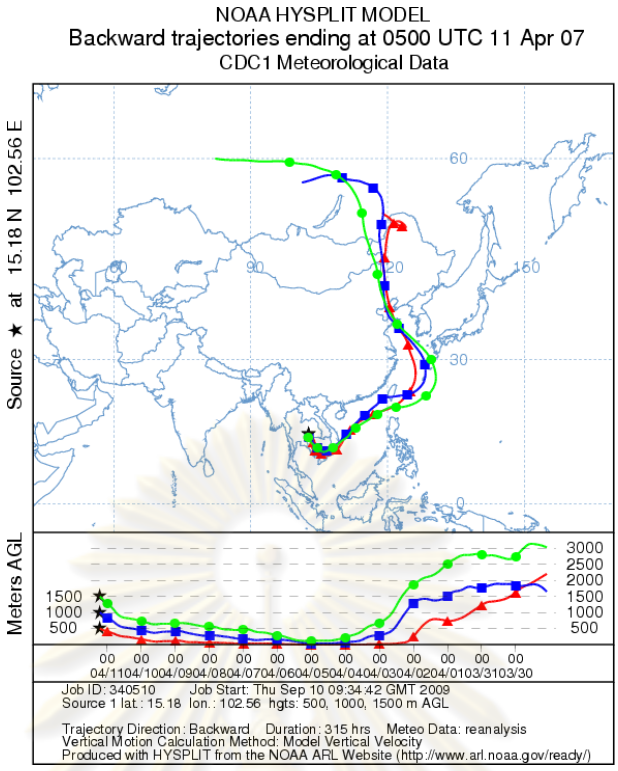

Figure D-21 Backward trajectories on 11 April 2007.

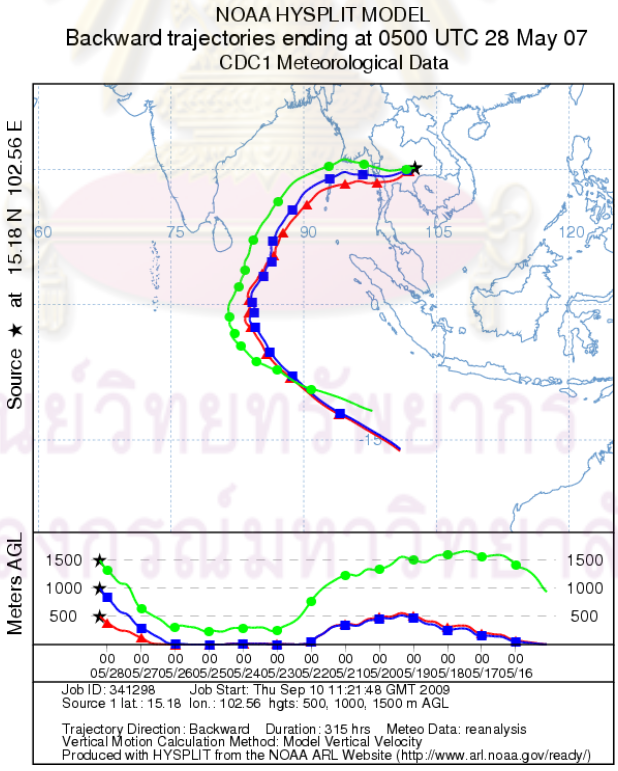

Figure D-22 Backward trajectories on 28 May 2007.

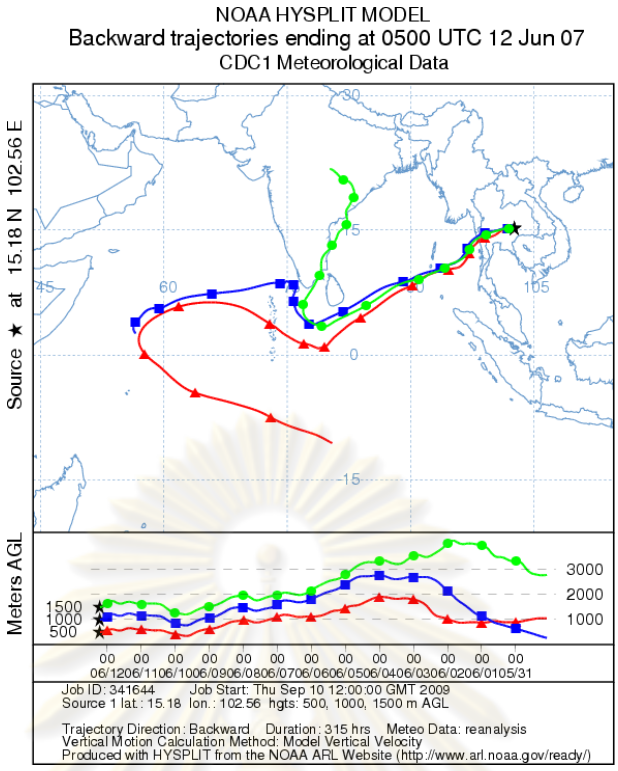

Figure D-23 Backward trajectories on 12 June 2007

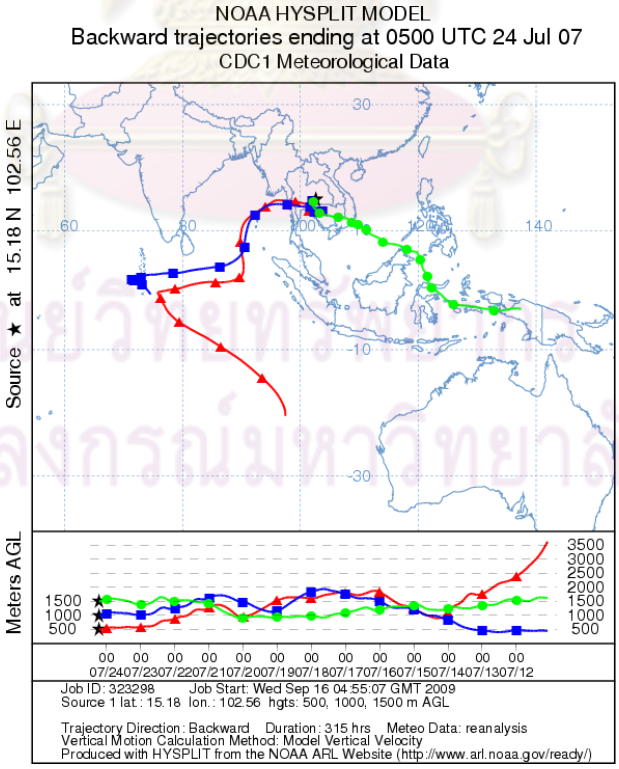

Figure D-24 Backward trajectories on 24 July 2007.

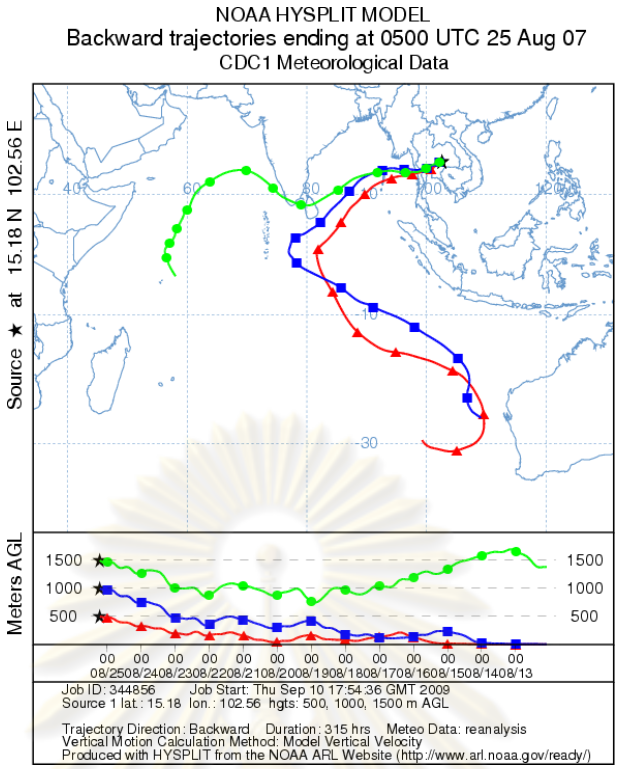

Figure D-25 Backward trajectories on 25 August 2007.

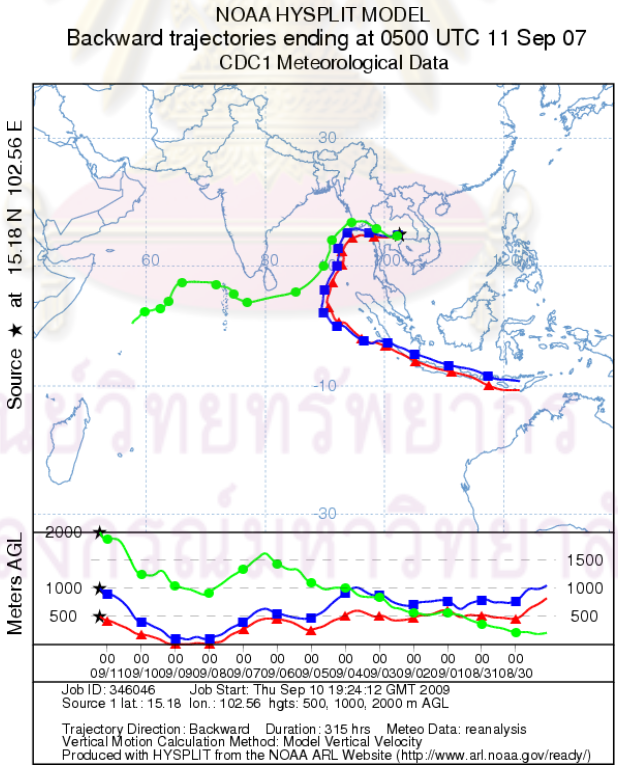

Figure D-26 Backward trajectories on 11 September 2007.

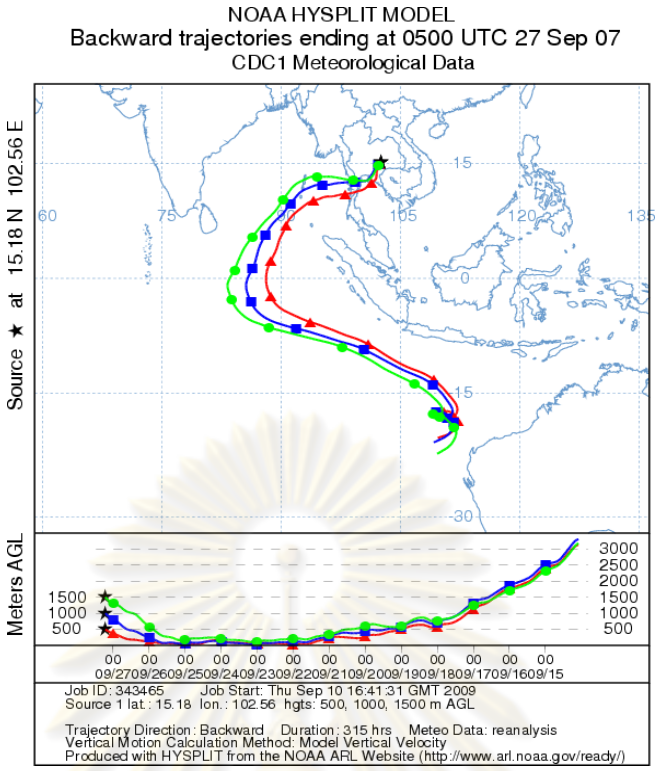

Figure D-27 Backward trajectories on 27 September 2007.

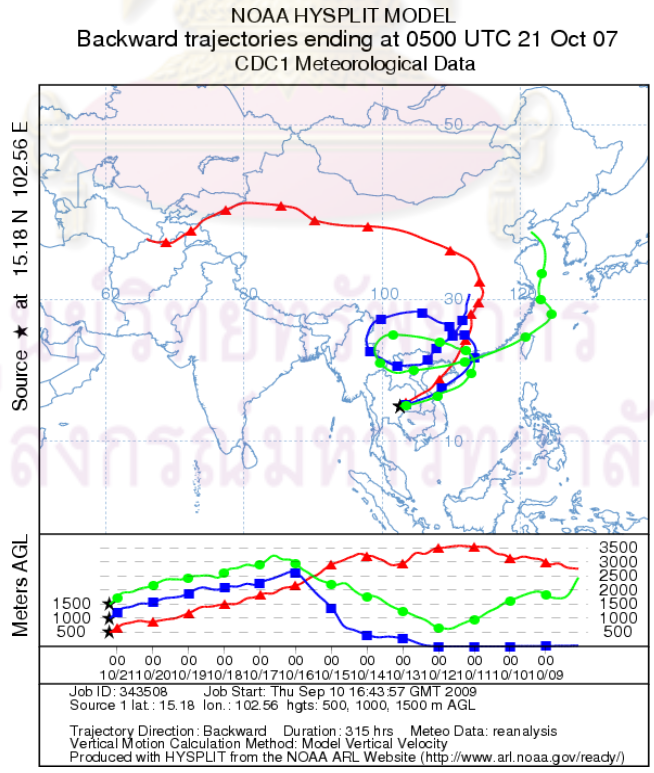

Figure D-28 Backward trajectories on 21 October 2007.

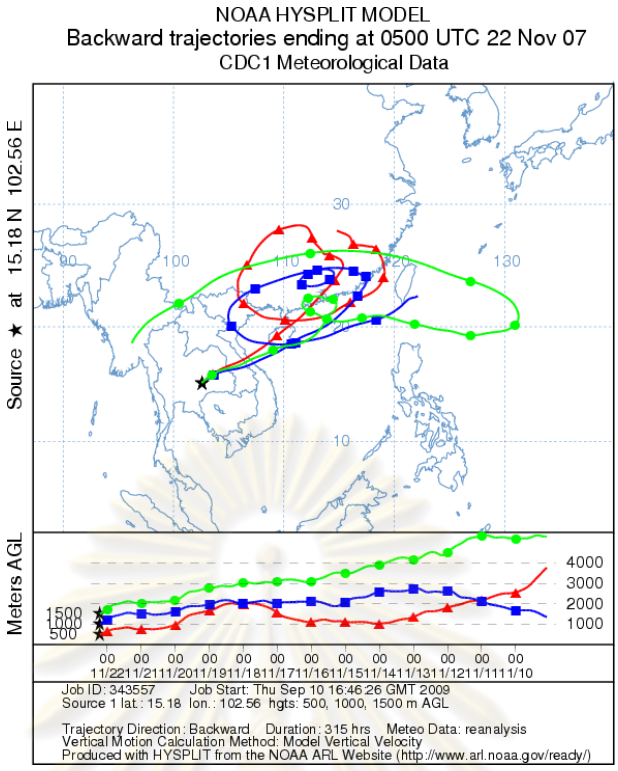

Figure D-29 Backward trajectories on 22 November 2007.

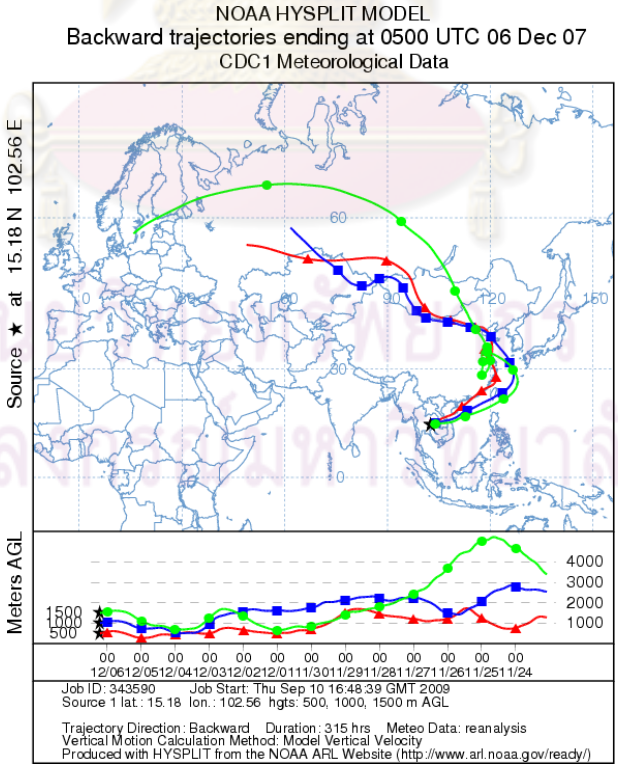

Figure D-30 Backward trajectories on 6 December 2007.

VITAE

Thawatchai Sudjai was born in Ratchaburi, Thailand. He received Bachelor Degree of Science (Physics) in 2006 from Chulalongkorn University. He serves as researcher in Atmospheric sciences, Earth Sciences Program, Department of Geology, Chulalongkorn Univeristy.